

Dear Editor,

Please find below:

- our point-by-point response to the reviews
- a list of all relevant changes made in the manuscript
- and a marked-up manuscript version.

## Reply to Anonymous Referee #1

We thank Anonymous Referee #1 for his/her positive review of this work.

Replies to Anonymous Referee #1's remarks and suggestions are given below. For clarity, we keep the reviewer's comments in blue and italic while our response is in black font.

*Nitrate is massively lost from the snowpack to the atmosphere making an interpretation of nitrate concentrations measured in the ice difficult if not impossible. Isotopes of N and O have been claimed to have the potential to disentangle post depositional processes from the initial nitrate deposition. Both isotopes have their specifics shedding light on different processes. Erbland et al. constructed a conceptual model for air snow interaction for nitrate including its isotopes. The model is not and does not claim to be perfect and include all the processes. However, the relevant processes are claimed to be included by parametrization.*

*The model and its concepts are well described. The simulations and discussions are hard to follow and naturally depend largely on the assumptions. That part of the manuscript would benefit from a bit of reorganization. State clearly what is working and even more what is not working. There are huge discrepancies between the model and the data. What is the motivation for the "modified Rayleigh plot"? The 21 year response time due to recycling in the model results in a major discrepancy in the concentration in the snow and points, in my view, to a major flaw in the concept of the model.*

Sections 3.2 and 3.3 ("Evaluation and discussion") have been largely reworked in order to clarify what is working and what is not. We also suggest to add a small paragraph in the conclusion of the paper.

The motivation for the modified Rayleigh plot is to offer a framework for the interpretation of nitrate isotope profiles in ice cores. Indeed, from ice cores, one can measure  $w(\text{FA})$ ,  $d_{15}\text{N}(\text{FA})$  et  $D_{17}\text{O}(\text{FA})$ . Given an assumption or constraints on the snow accumulation rates, one can calculate  $\text{FA} = w(\text{FA}) * A$ . In such a representation, we can observe the different impacts of changes in various variables and parameters. Since no direct information on  $\text{eps}_{\text{photo}}$  can be obtained from ice cores, one can use this representation to obtain indirect information.

Regarding the 21 years response time, the reviewer can refer to our reply to Prof. Wolff review, especially the second part of "Reply to the "Conceptual issue with the age of nitrate and number of recyclings" by Eric Wolff" when a detailed experiment illustrates this time response. We note that, in this case ("spike experiment"), the reported response time is 16 years while it is 21 years in the experiment described in the manuscript (FPI multiplied by a factor 10). The difference comes from the different criteria in determining the return to stable conditions.

*Still the model is a step forward in our approach to understand nitrate as a climate parameter at low accumulation Antarctic sites and certainly deserves being published.*

*Minor comments:*

*Title: the subtitle says “part 2”. I had difficulties finding part 1, published in 2013. I suggest to explicitly referring to part 1 in the introduction.*

The following sentence has been added at the beginning of section 1.4 in the introduction: “This paper is a companion paper of “Air-snow transfer of nitrate on the East Antarctic Plateau – Part 1: Isotopic evidence for a photolytically driven dynamic equilibrium in summer”, published in the same journal (Erbland, et al., 2013).”

*p. 6893, line 16 and 23:  $f$  is the remaining fraction. On line 23 it becomes “loss ( $f$ )” which is the opposite.*

Thank you for pointing this out. Sentences referring to the loss of nitrate (such as p. 6893 line 23) now refer to “ $1 - f$ ” and not to “ $f$ ”.

*p. 6894: eq 4 is identical to eq 2 written in a different form. The difference in epsilon is that  $e_{app}$  potentially includes more than one process while in eq. 4 epsilon is pure photolytic. I suggest to remove one of the equations and explain the difference properly.*

Indeed, equations 4 and 2 are almost the same equations. Following the reviewer’s suggestion, Eq 4 has been removed and the text has been changed to refer to the use of  $15\epsilon_{pho}$  when it comes to calculating the effects of the pure photolytic process on nitrogen isotopes of nitrate.

*p. 6894: eq 5: eq 5 is the accumulated product not the immediate product as the word emitted suggests. Please reword. Also where is eq 5 relevant? As the processes described later are fast I do not see where the accumulated product comes into play. I did not find any reference to Eq. 5. Therefore I suggest removing it entirely.*

Agreed. Eq 5 is removed as well.

*p. 6898, line 1: This is the isotopic mass balance. Please call it that.*

Agreed. The sentence has been changed to: “The isotopic mass-balance equations write...”.

*p. 6898, line 7: “Compartment” should be “box”*

Agreed. The text has been changed accordingly.

*p. 6901, line 28: typo should read “nitrate is kept the same”*

The text has been changed accordingly.

*section 2.4.2: I do not understand the consequence of  $f_{app}$ .  $f_{app}$  is not used later on as much as I can see. I suggest removing this section and discussing the effect in depth when D17O is discussed.*

Section 2.4.2 cannot be removed from the chapter on model description since it is an important process, which must be described. However, it is true that introducing  $f_{app}$  is not necessary. Therefore, the sentence “This results in an apparent remaining nitrate mass fraction denoted  $f_{app}$  which writes:  $f_{app} = f + f_{cage} \times (1 - f)$  and, consequently, to a lower apparent quantum yield” has been removed.

*p 6903: Can you please indicate the “Leighton cycle” in figure 1 and 2.*

Done. However, note that Figure 1 has been removed from the manuscript (cf our answers in the review process).

*p6907, line 16, 17: Why is the boundary layer set to 50m not 30m as others have found?*

The boundary layer height is set to 50 m which is the median height between winter (30m) and summer (ca. 100m) simulated by (Swain & Gallée, 2006) and (Gallée, et al., 2014), respectively. The text has been rephrased as follows: “The thickness of the atmospheric boundary layer is set to a constant value of 50 meters, a value which sits between the median wintertime value (ca. 30 m) simulated by Swain and Gallée (2006) and the mean value simulated around 27 December 2012 (Gallée et al., 2014)”.

A number of additional changes have been made to the model and the main text. The reviewers can refer to our other uploaded file.

## Reply to the review of Eric Wolff

We thank Prof. Eric Wolff for his positive review of this work.

Replies to Prof. Wolff's remarks and suggestions are given below. For clarity, we keep the reviewer's comments in blue and italic while our response is in black font.

*This paper presents a model that aims to trace the mass and isotopic changes of nitrate in the air and snow of the East Antarctic plateau. It builds on the insights obtained in a string of fieldwork by various of the authors, as well as some recent lab work (which has provided some essential parameters for the model). The paper provides a useful overall description of the processes that determine the processing and archiving of nitrate (and its isotopic values), with all the many factors that may be involved, and this is in itself useful. It provides a way of assessing the validity of some of the ideas that have been deduced from the fieldwork (generally with success). Finally the authors argue that it provides a framework for interpreting deep ice core records: I agree that it does although I am less confident than the authors that it will be possible to derive unique interpretations from the data using the model.*

*Overall the paper and the modelling effort are an impressive and fairly comprehensive attempt on the problem, and this will be a valuable contribution that should be published. The structure of the paper is logical, and the conclusions seem valid. I have one conceptual issue, regarding the number of recyclings that I would like to discuss. The paper is hard work to read: in fact I defy anyone to read it through at a single sitting. This is perhaps inevitable in a paper with so many parameters that have to be described: I will in any case suggest a couple of places where the reader might be given more help through summary paragraphs that would allow them to skip some of the more convoluted sections. I am also a little concerned about some of the figures: some of the multipart figures appear very small in the way they print as pdf (and in some cases coloured lines are hard to distinguish or not fully defined). While I realise readers can stretch them on screen, the authors should try and persuade the publishers to give some of them full pages in the print pdf format to help the reader who prints their papers.*

We thank Prof. Wolff for his appreciation of this work. Indeed, it is difficult to make the paper more concise given the different goals we want to reach. This is to say: describing the model, comparing it to observations for DC conditions, comparing it to observations for EAIS conditions and providing a framework for the interpretation of ice cores.

We will attempt to add summary paragraphs in order to help the reader skipping some parts of the text.

We will ask the publisher to print figures 5 and 6 in full page or, at least, the two on one full page.

*The paper should certainly be published in ACP, after revisions that are relatively minor, though important. (See below).*

*Abstract: last few lines. I think this gives an impression that is more positive than the reality about the likelihood of deriving particular changes from the ice core record. At least as presented later there are far more unknowns than measurements and for example it is not clear to me that it will be possible to infer any particular change in local processes from del170. Please reassess the wording.*

Please see our answers to your comments below.

*Page 6892, last few lines. I commented at pre-discussion stage about the figure (now revised to 120) for the average cycling of an archived nitrate. This recurs in various ways numerous times throughout the text (page 6936, line 7; page 6938, line 2 page 6940, line 11 – although it is often cited as 150). Presumably it is calculated as  $\tau_{\text{arch}}/\tau_{\text{photo}}$ , perhaps with a correction for seasonality in  $\tau_{\text{photo}}$ . 120 seems very high but I think I have argued myself into agreeing with you. I am less sure about  $\tau_{\text{arch}}$  itself though.*

To address this comment, we refer to our answer to the second comment of Prof. Wolff: “Reply to the “Conceptual issue with the age of nitrate and number of recyclings” by Eric Wolff”.

*$\tau_{\text{arch}}$  denotes the time it takes for the amount of nitrate in the top 50 cm to be archived. Putting some numbers in: with the values (for  $m_{50\text{cm}}$  and FA) in Tables 6 and 5,  $\tau_{\text{arch}}$  is 52 years. The time taken for snow to reach 50 cm is less than 6 years, so this number implies that nitrate molecules in the surface skin are already typically nearly 50 years old on average. Later on (section 3.3.3) you argue that the model converges after 20 years, which seems inconsistent with this number, so please think about that. In addition, later in the paper you will show that you get FA about right, but are almost a factor 3 low for  $m_{50\text{cm}}$ . This implies that an experimental value for  $\tau_{\text{arch}}$  is perhaps a factor 3 lower than you would infer. While obviously you have to run with your modelled values for now, I think it would be worthwhile to say that the real number might be lower, so as not to get weird numbers embedded in the literature.*

Here as well, to address this comment, we refer to our answer to the second comment of Prof. Wolff: “Reply to the “Conceptual issue with the age of nitrate and number of recyclings” by Eric Wolff”.

*Moving on to more detailed issues:*

*Page 6898, line 5. Be careful here. Almost all parameters in the tables are in units of meters (m) but now you introduce terms with cm. Please be sure you have correctly accounted for such unit changes.*

Unit changes in this equation have been checked. There is no mistake in the conversion.

However, the reader should read “ $\text{m}^{-3} \text{s}^{-1}$ ” for the unit of  $P_i$  and  $L_j$  (and not  $\text{cm}^{-3} \text{s}^{-1}$ ). In the text, the information about the unit of  $P_i$  and  $L_j$  has been removed to avoid any further

confusion. Indeed, providing this information only makes sense if the unit of  $X$  is provided as well.

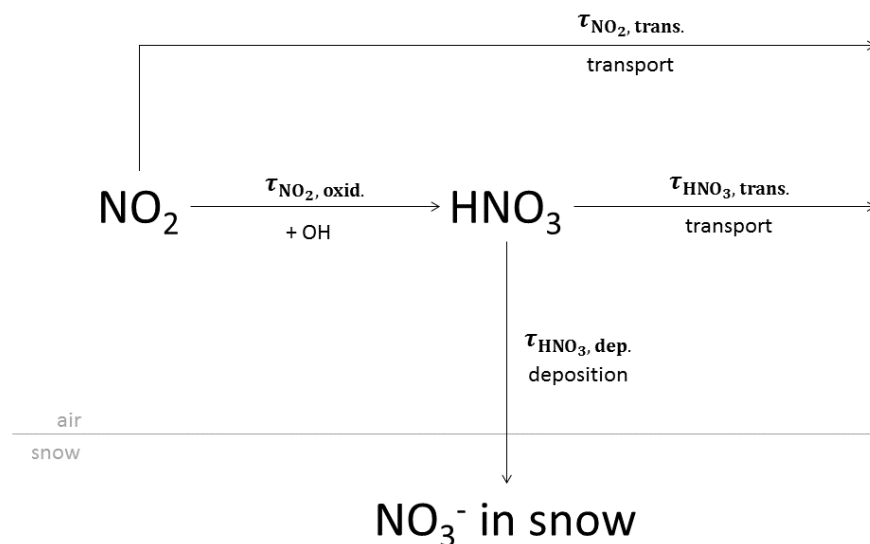
Also, for the sake of clarity, units for the atmospheric mixing ratios of  $\text{RO}_2$  and  $\text{OH}$  have changed to molecule  $\text{m}^{-3}$  and the unit for the diffusion coefficient has been changed to  $\text{m}^2 \text{s}^{-1}$ .

*Page 6908, line 23. I realise this is partly addressed later but why was 20% chosen. Was this a tuned parameter, ie 20% gives the best answer?*

The parameter  $f_{\text{exp}}$  is tuned (adjusted) and the value 20% gives realistic results. As mentioned in the text, setting  $f_{\text{exp}}$  to 0 (no export) would lead to unrealistic results: “ $\delta^{15}\text{N}$  values in [the atmosphere and skin layer] become highly negative ( $< -120 \text{‰}$ ) which is clearly not realistic when compared to the observations “. Also, in such conditions, the model does not converge within a reasonable time and nitrate endlessly builds up in the photic zone.

However,  $f_{\text{exp}}$  can be related to physical variables. Indeed,  $f_{\text{exp}}$  represents the competition between the export of  $\text{NO}_y$  ( $\text{NO}_2$  or  $\text{HNO}_3$ ) and the deposition of (to make it simple)  $\text{HNO}_3$ .

Let us consider the schematic below where  $\text{NO}_2$  and  $\text{HNO}_3$  are considered at steady-state. The deposition of  $\text{NO}_2$  is neglected because the deposition of  $\text{HNO}_3$  is a factor  $8.0 \pm 3.2$  faster than that of  $\text{NO}_2$  (Zhang, et al., 2009). Also, oxidation by  $\text{OH}$  is considered to be the only channel of  $\text{NO}_2$  oxidation (an assumption valid in summer).



The overall residence time of atmospheric  $\text{NO}_y$  ( $= \text{NO}_2 + \text{HNO}_3$ ) against deposition is expressed as follows:

$$\tau_{\text{dep}} = \tau_{\text{NO}_2, \text{oxi.} + \text{dep.}} = \tau_{\text{NO}_2, \text{oxi.}} + \tau_{\text{HNO}_3, \text{dep.}} \quad (\text{dry deposition of } \text{NO}_2 \text{ is neglected})$$

The residence time of atmospheric  $\text{NO}_y$  against horizontal export is expressed as follows:

$$\tau_{\text{exp}} = \frac{1}{\frac{1}{\tau_{\text{NO}_2, \text{trans.}}} + \frac{1}{\tau_{\text{NO}_2, \text{oxi.} + \text{trans.}}}}$$

with  $\tau_{\text{NO}_2,\text{oxi.}+\text{trans.}} = \tau_{\text{NO}_2,\text{oxi.}} + \tau_{\text{HNO}_3,\text{trans.}}$ .

$$\tau_{\text{NO}_2,\text{oxi.}} = \tau_{\text{NO}_2+\text{OH}} = \frac{1}{k_{\text{NO}_2+\text{OH}}(T,P) \times [\text{OH}]} = 3.5 \cdot 10^3 \text{ s.}$$

We use kinetic rate constants from (Atkinson, et al., 2004) and  $T$ ,  $P$  and  $[\text{OH}]$  for mean summertime conditions at DC (Kukui, et al., 2014).

For the calculation of  $\tau_{\text{HNO}_3,\text{dep.}}$ , we use  $v_{\text{dep}} = 0.8 \text{ cm s}^{-1}$  (Huey, et al., 2004) and assume an average boundary layer height of  $H = 100 \text{ m}$  representative of the 2011-2012 summer at DC (Gallée, et al., 2014).  $\tau_{\text{HNO}_3,\text{dep.}} = H / v_{\text{dep}} = 1.3 \cdot 10^4 \text{ s}$  (Jacob, 1999).

For the calculation of  $\tau_{\text{NO}_2,\text{trans.}}$  and  $\tau_{\text{HNO}_3,\text{trans.}}$ , we consider a characteristic horizontal length of  $L = 400 \text{ km}$  which represents the width of the East Antarctic plateau. We also consider the mean summertime wind speed at Dome C ( $v_{\text{wind}} = 3.1 \text{ m s}^{-1}$ , (Kukui, et al., 2014)).  $\tau_{\text{NO}_2,\text{trans.}} = \tau_{\text{HNO}_3,\text{trans.}} = L / v_{\text{wind}} = 1.3 \cdot 10^5 \text{ s}$ .

We then obtain  $f_{\text{exp}} = \frac{1}{1 + \frac{\tau_{\text{exp}}}{\tau_{\text{dep}}}} = 0.20$  in accordance to the chosen value of  $f_{\text{exp}}$  used to adjust the model.

We suggest to add the following sentences in section 3.1.1 where we discuss the choice of the “adjustment parameters”: “Following the approach of Jacob (1999), a summertime value for  $f_{\text{exp}}$  can be approached by considering the chemical lifetime of  $\text{NO}_2$  in its oxidation by  $\text{OH}$  and the residence times of  $\text{NO}_2$  and  $\text{HNO}_3$  in the atmosphere and against the deposition and horizontal export processes. Using kinetic rate constants from (Atkinson et al., 2004),  $T$ ,  $P$ , wind speeds and  $\text{OH}$  mixing ratios for mean summertime conditions at DC (Kukui, et al., 2014),  $\text{HNO}_3$  dry deposition velocity from Huey et al. (2004), and vertical and horizontal characteristic dimensions of  $100 \text{ m}$  (average summertime boundary layer height, Gallée et al., 2004) and  $400 \text{ km}$  (Antarctic plateau width), respectively, we obtain  $f_{\text{exp}} = 0.20$ , in accordance with the chosen value used to adjust the model.”

In a future version of the TRANSITS model, the  $f_{\text{exp}}$  parameter (or the deposition of  $\text{HNO}_3$  and the export of atmospheric nitrate) could be explicitly calculated at each time step.

*Page 6912, line 23. I don't understand this sentence since the figure shows a 1 year period starting in January not June.*

This is an error: this sentence referred to an earlier version of Figure 5. The sentence has been removed.

*Page 6914, line 9. This discrepancy between modelled and measured values in the skin layer needs more discussion. Later on, you say it may be an artefact of the discrete measurements (ie the data don't really show the skin layer), and this may be true, surely does not apply to the*



*factor 3 error in  $m_{50\text{cm}}$  (page 6915), so we can assume that at least that factor is genuinely a problem. Is it going to be possible to reconcile this with getting good agreement for the isotope values? This seems more fundamental than you allow, implying something is not quite understood yet.*

We agree, errors in sampling the skin layer cannot entirely explain the discrepancies between simulated and observed  $m_{50\text{cm}}$  values as shown on Fig. 7a. From the experiment where FPI has been multiplied by a factor 10, we have shown that the effect on  $m_{50\text{cm}}$  last for more than 10 years (actually 21 years) and this means that observations in 2007-2008 or 2009-2010 at Dome C could be sensitive to past changes in FPI.

Also, it is likely that a missing process in TRANSITS could explain the observed discrepancy. For example, the model does not include snow erosion, a process which could blow away a fraction of the skin layer and which may explain our observations in the field around 10 January 2010. Around this date, we observed a decrease of factor 2 in skin layer concentrations which was concurrent with an increase in wind speed (Erland, et al., 2013).

The following sentence has been added to the text in section 3.3.3.: “It is also likely that missing processes in TRANSITS could explain the observed discrepancy. For example, the model does not include snow erosion, a process which could blow away a significant fraction of the skin layer and thus lead to a rapid decrease in  $m_{50\text{cm}}(\text{NO}_3^-)$ ”.

*Page 6914, line 17. This value of 2% is of course entirely controlled by the decision to set  $f_{\text{exp}}$  at 20%!*

This is not exactly true. Indeed, not only  $f_{\text{exp}}$  controls the FA/FPI ratio. As discussed in section 4.1.1, parameters and variables controlling nitrate photolysis ( $f_{\text{cage}}$ , A,  $\rho$ , k, q,  $\Phi$  and the ozone column) also control this ratio (see also Table 7).

*Page 6917.  $F_{\text{exp}}$  is also bounded at the high end by  $(F_S+F_T/F_P)=25\%$ , because if it is higher than that then there is net export and eventually  $F_A$  must be negative.*

We think that Prof. Wolff is mistaking here. Indeed, here is how the horizontal export flux is calculated in the model ( $FE = f_{\text{exp}} * (FS + FT + FP)$ ). As a consequence,  $f_{\text{exp}}$  is bounded at the high end by  $f_{\text{exp}} = 1$  and greater values would lead to a net export of nitrate from the simulated combined atmosphere/snow box.

*Page 6922, line 23. You have shown that the model takes 20 years to reach equilibrium. Is this really the same as saying that the residence time is 20 years? I am sure this bears on the discussion above (and interesting that you don't get 50 years).*

Indeed, we are mistaking here. Showing that the model takes 20 years to reach equilibrium means that the slowest nitrate ions take 20 years to get through the top 1 m of snow. However, the residence time of nitrate in the top 1 m of snow is calculated as  $1/(A/\rho)$  and represents the average time that nitrate ions take to get though the top 1 m of snow (as

demonstrated in “Reply to the “Conceptual issue with the age of nitrate and number of recyclings” by Eric Wolff”). For DC conditions (as presented in this paper), the residence time is 10.7 years.

We have removed the reference to “more than 20 years” in sentence page 6922, line 23.

*Page 6932, line 20. Thank you for introducing this. However note that the speciation would also affect the cage effects (surely?). I think this issue needs to be mentioned also in the conclusions as it might strongly affect your interpretation of LGM data.*

We do not yet have a clue on how nitrate speciation would affect the cage effects. Would it directly affect them? Or would it be by affecting the ability to photolyze nitrate? Anyway, this is an important point and the following sentence has been added to the last paragraph of the conclusion: “To achieve this correction, the potential impact of nitrate speciation (association to H<sup>+</sup> or, e.g., Ca<sup>2+</sup>) on the cage effect will have to be taken into account (say, e.g. in the case of glacial conditions)”.

*Page 6934-5. This section is really hard to read (step back and look how much of it is symbols!). I suggest: (1) PSS needs to be listed in table 1 or somewhere, it took me ages to find where you had defined it, (2) Please give a summary paragraph explaining the outcome of section 4.2.2. You might consider this for other difficult sections.*

Good idea. We have added the acronym “PSS” in Table 1.

A summary paragraph explaining the outcome of section 4.2.2 has been written.

*Page 6936, line 7. 150 or 120?*

Our original calculation was wrong. The number of recyclings has been updated in light of our calculation in “Reply to the “Conceptual issue with the age of nitrate and number of recyclings” by Eric Wolff””. The number is now 3-4 cycles for DC conditions.

*Page 6938, line 22, ditto.*

Idem.

*Page 6938, line 3, not sure what you mean by “transcripts”.*

We meant “means”. The sentence now is: “Under the DC realistic simulation conditions, the quantum yield value which is necessary to reproduce the observations (0.026) means that nitrate lies in two different domains in or on the snow ice matrix (Meusinger et al., 2014)”

*Section 4.1 and 5. My problem with your optimism is that you have too many unknowns. For example if we consider Figure 10 and think about the LGM. We know accumulation rate will have changed, but under a different climate we can reasonably expect changes in O3 and FPI, (not to mention speciation with Ca). There will always be more than one combination, even if we can discriminate changes, that can move us to a new location on these diagrams. Similarly for 17O (page 6937, line 8): just what aspect of local atmospheric chemistry would we deduce had changed. I don't disagree with what is written but feel its presented in a too optimistic way at this stage.*

Yes, indeed, various parameters and variables could have changed under LGM conditions. However, it seems important to us to provide a tool which can classify the impacts of each parameter and variable in terms of mass and isotopic composition in the archived nitrate. Indeed, only  $\delta^{15}\text{N}(\text{FA})$  and  $[\text{NO}_3^-](\text{FA})$  (and  $\delta^{18}\text{O}(\text{FA})$  and  $\text{D17O}(\text{FA})$ ) can be measured from ice cores and the ways to discriminate changes in A, O3 or FPI (not to mention all the parameters and variables) is limited.

Regarding D17O, we state in the text that, if DC modern conditions prevail on the Antarctic plateau during, say, the LGM, then D17O(FA) must be mostly seen as harboring information about the past local and summertime oxidative conditions of NO and NO<sub>2</sub>. As it is written it seems, indeed, optimistic. However, what we mean is that, in such conditions, most of the potential global information (on D17O(FS) and D17O(FT)) is mostly lost. Rather, D17O(FA) holds local information. The sentence in the paper now reads "However, in such conditions,  $\Delta^{17}\text{O}(\text{FA}, \text{corr.})$  would rather hold information about the local and summertime atmospheric oxidation above the East Antarctic plateau."

*However having said that, it's an important statement that we cannot deduce changes in atmospheric oxidation at global scale and that should be highlighted.*

Yes. The last sentence in the conclusion now reads: "Therefore, if the modern DC conditions applied in the past as well (i.e. important loss by photolysis followed by the local recycling of nitrate), the determination of  $\Delta^{17}\text{O}(\text{FA}, \text{corr.})$  from ice cores drilled on the East Antarctic plateau are expected to deliver information about the oxidative chemistry occurring at the local and summertime scale rather than at the global scale".

*Table 1.  $m_{50\text{cm}}$  is a mass not a mass fraction.*

We agree. The text has been changed accordingly.

*Table 6.  $m_{50\text{cm}}$  should be in units of  $\text{mgN}^{-2}$ .*

We guess Prof. Wolff meant  $\text{mgN m}^{-2}$ . We agree that this unit should be the unit of  $m_{50\text{cm}}$ . Table 6 and the entire text have been changed accordingly.

*Fig 4. Part a must be wrong, with 52 timesteps this would give  $7.8 \text{ kg m}^{-2} \text{ a}^{-1}$ , which is a factor 3 too high. Anyway this flat line is pointless, just leave it out, after checking the accumulation is correct in your model.*

We agree that the representation of the snow accumulation rates in this figure is wrong: the flat line must be at a value of  $0.54 \text{ kg m}^{-2} \Delta t^{-1}$ . The figure has been updated and this panel has been removed.

*Fig 5, parts b and c, what are the different coloured lines. Please improve the caption.*

The different colored lines refer to the same caption as in panel a. The caption has been changed to avoid such confusion.

*Fig 5g. Please replot without the factor 4 scaling. This is confusing and unnecessary.*

Figure 5g has been updated accordingly.

A number of additional changes have been made to the model and the main text. The reviewers can refer to our other uploaded file.

## References

- Atkinson, R., Baulch, D. L., Cox, R. A., Crowley, J. N., Hampson, R. F., Hynes, R. G., . . . Troe, J. (2004). Evaluated kinetic and photochemical data for atmospheric chemistry: Volume I - gas phase reactions of Ox, HOx, NOx and SOx species. *Atmos. Chem. Phys.*, 4, 1461-1738.
- Erbland, J., Vicars, W. C., Savarino, J., Morin, S., Frey, M. M., Frosini, D., . . . Martins, J. M. (2013). Air-snow transfer of nitrate on the East Antarctic Plateau – Part 1: Isotopic evidence for a photolytically driven dynamic equilibrium in summer. *Atmos. Chem. Phys.*, 6403–6419.
- Gallée, H., Preunkert, S., Argentini, S., Frey, M. M., Genthon, C., Jourdain, B., . . . Legrand, M. (2014). Characterization of the boundary layer at Dome C (East Antarctica) during the OPAL summer campaign. *Atmos. Chem. Phys. Disc.*, 14, 33089-33116.
- Huey, L. G., Tanner, D. J., Slusher, D. L., Dibb, J. E., Arimoto, R., Chen, G., . . . Kosciuch, E. (2004). CIMS measurements of HNO<sub>3</sub> and SO<sub>2</sub> at the South Pole during ISCAT 2000. *Atmos. Environ.*, 38, 5411-5421.
- Jacob, D. J. (1999). *Introduction to Atmospheric Chemistry*. Princeton University Press.

Kukui, A., Legrand, M., Preunkert, S., Frey, M. M., Loisil, R., Gil Roca, J., & Jourdain, B. (2014). Measurements of OH and RO<sub>2</sub> radicals at Dome C, East Antarctica. *Atmos. Chem. Phys.*, *14*, 12373–12392. doi:10.5194/acp-14-12373-2014

Zhang, L., Vet, R., O'Brien, J. M., Mihele, C., Liang, Z., & Wiebe, A. (2009). Dry deposition of individual nitrogen species at eight Canadian rural sites. *J. Geophys. Res.*, *114*(D02301). doi:10.1029/2008JD010640

## Reply to the “Conceptual issue with the age of nitrate and number of recyclings” by Eric Wolff

We warmly thank Prof. Eric Wolff for his additional feedback on this very key conceptual issue. His critical and constructive views on the calculation of the number of recyclings helped us to imagine a different approach.

Replies to Prof. Wolff’s remarks and suggestions are given below. For clarity, we keep the reviewer’s comments in blue and italic while our response is in black font.

### *Problems with calculation of archiving lifetime and number of recyclings*

Before addressing Prof. Wolff’s comments and suggestions, let us recall the purpose of introductory section 1.2 (ACPD version). The goal of this section was to demonstrate the choice of the concepts used in the TRANSITS model for the conditions prevailing at Dome C. Indeed, we need:

1. To demonstrate that the NO/NO<sub>2</sub> cycling is fast enough to consider that 100% of the O atoms in NO<sub>2</sub> originate from the local summer NO<sub>x</sub> chemistry, and,
2. To demonstrate that NO<sub>y</sub> (the sum of nitrate + NO<sub>x</sub>) are recycled many times at the air-snow interface before being archived.

Reconsidering the second point, it appears that there is not such a need to convince the reader that multiple recyclings occurs at the air-snow interface. Indeed, the part 1 paper has already provided a demonstration for the recycling of nitrate to take place at the DC air-snow interface, as also suggested initially by (Davis, et al., 2008). The question that remains is the number of recycling before nitrate is definitely archived. Because the processes involved in nitrate recycling (loss, oxidation and deposition) are represented in the model, the model should be able to quantify such number of recycling.

We also note that our definition of the number of recyclings was not clear. Indeed, while we referred to the number of recyclings undergone by nitrate at the air/snow interface, our approach was an attempt to calculate the number of recyclings that the archived nitrate underwent and not the recyclings of the nitrate pool within the photic zone. This conceptual difference is essential because the information which can be extracted from ice core are only those hold by the archived nitrate. In the following, we will clarify this point.

After rethinking the issue, it turns out that the calculation of the number of nitrate recyclings is far from evident. As a result, we suggest to remove the calculation of the number of nitrate recyclings from section 1.2 (p6892 L12-26, ACPD version) and to replace it by a discussion later in the text (e.g., in section 3.3). To support our choice, we are addressing Prof. Wolff’s comments and suggestions below.

*When I wrote my main review of this paper, I confessed to some conceptual uncertainty about the meaning of  $\tau_{arch}$ , and some surprise about the number of recyclings estimated by the authors (page 6892, para 2 and many subsequent parts of paper). I have now thought some more about this,, and have convinced myself there is a problem that the authors need to*

address. I hope that others who have considered this problem might come in, either to explain more formally what the correct calculation is, or to explain why I have got it completely wrong.

*Tau-arch* of course can be calculated, and ( $m_{50cm}/FA$ ) is certainly the time it would take to deplete the 50 cm box purely by archiving nitrate. However the authors assert that this is the lifetime of nitrate in the top 50 cm and therefore use this to estimate the number of photochemical recyclings each nitrate ion has undergone.

There must be a misunderstanding here. Indeed, we do not assert that *Tau-arch* is the lifetime of nitrate in the top 50 cm but that it is “the lifetime of nitrate in the top 50 cm against archival” (p6892, L20-21, ACPD version). Therefore, it seems that we agree on this definition:  $Tau\_arch = m_{50cm}/FA$ .

What struck me as odd about this calculation is that is blind to the magnitude of the primary input ( $FPI=FT+FS$ ), or  $f_{exp}$ . So let’s do some thought experiments in which the some of the values in Table 5 are varied, but still within physically allowed ranges. I have included the value of  $m_{50cm}$  and a calculated  $f_{exp}$ . All units are  $mg$  (or  $10^{-6} kg$ )  $N m^{-2}$ , or  $mg N m^{-2} a^{-1}$  as in the paper. Case A is the one in the paper. Cases B and C are the extreme ends of what is possible. In each case the amount in the top 50 cm and the amount archived (FA) are kept the same as in the base case. But FPI is varied between the minimum that allows mass balance (FA), and a very large number. I simply have to alter FE (and hence  $f_{exp}$ ) to balance the calculation.

	A (as in paper)	B	C
$m_{50cm}$	8.3	8.3	8.3
FP	32.00	32.00	32.00
FD	32.16	32.16	32.16
FE	8.04	999.84	0
FA	0.16	0.16	0.16
FPI	8.2	1000	0.16
$f_{exp}$	20%	Close to 100%	0%

Because of the fast photochemistry, the 50 cm firn box and the atmosphere are essentially a single box as far as mixing with the primary input is concerned. In case B there is a huge primary input. When nitrate in the firn is photolyzed, it is quickly swamped by new (FPI) input, and whatever is deposited is almost entirely new input. In this case the lifetime of nitrate in the combined firn/atmosphere box (ignoring the physical transit time for an ion to be advected with the snow from the skin layer to below 50 cm) is close to zero, and all the ions that survive have likely never been recycled (zero recyclings).

Agreed.

In case C on the other hand, the primary input balances FA and the only way an ion can escape the combined box is by being archived. In this case the lifetime in the combined box is indeed 50 years, but that is calculated as  $FP/FPI$ , not as  $FP/FA$  as in the calculation of  $\tau_{arch}$  in the paper. The number of recyclings in this case is very high and may well be 120.

We agree that, in case C,  $\tau_{\text{arch}} = m_{50\text{cm}}/FA \approx 52$  years. We also note that the absence of an export on nitrate ( $FE = 0$ ) leads to the equivalence between the lifetime of nitrate against archival  $\tau_{\text{arch}}$  and the lifetime of  $\text{NO}_y$  in the combined atmosphere/snow box.

In correspondence with Prof. Wolff, he acknowledges that he wrote FP/FPI and FP/FA when he intended  $m_{\text{arch}}/FPI$  and  $m_{\text{arch}}/FA$ .”

*So, here is the point. The lifetime of nitrate (or perhaps I should say of  $\text{NO}_y$ ) in the combined 50cm/atmosphere box is NOT  $m_{50\text{cm}}/FA$ , but  $m_{50\text{cm}}/(FA+FE) = m_{50\text{cm}}/FPI$ , and this is what determines how old the nitrate in the box is and how many recyclings it has experienced. For the base case in the paper this is then of order 1 year and the average number of recyclings will be of order 10 I suppose.*

We thank Prof. Wolff for his demonstration that our assumption and the 120 cycles we report were incorrect. In the ACPD version, here is how we calculated the number of cycles:  $n_{\text{cycles}} = \tau_{\text{arch}} / \tau_{\text{photo}} = FP/FA$ . This choice was made by analogy with our calculation of the number of  $\text{NO}/\text{NO}_2$  cycles before  $\text{NO}_2$  is converted to  $\text{HNO}_3$  (section 1.2). It is now clear that this definition of  $n_{\text{cycles}}$  is not correct. Indeed, it seems unrealistic that this number can be as high as 120. While  $\text{NO}_y$  only remains in the combined 50cm/atmosphere box for one year on average, it is clear also that nitrate archived is older and as suggested by Prof. Wolff, 10 recyclings is probably more realistic.

In his demonstration, Prof. Wolff has to make a simple assumption by considering the photic zone as a single box and his calculation can only give an order of magnitude for the number of recyclings. In detail, this simple assumption ignores the heterogeneity of the photic zone box. The TRANSITS model is the perfect tool to make the correct calculation of the number of recyclings. Below, we suggest another approach to calculate  $n_{\text{cycles}}$  using the TRANSITS model.

*The critical point here is that the lifetime in a box is based on all the processes involved (Jacob 1999, eq 3.1). What we need to know the age of  $\text{NO}_y$  (the sum of nitrate +  $\text{NO}_x$ , for which we don't care about photolysis to  $\text{NO}_x$  except in so much as it mixes the 50 cm and atmosphere box) is, analogous to Jacob's eq 3.1*

$\tau = m_{50\text{cm}}/(F_{\text{out}}+D)$  ( $L$  is zero in this case as there is no chemical loss of  $\text{NO}_y$ ), ie

$\tau = m_{50\text{cm}}/(FE+FA)$ .

*What the authors calculate as  $\tau_{\text{arch}}$  is  $m_{50\text{cm}}/FA$  which is the lifetime against archiving, but is not the one you need to estimate the age of the archived nitrate!*

We agree with Prof. Wolff as long as the photic zone is considered as a single box but this assumption is not true because the snow nitrate age is not homogeneous and 90% of the mass is within the first mm of the photic zone. This heterogeneity in age and concentration forbid the use of a two-box model. This is the reason why TRANSITS was built as a multi-layer model. Put in other words, FPI concerns only the “skin layer”, not the layers below. The lifetime



definition given by Prof. Wolff concerns essentially the lifetime of nitrate within the first top layer. Since this layer contains 90% of the mass, as a first approximation one can consider this lifetime as the lifetime of nitrate for the whole photic zone but in reality, this is not true. A good analogy is the atmosphere where the troposphere and stratosphere cannot be treated as a single box due to the large difference in lifetime within these two compartments. In the case of the photic zone, it is the same: the large heterogeneity between the top and the bottom precludes the use of a single box for the snow. For the DC atmospheric box, the BL is a well-mixed (at least at our time scale) and a single box approximation is valid. Only a multi-layer model can actually calculate the number of recycling as we will show below.

*Please tell me how I am wrong, but I think I am not! I am unsure why your model takes 20 years to equilibrate, but given that it takes around 15 years for surface snow to sink through the 1 meter snow model domain, it may simply be that. If I am right, the paper needs changing in several places including Fig 1, page 6938, 6936 and especially 6892, but the whole paper should be checked for errors based on this.*

### *Calculation of the average number of recyclings undergone by the archived nitrate using the TRANSITS model*

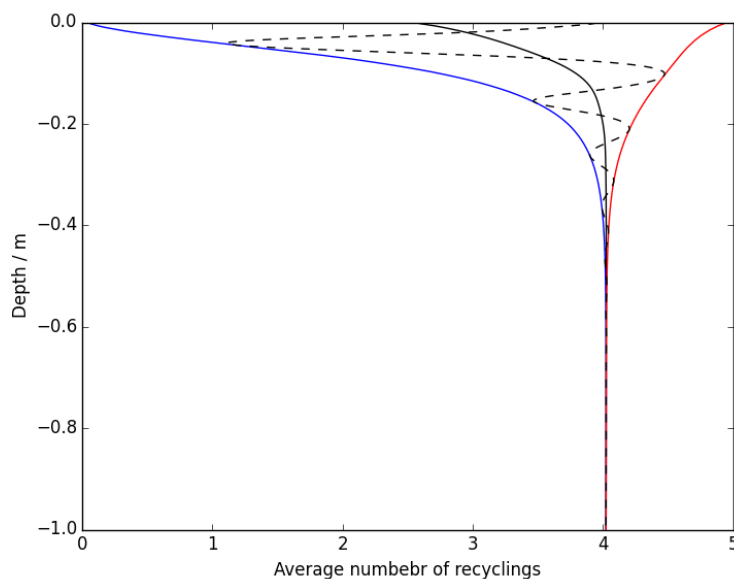
As clarified earlier in this document, we seek an information about the average number of recyclings undergone by the nitrate ions which are actually archived. We acknowledge that the range of number of recyclings undergone by the archive nitrate ions must be wide since some nitrate ions may well have travelled through the entire snowpack zone of active photochemistry without been recycled while some did undergo a lot of recyclings. We recall that one should not confuse “the average number of recyclings at the surface” and “the average number of recyclings of the archived nitrate ions”.

#### Method:

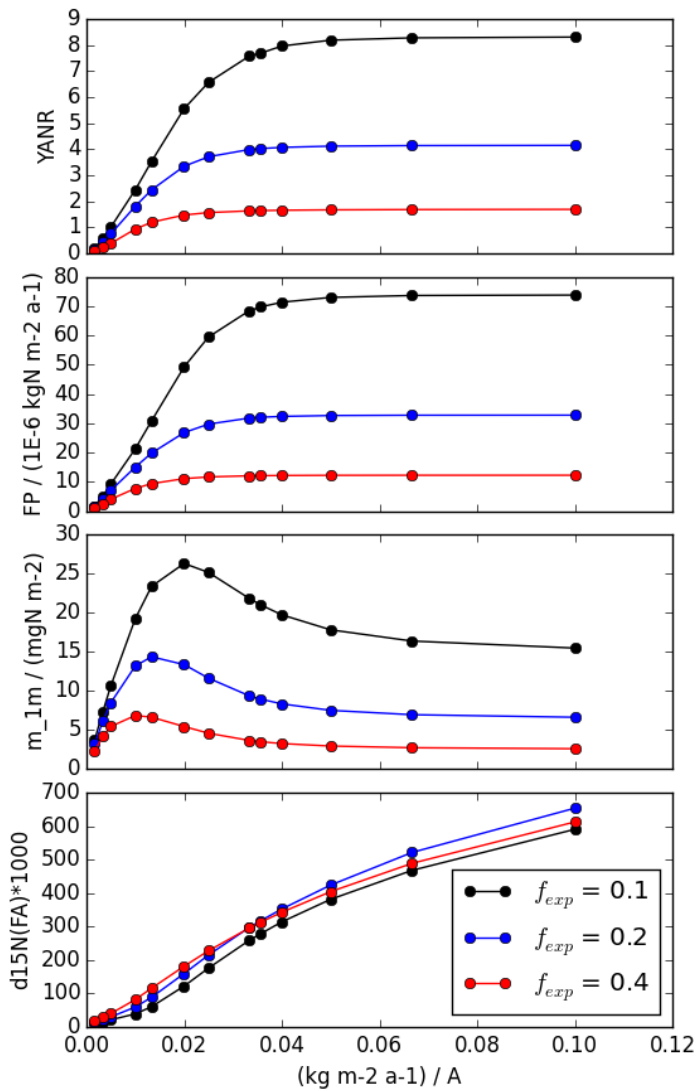
A new tracer, denoted “CYCL”, has been introduced in the TRANSITS model. In a given box (snow layer or atmosphere), *CYCL* represents the average number of recyclings undergone by nitrate in the considered box. The *CYCL* variable follows a numerical treatment which is comparable to that of  $\delta^{15}\text{N}$  and  $\Delta^{17}\text{O}$ , i.e. a “recycling” (instead of an isotopic) mass balances, diffusion and the calculation of *CYCL* values in the macroscopic fluxes (*FP*, *FD*, *FE*, *FA*). The *CYCL* value for primary nitrate is set to 0 and *CYCL* variables in the boxes are incremented by 1 in the only case of the upward crossing of the air-snow interface by  $\text{NO}_2$  molecules (i.e. in the case of every photolytically produced  $\text{NO}_2$  molecules which do not undergo cage effect). Hereafter, *YANR* denotes the “Yearly Average Number of Recyclings” undergone by the archived nitrate. *YANR* is calculated as a mass-weighted average of the *CYCL* values of the 52 snow layers which are archived below 1 m over the course of one year. We have checked that *YANR* is insensitive to the chosen steps for time and space (snow) discretization (approx. one week and 1 mm for the DC realistic simulation, respectively).

For the Dome C simulation, we obtain  $YANR = 4.02$  which means that, on average, the archived nitrate at Dome C has undergone 4.02 recyclings (i.e. loss, local oxidation, deposition). The figure below shows the profile of ANR for summer solstice at Dome C.

The figure below shows the average number of recyclings as a function of depth in the DC realistic simulation. The black line represents the yearly average depth profile which shows that nitrate in the skin layer has undergone 2.6 recyclings on average and that CYCL values quickly increase in the top 20 cm where nitrate photolysis is the most active. The curves in blue and red indicate the yearly minimum and maximum of CYCL as a function of depth. This draws an envelope as observed in the case of the CYCL profile at summer solstice (black dashed line) which shows one-year period oscillations corresponding to the burial of the former “skin layers” which have high CYCL values. The dampening of the CYCL oscillations at depth is the result of nitrate diffusion in the snowpack.



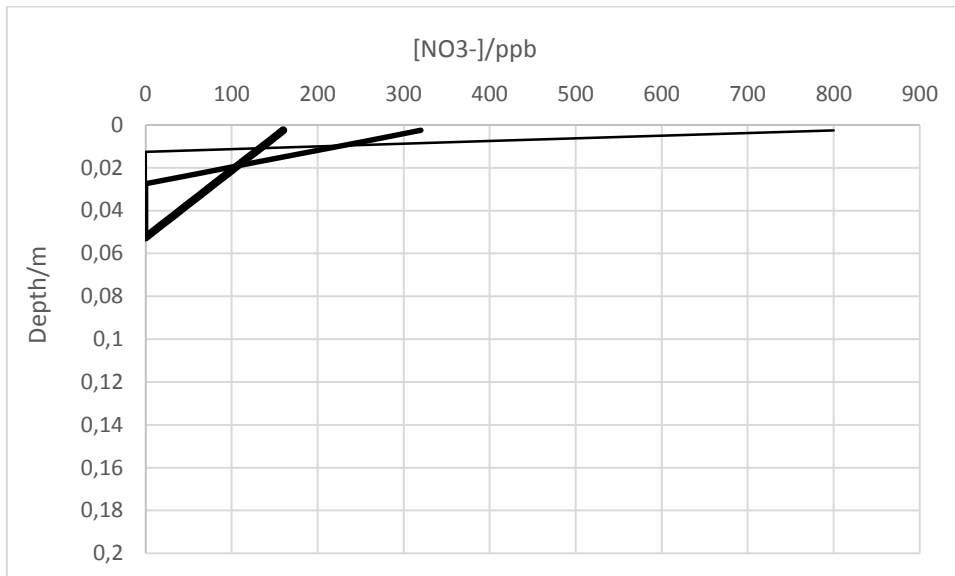
The figure below presents the results of an experiment where the annual snow accumulation rate ( $A$ ) and the export parameter ( $f_{exp}$ ) have been varied. We report  $YANR$ ,  $FP$ ,  $m_{1m}$  (the nitrate mass in the top 1m of the snowpack) and  $d_{15N}(FA)$  in the archived nitrate as a function of the inverse of the snow accumulation rate ( $1/A$ ).



At a given  $f_{exp}$  value and for  $A > 50 \text{ kg m}^{-2} \text{ a}^{-1}$  ( $1/A < 0.02$ ), YANR first linearly increases with the increase in  $1/A$  which means that the burial of snow layers controls nitrate recycling. For low snow accumulation rates ( $A < 20 \text{ kg m}^{-2} \text{ a}^{-1}$ , i.e.  $1/A > 0.05$ ), YANR reaches a plateau at 4.1 in the case where  $f_{exp} = 0.2$  (DC case). The second panel on the above figure shows that YANR and FP have concurring variations. We recall that FPI is kept constant at  $8.2 \times 10^{-6} \text{ kgN m}^{-2} \text{ a}^{-1}$  in these experiments and observe that  $\text{YANR} = \text{FP}/\text{FPI}$ . In this second regime, the burial of snow is no longer limiting and the snowpack control on YANR ceases because nitrate is confined in the top layers (discussed below).

For low snow accumulation rates ( $A < 20 \text{ kg m}^{-2} \text{ a}^{-1}$ , i.e.  $1/A > 0.05$ ), we also observe that FP remains constant, e.g. at  $32.8 \times 10^{-6} \text{ kgN m}^{-2} \text{ a}^{-1}$  for  $f_{exp} = 0.2$ . The reason is that, while the residence time of nitrate in the photic zone increases with the decrease of  $A$  (mass loss increases for a fixed time step), the nitrate concentration profile at depth diminishes (the mass loss decreases for the same time step), so that at the end, FP levels off due to the negative

feedback of the decreasing nitrate concentration. In this extreme case,  $m_{1m}$  does not change significantly (third panel on the figure above). The schematic figure below shows how nitrate distributes with depth with the decrease of  $A$ . The decrease in line thickness represents the decrease in snow accumulation rates ( $A$ ). When  $A$  decreases, most of nitrate gets confined in a layer at the top which becomes thinner.



Our finding of  $YANR = FP/FPI$  is an independent confirmation of the definition given by Davis et al (2008) on the basis of the macroscopic yearly primary and photolytic fluxes: the “Nitrogen Recycling Factor”,  $NRF = \text{ratio of nitrogen emission and nitrogen deposition}$ . While we are satisfied to end up with the Davis et al (2008) expression for  $YANR$  using our independent model-based tracer experiment, we must observe that we define  $YANR$  is the average number of recyclings undergone by the archived nitrate while Davis et al (2008) define it as the “nitrogen recycling factor within a photochemical season”.

In our experiments above, we have observed that a key control on  $FP$  and, thus,  $YANR$  is  $f_{exp}$  which sets the degree of horizontal export of nitrate in the atmosphere. All else being equal, increasing values of  $f_{exp}$  lead to the increase of the exported flux ( $FE$ ), to the lower incorporation of atmospheric nitrate to the snow and, in turn, to lower  $FP$  values.

### Conclusions:

From this small study, it seems that the average number of recyclings undergone by the archived nitrate at Dome C is around 4.02. This value seems more reasonable than the value 120 we have calculated previously. We recall that our definition of  $YANR$  was wrong in the ACPD version of the paper and led to this false value. If Prof. Wolff agrees with our approach to calculate  $YANR$ , we suggest:

1. to remove the reference in the calculation of the number of recyclings in the introduction (second paragraph of section 1.2)
2. to remove the mention of a number of cycles of 120 (and of course 150) in the text
3. to update figures 1 and 11

4. to incorporate the results and discussion of the above small study in section 3.3 where we discuss the model results.

### *Note on the time for the model to reach equilibrium*

In the paper we state that the model takes 20 years to equilibrate. Given that it takes approximately 10 years for a surface layer to get buried below 1m depth in conditions close to DC conditions ( $A = 30 \text{ kg m}^{-2} \text{ a}^{-1}$  and  $\rho = 300 \text{ kg m}^{-3}$ ), why are those two numbers different?

In order to get an objective view on the time to equilibrium (hereafter denoted “TTE”), we simulate a “spike” of nitrate in the atmospheric box. In the middle of summer, a nitrate mass equivalent to one year of nitrate input (FPI) is deposited to the top layer. We could label this nitrate with a very special isotope signature but we can also simply monitor the time the archived nitrate mass takes to reach equilibrium after the “spike nitrate” has escaped below 1m.

The sudden nitrate mass which adds up to the atmospheric box is simulated as follows:

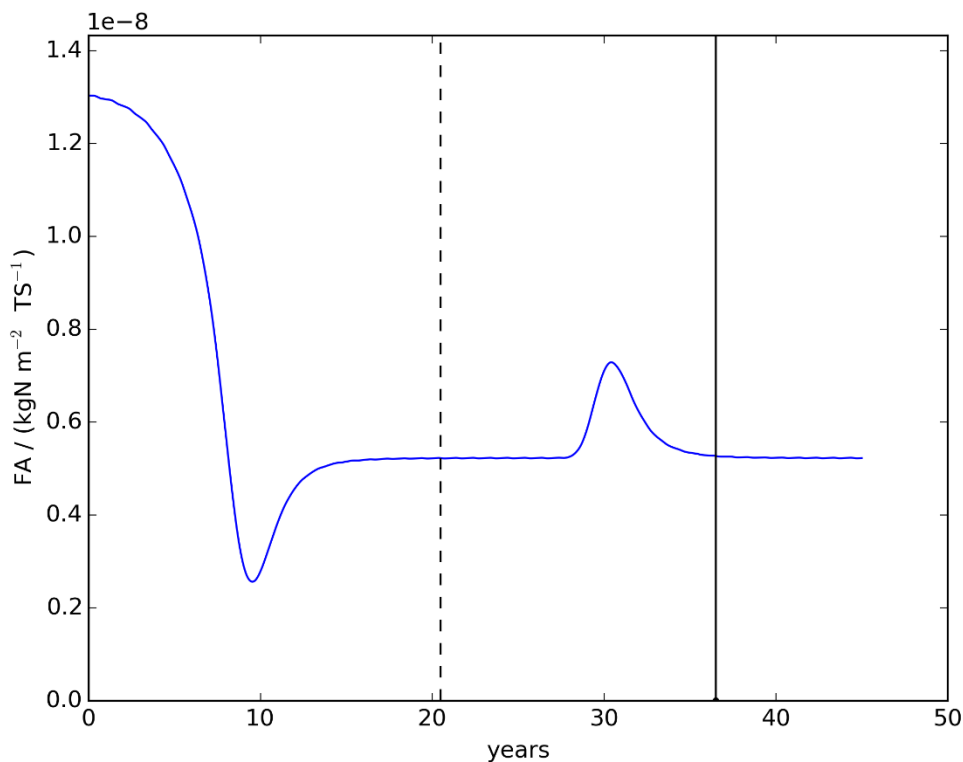
- mass =  $8.2 \cdot 10^{-6} \text{ kgN m}^{-2}$  (same as one year in a week)
- Sudden mass gain happens after 20 years of computation when the model has reached stability and at summer solstice (time step 26)

The model is used in DC conditions:

- $\Phi = 0.026$
- $\text{Diff} = 1.33 \cdot 10^{-11} \text{ cm}^2 \text{ s}^{-1}$
- To simplify, we use  $A = 30 \text{ kg m}^{-2} \text{ a}^{-1}$
- $\rho = 300 \text{ kg m}^{-3}$

The residence time of nitrate in the top 1m of the modeled snowpack is the average time for the nitrate ions from the spike to get below 1m. However, when it comes to looking at equilibrium, we look for the time it takes to – ideally – archive 100% of the nitrate ions from the spike. To calculate this duration, we observe the time when the archived mass (FA) is getting back to its “equilibrium value” within 1%.

Below is an example with the DC case described above (Case 1 in table below). The y-axis represents the nitrate mass which is archived below 1m at every time step. The x-axis represents the time (in years) after the beginning of the computation. The first phase (0-20 years) shows the equilibration of the model. The vertical dashed line represents the time when the sudden nitrate mass adds up in the atmosphere (i.e. after  $20 + 26/52 = 20.5$  years). The vertical line to the right represents the time when FA gets back within +/- 1% of the “equilibrium value” (i.e. approx.  $5 \cdot 10^{-9} \text{ kgN m}^{-2} \text{ TS}^{-1}$ ). In this case, the “spike nitrate” took 16 years to fully escape the photic zone. We also observe that the very first ions originating from this “spike nitrate” archive 8 years only after deposition, which means, faster than the snow (10 years). This results from the nitrate diffusion in the snowpack.



We have investigate 2 other cases as depicted in the table below.

	Local recycling	Diffusion	Photolysis	TTE / years
1	Yes, $f_{exp} = 0.2$	$1.33 \cdot 10^{-11}$	0.026	16
2	Yes, $f_{exp} = 0.2$	No	No	11
3	Yes, $f_{exp} = 0.2$	No	0.026	16

Case 1 represents the conditions for the run displayed in the above figure. Case 2 represents the case where there is no photolysis and no diffusion. In this case, nitrate archives at the same rate as snow does and the TTE value (11 years) compares well with the residence time which is calculated ( $1m / (A / \rho) = 10$  years). Note, that the TTE value is an approximation which is overestimated given the way we calculate it.

The comparison of cases 1 and 2 shows that the photolytic and diffusion processes lead to a TTE which is increased by 5 years. In case 3, the diffusion process is switched off and we observe that the TTE is not changed. This shows that the N recycling initiated by nitrate photolysis is mostly responsible for the observed 5-year delay. In other words, the 6.4 recyclings undergone by the archived nitrate induces a 5-years delay in its burial.

Our observation in case 1 explains why the model takes almost 20 years to equilibrate. Note that the 20-year value reported in the ACPD version of the paper was an approximate value.

At last, we note that the experiment presented here could be helpful to discuss the potential archive of the nitrate production effects of Solar Proton Events (SPE) in Antarctic plateau firn and ice (see discussion in (Wolff, Jones, Bauguitte, & Salmon, 2008)). The small study above

for example shows that a fraction of the nitrate mass brought by a SPE could potentially be archived. Measuring  $\delta^{15}\text{N}$ ,  $\delta^{18}\text{O}$  and  $\delta^{17}\text{O}$  profiles in this archived nitrate could potentially help assessing whether or not an archived spike originates from a SPE. Of course, this is out of the scope of the present paper.

## References

- Davis, D. D., Seelig, J., Huey, G., Crawford, J., Chen, G., Wang, Y., . . . Eisele, F. (2008). A reassessment of Antarctic plateau reactive nitrogen based on 2003 airborne and ground based measurements. *Atmos. Environ.*, *42*, 2831-2848.
- Wolff, E. W., Jones, A. E., Bauguitte, S. J.-B., & Salmon, R. A. (2008). The interpretation of spikes and trends in concentration of nitrate in polar ice cores, based on evidence from snow and atmospheric measurements. *Atmos. Chem. Phys.*, *8*, 5627-5634.

## Changes brought to the TRANSITS model and additional changes brought to the manuscript after the review process

### Diffusion calculation

Currently, the model runs at a time step ( $\Delta t$ ) of one approx. one week and the diffusion routine runs at a time step ( $\Delta t_{\text{short}}$ ) of 4 hours. In order to scale this routine to the main time step and allow the model to be used in different conditions, the ratio  $\Delta t/\Delta t_{\text{short}} = 50$  has been introduced in the model. In this case,  $\Delta t_{\text{short}} \approx 3.4$  hours. This modification does not change the results of our study. Indeed, the time step for the diffusion routine must be short enough to allow convergence.

We have edited the text which now writes: “Nitrate diffusion is assumed to occur in the snowpack and is solved at a time resolution 50 times shorter than the model main time resolution (i.e. approx. 3.4 hours)” and, later in the text “Equation (14) is solved at a time step of 3.4 hours”.

### Description of D17O(OH).

A number of errors have been made in the calculation of D17O(OH). First, a detailed reading of Kukui et al. (2014) indicates that HONO may contribute much less than 56% to the formation of OH because real HONO concentrations may be decreased by a factor 4 to provide a good match between modeled and measured HOx. Second, the calculation of D17O(OH) requires that of  $\beta = \frac{\sum_i L_i}{\sum_i L_i + k_{\text{HO}+\text{H}_2\text{O}} [\text{OH}][\text{H}_2\text{O}]}$ , a parameter which accounts for the competition of the isotopic exchange reaction with the OH sink reactions. Under the cold DC conditions,  $\beta$  is significantly different from 0 and  $\text{D17O(OH)} = \beta * \text{D17O(OH, prod)}$  shows that D17O(OH) will hold a fraction of the 17O-excess value set by its production channels.

In the frame of the OPALE campaign, D17O(OH) has been discussed in a submitted paper (Savarino et al., submitted to OPALE Special Issue, ACPD). The results of this study show that D17O(OH) varies in a narrow range, between 1 and 3 ‰, around summer solstice 2011-2012. We have changed the model to account for the changes described above. The text has been changed as follows:

“In the frame of the OPALE campaign,  $\Delta^{17}\text{O(OH)}$  has been discussed in a submitted paper (Savarino et al., in prep.). The results of this study show that  $\Delta^{17}\text{O(OH)}$  varies in a narrow range, between 1 and 3 ‰, around summer solstice 2011-2012. As a result, we set  $\Delta^{17}\text{O(OH)} = 3\text{‰}$  throughout the entire sunlit season”.

Since the variable  $\Delta^{17}\text{O(OH)}$  is introduced in the model, we will consider it for the sensitivity tests and when discussing the contributors to D17O(FA, corr.) (section 4).

### Diffusion coefficient as an adjustment parameter

In the model version used for the ACPD version of the paper, we made a mistake in not converting units in  $\text{cm}^2 \text{s}^{-1}$  from (Thibert & Domine, 1998) into  $\text{m}^2 \text{s}^{-1}$  in the expression of the



diffusivity coefficient ( $D$ ). As a result, a value of  $D$  four orders of magnitude higher than the Thibert & Domine value must be used in order to reproduce realistic nitrate profiles at depth. We note that this diffusion coefficient was measured on a single monocrystal of ice and thus do not take into account the complex polycrystalline nature of the snow, but most obviously the diffusion coefficient does not include the diffusivity of  $\text{HNO}_3$  in the interstitial air pack (see below).

In the current revised version of the TRANSITS model, we now use  $D$ , the  $\text{HNO}_3$  diffusion coefficient, as an adjustment parameter. Using a value of  $D = 1.0 \times 10^{-11} \text{ m}^2 \text{ s}^{-1}$  allows to obtain smooth nitrate profiles consistently with the observations.

In section 3.3.1, we discuss the  $D$  value and compare it to the literature. The adjusted value is almost 4 orders of magnitude higher than the diffusion coefficient of solid solution of  $\text{HNO}_3$  in ice which is  $2.6 \times 10^{-15} \text{ m}^2 \text{ s}^{-1}$  for DC summertime conditions ( $T=244 \text{ K}$ , Kukui et al., 2014) (Thibert et al., 1998).

$\text{HNO}_3$  is a sticky gas and its effective diffusivity in snow (denoted  $D_{\text{eff}}$ ) can be calculated as in Herbert et al. (2006) and by assuming that the snow layers are always under-saturated in nitrate. The  $D_{\text{eff}}$  coefficient is a function of the diffusivity of  $\text{HNO}_3$  in the interstitial air which depends on temperature and pressure (Massmann, 1998). Using a Surface Specific Area of snow of  $38 \text{ m}^2 \text{ kg}^{-1}$  (Gallet et al., 2011), a snow density of  $300 \text{ kg m}^{-3}$ , median temperature and pressure for DC summer 2012 (Kukui et al., 2014) and a partition coefficient in the uptake of  $\text{HNO}_3$  on ice (Crowley et al., 2010), we find  $D_{\text{eff}} = 7.3 \times 10^{-12} \text{ m}^2 \text{ s}^{-1}$ , a value close to the adjusted value.

The paper has been changed as follows:

- $D$  is now an adjustment parameter set to  $1.0 \times 10^{-11} \text{ m}^2 \text{ s}^{-1}$  (Figure 3 and Table 3 are modified accordingly)
- Sensitivity tests were modified (Figure 10 is changed)
- We have added the following text in section 3.3.1 to discuss the choice of the value  $1.0 \times 10^{-11} \text{ m}^2 \text{ s}^{-1}$  for  $D$ :

“Nitric acid is a sticky gas and its effective diffusivity in snow (denoted  $D_{\text{eff}}$ ) can be calculated as in Herbert et al. (2006) and by assuming that the snow layers are always under-saturated in nitrate. The  $D_{\text{eff}}$  coefficient is a function of the diffusivity of  $\text{HNO}_3$  in the interstitial air which depends on temperature and pressure (Massmann, 1998). Using a Surface Specific Area of snow of  $38 \text{ m}^2 \text{ kg}^{-1}$  (Gallet et al., 2011), a snow density of  $300 \text{ kg m}^{-3}$ , median temperature and pressure for DC summer 2012 (Kukui et al., 2014) and a partition coefficient in the uptake of  $\text{HNO}_3$  on ice (Crowley et al., 2010), we find  $D_{\text{eff}} = 7.3 \times 10^{-12} \text{ m}^2 \text{ s}^{-1}$ , a value very close to our chosen value for  $D$  ( $1.0 \times 10^{-11} \text{ m}^2 \text{ s}^{-1}$ ) which means that the macroscopic mobility of nitrate in the snowpack is mostly the consequence of  $\text{HNO}_3$  mobility. We recall that our description of nitrate diffusion in the snowpack is basic and that the picture may well be more complicated with, e.g. wind pumping effects.”

On the use of the (Brizzi, et al., 2009) reference

In the ACPD version of the paper, we referred to (Brizzi, et al., 2009) in which atmospheric H<sup>15</sup>NO<sub>3</sub>/H<sup>14</sup>NO<sub>3</sub> isotope ratio profiles were measured by the Earth observation instrument MIDAS operated onboard of the Environmental Satellite (ENVISAT). On the basis of that work, we attempted to provide an additional constrain on the d<sup>15</sup>N(FS) value.

We acknowledge that we have misread Figure 5h in (Brizzi, et al., 2009). Indeed, HNO<sub>3</sub> at 15 km above South Pole at summer solstice has a d<sup>15</sup>N value of (210 ± 40) ‰ and not (21 ± 4) ‰.

It seems that (Brizzi, et al., 2009) cannot be directly used to constrain d<sup>15</sup>N(FS) and the reason is threefold. First, we note that uncertainties in the reported profiles are important even at altitudes where most HNO<sub>3</sub> seems to be observed (from 15 to 25 km). Second, there is no winter profile reported. Third, further assumptions must be made to derive d<sup>15</sup>N values in the condensed nitric acid from the d<sup>15</sup>N values in the gaseous HNO<sub>3</sub>.

As a consequence, we decide not to refer to the work from (Brizzi, et al., 2009) in the final version of this paper. We recall that the reference to (Savarino, Kaiser, Morin, Sigman, & Thieme, 2007) already allows us to provide a constrain on d<sup>15</sup>N(FS).

## On the structure of the paper

In their quick reports, the reviewers suggested to reorganize the manuscript and to put information in appendixes. We acknowledge that the paper is long and that we should have wrote, ideally, two different papers (1. model description/validation, 2. Framework for the interpretation of ice cores). In this stage and given our schedule with this publication, we unfortunately won't be able to split the paper and we now have to live with its length.

Sadly, we do not see how to reorganize the paper without having the reader going back and forth from the main text to appendixes where some information would sit. Therefore, we would like to keep the main text as it is and not to move information to appendixes. However, we have worked on a better organization of Section 3 as advised by Anonymous Reviewer #1.

Below are most changes to the structure of the paper:

- 1. Introduction :
  - The sub-sections have been removed
  - Former section 1.3 has been removed. The important material has been moved to the appropriate parts of section 2 (model description)
  - Figure 1 has been removed
- 2. Description of the TRANSITS model
  - Structure unchanged
- 3. "Model setup, runs and evaluation" renamed to "Model evaluation"
  - 3.1 "Method" renamed to Method: observational constraints, model setup and runs
  - 3.3 "Evaluation and discussion" reorganized as follows:

- 3.3.1 “Validation of the mass loss, diffusion and  $^{15}\text{N}/^{14}\text{N}$  fractionation process”
- 3.3.2 “Validation of the cage effects”
- 3.3.3 “Validation of the macroscopic fluxes”
- 3.3.4 “Validation of the residence time in the photic zone and calculation of the average number of recyclings”
- 3.3.5 “Validation of the nitrate mass in each compartment”
- 3.3.6 “Validation of the  $\delta^{15}\text{N}$  values in each compartment”
- 3.3.7 “Photolytically-driven dynamic equilibrium at the air-snow interface”
- 3.3.8 “On the discrepancies between simulated and observed  $\Delta^{17}\text{O}$  values”

## References:

- Atkinson, R., Baulch, D. L., Cox, R. A., Crowley, J. N., Hampson, R. F., Hynes, R. G., . . . Troe, J. (2004). Evaluated kinetic and photochemical data for atmospheric chemistry: Volume I - gas phase reactions of Ox, HOx, NOx and SOx species. *Atmos. Chem. Phys.*, *4*, 1461-1738.
- Brizzi, G., Arnone, E., Carlotti, M., Dinelli, B. M., Flaud, J.-M., Papandrea, E., . . . Ridolfi, M. (2009). Retrieval of atmospheric  $\text{H}^{15}\text{NO}_3/\text{H}^{14}\text{NO}_3$  isotope ratio profile from MIPAS/ENVISAT limb-scanning measurements. *J. Geophys. Res.*, *114*(D16301). doi:10.1029/2008JD011504
- Crowley, J. N., Ammann, M., Cox, R. A., Hynes, R. G., Jenkin, M. E., Mellouki, A., . . . Wallington, T. J. (2010). Evaluated kinetic and photochemical data for atmospheric chemistry: Volume I - heterogeneous reactions on solid substrates. *Atmos. Chem. Phys.*, *10*, 9059-9223.
- Gallée, H., Preunkert, S., Argentini, S., Frey, M. M., Genthon, C., Jourdain, B., . . . Legrand, M. (2014). Characterization of the boundary layer at Dome C (East Antarctica) during the OPAL summer campaign. *Atmos. Chem. Phys. Disc.*, *14*, 33089-33116.
- Herbert, B., Halsall, C., Jones, K., & Kallenborn, R. (2006). Field investigation into the diffusion of semi-volatile organic compounds into fresh and aged snow. *Atmos. Environ.*, *40*(8), 1385-1393.
- Kukui, A., Legrand, M., Preunkert, S., Frey, M. M., Loisil, R., Gil Roca, J., & Jourdain, B. (2014). Measurements of OH and RO<sub>2</sub> radicals at Dome C, East Antarctica. *Atmos. Chem. Phys.*, *14*, 12373–12392. doi:10.5194/acp-14-12373-2014
- Massmann, W. J. (1998). A review of the molecular diffusivities of  $\text{H}_2$ ,  $\text{CO}_2$ ,  $\text{CH}_4$ ,  $\text{CO}$ ,  $\text{O}_3$ ,  $\text{SO}_2$ ,  $\text{NH}_3$ ,  $\text{N}_2\text{O}$ ,  $\text{NO}$ , and  $\text{NO}_2$  in air,  $\text{O}_2$  and  $\text{N}_2$  near  $\{\text{STP}\}$ . *Atmos. Environ.*, *32*(6), 1111-1127.
- Morin, S., Sander, R., & Savarino, J. (2011). Simulation of the diurnal variations of the oxygen isotope anomaly ( $\Delta^{17}\text{O}$ ) of reactive atmospheric species. *Atm. Chem. Phys.*, *11*(8), 3653-3671.

Savarino, J., Kaiser, J., Morin, S., Sigman, D. M., & Thieme, M. H. (2007). Nitrogen and oxygen isotopic constraints on the origin of atmospheric nitrate in coastal Antarctica. *Atmos. Chem. Phys.*, 7, 1925-1945.

Thibert, E., & Domine, F. (1998). Thermodynamics and kinetics of the solid solution of  $\text{HNO}_3$  in ice. *J. Phys. Chem. B*, 102, 4432-4439.

1 **Air-snow transfer of nitrate on the East Antarctic plateau –**  
2 **Part 2: An isotopic model for the interpretation of deep ice-**  
3 **core records**

4  
5 **J. Erbland<sup>1,2</sup>, J. Savarino<sup>1,2</sup>, S. Morin<sup>3</sup>, J.L. France<sup>4,5</sup>, M.M. Frey<sup>6</sup>, M.D. King<sup>4</sup>**

6 [1] {Université Grenoble Alpes, LGGE, F-38000 Grenoble, France }

7 [2] {CNRS, LGGE, F-38000 Grenoble, France }

8 [3] {Météo-France - CNRS, CNRM – GAME UMR 3589, CEN, Grenoble, France }

9 [4] {Department of Earth Sciences, Royal Holloway University of London, Egham, Surrey,  
10 TW20 0EX, UK }

11 [5] {Now at School of Environmental Sciences, University of East Anglia, Norwich, NR4 7TJ,  
12 United Kingdom }

13 [6] {British Antarctic Survey, Natural Environment Research Council, Cambridge, UK }

14 Correspondence to: J. Savarino (joel.savarino@ujf-grenoble.fr)

15

16 **Abstract**

17 Unraveling the modern budget of reactive nitrogen on the Antarctic plateau is critical for the  
18 interpretation of ice core records of nitrate. This requires accounting for nitrate recycling  
19 processes occurring in near surface snow and the overlying atmospheric boundary layer. Not  
20 only concentration measurements, but also isotopic ratios of nitrogen and oxygen in nitrate,  
21 provide constraints on the processes at play. However, due to the large number of intertwined  
22 chemical and physical phenomena involved, numerical modelling is required to test hypotheses  
23 in a quantitative manner. Here we introduce the model “TRansfer of Atmospheric Nitrate Stable  
24 Isotopes To the Snow” (TRANSITS), a novel conceptual, multi-layer and one-dimensional  
25 model representing the impact of processes operating on nitrate at the air-snow interface on the  
26 East Antarctic plateau, in terms of concentrations (mass fraction) and ~~the~~ nitrogen ( $\delta^{15}\text{N}$ ) and  
27 oxygen isotopic composition ( $^{17}\text{O}$ -excess,  $\Delta^{17}\text{O}$ ) in nitrate. At the air-snow interface at Dome  
28 C (DC,  $75^{\circ}06'\text{S}$ ,  $123^{\circ}19'\text{E}$ ), the model reproduces well the values of  $\delta^{15}\text{N}$  in atmospheric and

1 surface snow (skin layer) nitrate as well as in the  $\delta^{15}\text{N}$  profile in DC snow including the  
2 observed extraordinary high positive values (around +300 ‰) below 20 cm. The model also  
3 captures the observed variability in nitrate mass fraction in the snow. While oxygen data are  
4 qualitatively reproduced at the air-snow interface at DC and in East Antarctica, the simulated  
5  $\Delta^{17}\text{O}$  values underestimate the observed  $\Delta^{17}\text{O}$  values by a few several ‰. This is explained by  
6 the simplifications made in the description of the atmospheric cycling and oxidation of  $\text{NO}_2$ : as  
7 well as by our lack of understanding of the  $\text{NO}_x$  chemistry at Dome C. The model reproduces  
8 well the sensitivity of  $\delta^{15}\text{N}$ ,  $\Delta^{17}\text{O}$  and the apparent fractionation constants ( $^{15}\epsilon_{\text{app}}$ ,  $^{17}\epsilon_{\text{app}}$ ) to the  
9 snow accumulation rate. Building on this development, we propose a framework for the  
10 interpretation of nitrate records measured from ice cores. Measurement of nitrate mass fractions  
11 and  $\delta^{15}\text{N}$  in the nitrate archived in an ice core, may be used to derive information about past  
12 variations in the total ozone column and/or the primary inputs of nitrate above Antarctica as  
13 well as in nitrate trapping efficiency (defined as the ratio between the archived nitrate flux and  
14 the primary nitrate input flux). The  $\Delta^{17}\text{O}$  of nitrate could then be corrected from the impact of  
15 cage recombination effects associated with the photolysis of nitrate in snow. Past changes in  
16 the relative contributions of the  $\Delta^{17}\text{O}$  in the primary inputs of nitrate and the  $\Delta^{17}\text{O}$  in the locally  
17 cycled  $\text{NO}_2$  and that inherited from the additional O atom in the oxidation of  $\text{NO}_2$  could then  
18 be determined. Therefore, information about the past variations in the local and long range  
19 processes operating on reactive nitrogen species could be obtained from ice cores collected in  
20 low accumulation regions such as the Antarctic plateau.

21

## 22 **1 Introduction**

23 Ice cores from the East Antarctic plateau provide long-term archives of Earth's climate and  
24 atmospheric composition such as past relative changes in local temperatures and global  
25 atmospheric  $\text{CO}_2$  levels (EPICA community members, 2004, for example). Soluble impurities  
26 have been used in such cores as tracers of biogeochemical processes. As the end product of the  
27 atmospheric oxidation of  $\text{NO}_x$  ( $\text{NO} + \text{NO}_2$ ), nitrate ( $\text{NO}_3^-$ ) is a major ion found in Antarctic  
28 snow (Wolff, 1995). Its primary origins are a combination of inputs from the stratosphere and  
29 from low latitude sources (Legrand and Delmas, 1986; Legrand and Kirchner, 1990).  
30 Stratospheric inputs of nitrate are believed to be mostly caused by the sedimentation of Polar  
31 Stratospheric Clouds (PSCs) in winter (Seinfeld and Pandis, 1998; Jacob, 1999). The  
32 interpretation of nitrate deep ice-core records remains elusive (e.g. Wolff et al., 2010) mainly

1 because its deposition to the snow is not irreversible (Traversi et al., 2014 and references  
2 therein) at low accumulation sites such as Dome C or Vostok (78°27'S, 106°50'E, elevation  
3 3488 m.a.s.l.).

#### 4 ~~—~~ Nitrate recycling

5 Nitrate loss from snow can occur through the physical release of HNO<sub>3</sub> (via evaporation and/or  
6 desorption, also referred to as simply “evaporation”) or through the UV-photolysis of the NO<sub>3</sub><sup>-</sup>  
7 ion (Röthlisberger et al., 2000). At wavelengths ( $\lambda$ ) below 345 nm, NO<sub>3</sub><sup>-</sup> photolyses to form  
8 NO<sub>2</sub> (Chu and Anastasio, 2003) or NO<sub>2</sub><sup>-</sup> ion (Chu and Anastasio, 2007) which can form HONO  
9 at pH < 7. Nitrate photolysis is quantitatively represented by its rate constant ( $J$ ) expressed as  
10 follows:

$$11 \quad J = \int \Phi(\lambda, T) \sigma(\lambda, T) I(\lambda, \theta, z) d\lambda \quad (1)$$

12 with  $\Phi$  the quantum yield,  $\sigma$  the absorption cross section of NO<sub>3</sub><sup>-</sup>,  $I$  the actinic flux,  $\lambda$  the  
13 wavelength,  $T$  the temperature,  $\theta$  the solar zenith angle and  $z$  the depth. Two recent laboratory  
14 studies have investigated nitrate photolysis in DC snow. Meusinger et al. (2014) have reported  
15 the quantum yields for the photolysis of either photolabile or buried nitrate. The terms  
16 “photolabile” and “buried” were introduced by Meusinger et al. (2014) as different “domains”,  
17 i.e. different physico-chemical properties of the region around the nitrate chromophore.  
18 Berhanu et al. (2014a) have reported the absorption cross-section of <sup>14</sup>NO<sub>3</sub><sup>-</sup> and <sup>15</sup>NO<sub>3</sub><sup>-</sup> in  
19 Antarctic snow at a given temperature, using a new semi-empirical zero point energy shift  
20 ( $\Delta ZPE$ ) model.

21 Nitrate deposition to the snow can occur through various mechanisms including co-  
22 condensation and dry deposition (Röthlisberger et al., 2000; Frey et al., 2009). Within the  
23 snowpack, nitrate can be contained as HNO<sub>3</sub> in the gas phase, adsorbed on the surface or  
24 dissolved in the snow ice matrix. It can be exchanged between these compartments by  
25 adsorption, desorption or diffusion processes (Dominé et al., 2007) which can lead to a  
26 redistribution of nitrate inside the snowpack, a process which tends to smooth the nitrate mass  
27 fraction profiles (Wagenbach et al., 1994). Phase change and recrystallization processes (snow  
28 metamorphism) can further promote the mobility of nitrate thus potentially modify~~ing~~  
29 the location of nitrate (Dominé and Shepson, 2002; Kaempfer and Plapp, 2009), with implications  
30 for its availability for photolysis and desorption processes (Dominé and Shepson, 2002). For  
31 instance, it is more available for photolysis when adsorbed on the snow ice matrix surface where

1 cage recombination effects are less likely to occur (Chu and Anastasio, 2003; Meusinger et al.,  
2 2014 and references therein).

3 The photolysis of nitrate has been identified to be an important mechanism for nitrate mass loss  
4 in the snow on the Antarctic plateau (Frey et al., 2009; France et al., 2011). ~~OneAs a~~  
5 consequence ~~of~~ the release of nitrogen oxides through this process ~~is the leads to a~~ complex  
6 recycling of nitrate at the air-snow interface (Davis et al., 2008). Here we refer to “nitrate  
7 recycling” as the combination of ~~nitrate photolysis in snow and the~~  $\text{NO}_x$  production ~~from nitrate~~  
8 ~~photolysis in snow of~~  $\text{NO}_x$ , the subsequent atmospheric ~~processing and oxidation of~~  $\text{NO}_x$  to form  
9 ~~gas phase chemistry to form~~ atmospheric nitrate ~~from~~  $\text{NO}_x$ , ~~the its partial dry or wet~~ deposition  
10 ~~(dry and/or wet-) of a fraction of the producte~~ and the export of ~~another fraction the remaining~~.  
11 Davis et al. (2008) and Frey et al. (2009) suggested the following conceptual model for nitrate  
12 recycling in the atmosphere-snow system for the Antarctic plateau where annual snow  
13 accumulation rates are low. The stratospheric component of nitrate is deposited to the surface  
14 in late winter, in a shallow surface snow layer of approximately uniform concentration  
15 (Savarino et al., 2007). The increase in surface UV radiation in spring initiates a photolysis-  
16 driven redistribution process of  $\text{NO}_3^-$ , which continues throughout the sunlit season resulting in  
17 the almost complete depletion of the bulk snow nitrate reservoir. In summer, this results in a  
18 strongly asymmetric distribution of total  $\text{NO}_3^-$  within the atmosphere-snow column as  
19 previously noted by Wolff et al. (2002), with the majority of the mass of nitrate residing in a  
20 “skin layer” (the top mm of snow, often under form of surface hoar) and only a small fraction  
21 in the atmospheric column above it or in the snow below.

Mis en forme : Indice

Mis en forme : Indice

#### 22 4.1— Nitrogen cycles overlapping at the air-snow interface at Dome C

23 ~~The second cycle concerns~~  $\text{NO}_3^-$  ~~in the snow photic zone (the zone of active photochemistry),~~  
24 ~~which corresponds to ca. 50 cm, i.e. 3 times the observed typical e-folding depth (France et al.,~~  
25 ~~2011), a depth below which 95% of the UV radiation is lost. There, it accumulates by deposition~~  
26 ~~of atmospheric  $\text{HNO}_3$  and is removed by UV photolysis or is “archived” below the photic zone.~~  
27 ~~The lifetime of nitrate in the top 50 cm against photolysis can be calculated as  $\tau_{\text{photo}}(\text{NO}_3^-) =$~~   
28  ~~$m_{50\text{cm}}(\text{NO}_3^-) / F(\text{NO}_2)$  (section 3.1.1 in Jacob, 1999), with  $m_{50\text{cm}}(\text{NO}_3^-)$  the integrated mass of~~  
29 ~~nitrate per unit horizontal surface area in the top 50 cm of the snowpack and  $F(\text{NO}_2)$ , the annual~~  
30 ~~potential flux of photolytically produced  $\text{NO}_2$  per unit horizontal surface area. The lifetime of~~  
31 ~~nitrate in the top 50 cm against archival can be calculated as  $\tau_{\text{arch}}(\text{NO}_3^-) = m_{50\text{cm}}(\text{NO}_3^-) / FA$~~   
32 ~~(Jacob, 1999), with  $FA$ , the archived nitrate mass flux per unit horizontal surface area. Using~~

Mis en forme : Surlignage



1 representative annual values for the above physical (potential NO<sub>2</sub> flux, France et al., 2011;  
2 updated  $\Phi$  value, Meusinger et al., 2014; archived nitrate flux, Frey et al., 2009, Erbland et al.,  
3 2013.), it is found that nitrate in snow is cycled on average  $\approx$  120 times in the snow photic zone  
4 before being buried below the photic zone.

#### 5 4.1— Isotopic signatures of processes involved in nitrate recycling

6 The post-depositional processes as described above thus strongly imprint the stable isotopic  
7 composition of nitrate in snow at low accumulation sites (Blunier et al., 2005, Frey et al., 2009,  
8 Erbland et al., 2013). Nitrate is composed of N and O atoms and has the following stable isotope  
9 ratios: <sup>15</sup>N/<sup>14</sup>N, <sup>17</sup>O/<sup>16</sup>O and <sup>18</sup>O/<sup>16</sup>O, from which isotopic enrichment values  $\delta^{15}\text{N}$ ,  $\delta^{17}\text{O}$ ,  $\delta^{18}\text{O}$   
10 can be computed. The  $\delta$  scale is defined as  $\delta = R_{\text{spl}}/R_{\text{ref}} - 1$  with  $R$  denoting the isotope ratios,  
11 the references being N<sub>2</sub>-AIR for N and VSMOW for O. The quantification of the integrated  
12 isotopic effects of post-depositional processes is achieved by calculating apparent fractionation  
13 constants (<sup>15</sup> $\epsilon_{\text{app}}$ , <sup>17</sup> $\epsilon_{\text{app}}$  and <sup>18</sup> $\epsilon_{\text{app}}$ ) from isotopic and mass fraction profiles of nitrate in the top  
14 decimeters of snow (Blunier et al., 2005, Frey et al., 2009, Erbland et al., 2013). For instance,  
15 <sup>15</sup> $\epsilon_{\text{app}}$  is calculated from the following equation, which represents a Rayleigh model and assumes  
16 a single loss process and the immediate and definitive removal of the lost nitrate fraction:

$$17 \ln(\delta^{15}\text{N}_f + 1) = {}^{15}\epsilon_{\text{app}} \cdot \ln f + \ln(\delta^{15}\text{N}_0 + 1) \quad (2)$$

18 with  $\delta^{15}\text{N}_f$  and  $\delta^{15}\text{N}_0$  the  $\delta$ -value in the remaining and initial snow nitrate,  $f$  is the remaining  
19 mass fraction. Comparing apparent fractionation constants obtained in the field to the  
20 fractionation constants associated with the physical and photochemical nitrate loss processes  
21 has demonstrated that the UV-photolysis of nitrate is the dominant mass loss process on the  
22 Antarctic plateau (Erbland et al., 2013). As a consequence,  $\delta^{15}\text{N}$  in nitrate archived beyond the  
23 snow photic zone (the zone of active photochemistry) on plateau sites depends on <sup>15</sup> $\epsilon_{\text{pho}}$ , the  
24 <sup>15</sup>N/<sup>14</sup>N fractionation constant associated with nitrate photolysis (Frey et al., 2009; Erbland et  
25 al., 2013) and the magnitude of the loss ( $1-f$ ) (Eq. (2)). Because of its link with the residence  
26 time of nitrate in the photic zone, a strong relationship has been found between the snow  
27 accumulation rate ( $A$ ) and the degree of isotopic fractionation  $\delta^{15}\text{N}$  in the archived (asymptotic,  
28 “as.”) nitrate (Freyer et al., 1996, Erbland et al., 2013). At a given actinic flux  $I$ , the <sup>15</sup>N/<sup>14</sup>N  
29 fractionation constant induced by nitrate photolysis is calculated as the ratio of the photolysis  
30 rate constants:

$$31 {}^{15}\epsilon_{\text{pho}} = \frac{I'}{I} - 1 \quad (3)$$

1 with  $J$  and  $J'$  the photolytic rate constants of  $^{14}\text{NO}_3^-$  and  $^{15}\text{NO}_3^-$  respectively. The Rayleigh  
 2 distillation model applied to a single process in an open system gives the  $\delta^{15}\text{N}$  values in the  
 3 ~~emitted and remaining fractions by applying Eq. (2) using  $^{15}\epsilon_{\text{photo}}$  as follows:~~

$$4 \delta^{15}\text{N}_{\text{rem}} = (1 + \delta^{15}\text{N}_0) \times f^{15\epsilon} - 1 \quad (4)$$

$$5 \delta^{15}\text{N}_{\text{em}} = (1 + \delta^{15}\text{N}_0) \times \frac{1 - f^{(15\epsilon+1)}}{1-f} - 1 \quad (5)$$

6 ~~with  $f$  the remaining nitrate mass fraction,  $^{15}\epsilon$  the fractionation constant and  $\delta^{15}\text{N}_0$  which~~  
 7 ~~represents the  $\delta^{15}\text{N}$  in the initial nitrate.~~

8 The three stable isotopes of oxygen allow to define a unique tracer,  $\Delta^{17}\text{O} = \delta^{17}\text{O} - 0.52 \times \delta^{18}\text{O}$   
 9 which is referred to as “oxygen isotope anomaly” or also “ $^{17}\text{O}$ -excess”. An apparent  
 10 fractionation constant ( $^{17}E_{\text{app}}$ ) can be computed for  $\Delta^{17}\text{O}$  using ~~equation Eq. (2)~~, similarly to  
 11 what can be done for isotopic enrichment values ( $\delta$ ). Most oxygen-bearing species feature  $\Delta^{17}\text{O}$   
 12 = 0 ‰ but some species such as atmospheric nitrate can partially inherit the large positive  
 13 oxygen isotope anomaly transferred from ozone thus reflecting the relative contribution of  
 14 various oxidants involved in its formation (Michalski et al., 2003, Morin et al., 2007, 2008,  
 15 2009, 2011, Kunasek et al., 2008, Alexander et al., 2009).

16 Erbland et al. (2013) documented year-round measurements of  $\Delta^{17}\text{O}$  in atmospheric and skin  
 17 layer nitrate at Dome C and on the Antarctic plateau, which revealed a photolytically driven  
 18 isotopic equilibrium between the two compartments, i.e. the  $\Delta^{17}\text{O}$  atmospheric signal is mostly  
 19 conserved in the skin layer. In contrast to  $\delta^{15}\text{N}$ , post-depositional processes have a small impact  
 20 on  $\Delta^{17}\text{O}$  in nitrate snow profiles (Frey et al., 2009) so that a large portion of the atmospheric  
 21 signature is transferred in snow nitrate at depth despite a small dampening effect (Erbland et  
 22 al., 2013). Indeed, laboratory studies have shown that although nitrate photolysis in snow has a  
 23 purely mass-dependent isotopic effect (i.e. in theory not impacting the  $\Delta^{17}\text{O}$ ), this process leads  
 24 to a lower  $\Delta^{17}\text{O}(\text{NO}_3^-)$  in the remaining phase because of the cage recombination (hereafter  
 25 termed “cage effects”) of the primary photo-fragment of  $\text{NO}_3^-$  (McCabe et al., 2005).  
 26 Immediately following nitrate photolysis, a fraction of the photo-fragment  $\text{NO}_2$  reacts back with  
 27 OH radicals to form  $\text{HNO}_3$  but some of the OH radicals exchange O atoms with water molecules  
 28 in the ice lattice, so that the recombined  $\text{HNO}_3$  contains an oxygen atom replaced by one  
 29 originating from  $\text{H}_2\text{O}$  and featuring  $\Delta^{17}\text{O}(\text{H}_2\text{O}) = 0$  ‰.

## 1.2 Goals of this article

This article is a companion paper of “Air-snow transfer of nitrate on the East Antarctic Plateau – Part 1: Isotopic evidence for a photolytically driven dynamic equilibrium in summer”, published in the same journal (Erbland, et al., 2013). In this paperstudy, we test the nitrate recycling theory and evaluate it in light of the field isotopic measurements presented in Erbland et al. (2013) and obtained at the air-snow interface at Dome C as well as in several shallow snow pits collected at this site and on a large portion of the East Antarctic plateau. Testing this theory requires the building of a numerical model which represents nitrate recycling at the air-snow interface and describes the evolution of the nitrogen and oxygen stable isotopic composition of nitrate with various constraints from key environmental variables such as the solar zenith angle and the available UV radiation. Various models have been developed to investigate the physical and chemical processes involving nitrate in snow and their impact on the atmospheric chemistry in Antarctica (Wang et al., 2007; Liao and Tan, 2008; Boxe and Saiz-Lopez, 2008) and in Greenland (Jarvis et al., 2008; 2009; Kunasek et al., 2008; Thomas et al., 2011; Zatko et al., 2013). Those models are adapted to short time periods (hours to days, typically) and focus on processes at play in the atmosphere and in the near-surface snowpack. In this article, we present a new model called TRANSITS (“TRansfer of Atmospheric Nitrate Stable Isotopes To the Snow”), which shares some hypotheses with the modeling effort of Wolff et al. (2002) and the conceptual model of Davis et al. (2008). Together with a more realistic representation of some processes, the main novelty brought by the TRANSITS model is the incorporation of the oxygen and nitrogen stable isotopic ratios in nitrate as a diagnostic and evaluation tool in the ideal case of the East Antarctic plateau where snow accumulation rates are low and where nitrate mass loss can be mostly attributed to UV-photolysis. The following key questions are addressed in this work:

1. Is the theory behind the TRANSITS model compatible with the available field measurements?
2. What controls the mass and isotopic composition ( $\delta^{15}\text{N}$  and  $\Delta^{17}\text{O}$ ) of the archived nitrate?

The model is first described. Then it is evaluated by comparing its outputs to observations in the case of simulations at the air-snow interface at Dome C as well as in East Antarctic sites. A framework for the interpretation of the nitrate isotope record in deep ice cores is then given in light of sensitivity tests of the model.

Code de champ modifié

Mis en forme : Ne pas vérifier l'orthographe ou la grammaire

1

## 2 2 Description of the TRANSITS model

### 3 2.1 Overview

4 TRANSITS is a multi-layer, 1-D isotopic model which represents a snow and atmosphere  
5 column with an arbitrary surface area taken sufficiently large to neglect local lateral air mass  
6 movement (i.e. at the scale of the East Antarctic plateau). The snowpack is set to a constant  
7 height of one meter and a snow density ( $\rho$ ) is assumed to be constant. The one-meter snowpack  
8 is divided into 1000 layers of a 1-mm thickness, which means that the snow mass is the same  
9 in each layer. The atmospheric boundary layer (ABL) is represented by a single box of a  
10 constant height.

11 The aim of the model is to conceptually represent nitrate recycling at the air-snow interface  
12 (UV-photolysis of  $\text{NO}_3^-$ , emission of  $\text{NO}_x$ , local oxidation, deposition of  $\text{HNO}_3$ ) and to model  
13 the impact on nitrogen and oxygen stable isotopic ratios in nitrate in both reservoirs. For the  
14 sake of simplicity, we will focus on  $\delta^{17}\text{O}$  and  $\delta^{15}\text{N}$ ;  $\delta^{18}\text{O}$  is not included in the TRANSITS  
15 model. The TRANSITS model is neither a snowpack nor a gas-phase chemistry model and it  
16 does not aim at representing all the mechanisms responsible for nitrate mobility neither at the  
17 snowpack scale nor at the snow microstructure scale.

18 Figure ~~1~~<sup>2</sup> provides an overview of the TRANSITS model. The loss of nitrate from snow is  
19 assumed to only occur through UV-photolysis, because the physical release of  $\text{HNO}_3$  is  
20 negligible (Erbland et al., 2013). TRANSITS does not treat different nitrate domains in snow  
21 and it is hypothesized that its photolysis only produces  $\text{NO}_2$ .  $\text{NO}_2$  undergoes local cycling with  
22  $\text{NO}_x$  which modifies its oxygen isotope composition while the N atom is preserved. One  
23 computed year is divided into 52 time steps of approximately one week ( $\Delta t = 606\,877$  s), a time  
24 step sufficiently long to assume quantitative oxidation of  $\text{NO}_2$  into  $\text{HNO}_3$ . The chosen time step  
25 also allows to operate at the annual timescale, which is best suited to long simulation durations.  
26 For simplicity, we assume that  $\text{NO}_2$  oxidation occurs through reaction with OH radicals. The  
27 deposition of atmospheric  $\text{HNO}_3$  is assumed to occur by the uptake at the surface of the  
28 snowpack. Nitrate diffusion is assumed to occur in the snowpack at the macroscopic scale and  
29 is solved at a time ~~step of resolution 50 times shorter~~ 4 hours within each main ~~than the model~~  
30 main time resolution (i.e. approx. 3.4 hours) ~~model time step~~.

1 ~~The lower limit of the modeled snowpack is set at one meter depth. Below one meter,~~ a depth  
2 ~~below which where~~ the actinic flux is always negligible. ~~Below this depth, nitrate is considered,~~  
3 ~~the nitrate is to be~~ archived. ~~At every time step, the new snow layer accumulated at the top~~  
4 ~~pushes a layer of snow below one meter depth. This snow layer is archived and its nitrate mass~~  
5 ~~fraction is frozen (and denoted  $\omega(FA)$ ), thus allowing the calculation of the archived nitrate~~  
6 ~~mass flux ( $FA$ , the product of  $\omega(FA)$  and the archived snow mass during one time step).~~ Table  
7 1 provides a glossary of the acronyms used in this paper, as well as their definition.

## 8 2.2 Mass balance equations

9 In each box, the model solves the general “mass-balance” equation, which describes the  
10 temporal evolution of the concentration of the species  $X$  (i.e. nitrate or  $\text{NO}_2$ ):

$$11 \frac{d}{dt} [X] = \Sigma_i P_i - \Sigma_j L_j \quad (64)$$

12 The isotopic mass-balance equations ~~also apply to the products  $[X] \times \delta^{15}\text{N}$  and  $[X] \times \Delta^{17}\text{O}$  write~~  
13 (Morin et al., 2011):

$$14 \frac{d}{dt} ([X] \times \delta^{15}\text{N}) = \Sigma_i (P_i \times \delta^{15}\text{N}_i(X)) - (\Sigma_j (L_j \times (\delta^{15}\text{N}(X) - {}^{15}\epsilon_j))) \quad (75)$$

$$15 \frac{d}{dt} ([X] \times \Delta^{17}\text{O}) = \Sigma_i (P_i \times \Delta^{17}\text{O}_i(X)) - (\Sigma_j L_j) \times \Delta^{17}\text{O}(X) \quad (86)$$

16 where  $P_i$  and  $L_j$  respectively represent sources and sinks rates ~~(in  $\text{cm}^{-3}\text{s}^{-1}$ )~~ and  $\delta^{15}\text{N}_i(X)$  and  
17  $\Delta^{17}\text{O}_i(X)$  the isotopic compositions of the  $i$  sources. A  $^{15}\text{N}/^{14}\text{N}$  fractionation constant ( ${}^{15}\epsilon_j$ ) can  
18 be associated with loss process  $j$ . Within each ~~compartment~~box, incoming fluxes are positive  
19 and outgoing fluxes are negative. The concentration of nitrate in a snow layer is handled as  
20 “nitrate mass fraction” which is denoted  $\omega(\text{NO}_3)$ .

21 For simplicity, fluxes will be hereafter denoted “ $FY$ ”, with “ $Y$ ” a chain of capital letters. The  
22 primary input of nitrate to the modeled atmosphere is denoted  $FPI$  and is ~~the~~ combination of  
23 a stratospheric flux ( $FS$ ) and the horizontal long distance transport ( $FT$ ) of nitrate. Therefore,  
24  $FPI = FS + FT$ . The two primary origins of nitrate are defined by constant  $\Delta^{17}\text{O}$  and  $\delta^{15}\text{N}$   
25 signatures denoted  $\Delta^{17}\text{O}(FS)$ ,  $\Delta^{17}\text{O}(FT)$ ,  $\delta^{15}\text{N}(FS)$  and  $\delta^{15}\text{N}(FT)$ . The secondary source of  
26 nitrate to the atmosphere is the local oxidation of  $\text{NO}_2$  occurring after nitrate photolysis in the  
27 snow ( $FP$ ).

28 Nitrate is removed from the atmospheric box via two processes. Large scale horizontal air  
29 masses movement can lead to a loss of nitrate, hereafter named “horizontal export flux” ( $FE$ ).

1 ~~The  $FE$  flux is modeled as a constant fraction of all incoming nitrate fluxes to the atmosphere~~

2  ~~$FE = f_{\text{exp}} \times (FP + FS + FT)$ .~~ The export of nitrate is assumed to preserve the  $\Delta^{17}\text{O}$  and  $\delta^{15}\text{N}$   
3 values. Nitrate can also be lost via deposition ( $FD$ ) to the snow, which is the sole nitrate source  
4 to the snowpack. This flux is obtained by solving the mass balance in the atmospheric box and  
5 is added to the topmost layer of the snowpack at each model time step.

6 The loss of nitrate from the snowpack is assumed to occur through nitrate UV-photolysis only.  
7 Within the snowpack, nitrate is redistributed by macroscopic diffusion, which is assumed to  
8 preserve  $\Delta^{17}\text{O}$  and  $\delta^{15}\text{N}$ .

### 9 **2.3 Physical properties of the atmosphere and the snowpack**

10 The ~~constant~~ height of the ABL is denoted  $h_{\text{AT}}$ . This single atmospheric box is assumed to be  
11 well mixed at all times which is justified at the time resolution of the model (ca. one week).  
12 Hereafter we denote  $\gamma(\text{NO}_3^-)$  the nitrate concentration in the atmospheric box. In TRANSITS,  
13 the time evolution of this variable is prescribed by observations.

14 Physical properties of the snowpack influencing radiative transfer in snow are fixed, according  
15 to a typical Dome C snowpack with a constant layering throughout the year as defined in France  
16 et al. (2011): it is made of 11 and 21 cm of soft and hard windpack snow at the top and hoar-  
17 like snow below with their respective snow densities, scattering and absorption coefficients at  
18 350 nm. At Dome C, the e-folding attenuation depths (denoted  $\eta$ ) for the three snow layers are  
19 fairly constant in the range 350–400 nm (France et al., 2011) and this observation can be  
20 extended to the 320–350 nm range (James France, unpublished). The snow optical properties  
21 taken at 350 nm are therefore assumed to be valid for the whole 280–350 nm range of interest  
22 for nitrate photolysis. This hypothesis is supported twofold. First, e-folding attenuation depths  
23 measured at Alert, Nunavut show no significant sensitivity to wavelengths in the 310–350 nm  
24 range (King and Simpson, 2001). Secondly,  $\eta$  values measured in a recent laboratory study only  
25 show a weak (10 %) decrease from 350 nm to 280 nm (Meusinger et al., 2014). Under Dome  
26 C conditions, the absorption of UV by impurities is small and the depth attenuation of UV light  
27 is mostly driven by light scattering (France et al., 2011). As a consequence,  $\eta$  is assumed to be  
28 independent on the impurities content in the snow, in this case, nitrate itself.

29 While optical calculations are based on a realistic snowpack, nitrate mass and isotopic  
30 computations are performed assuming a constant ~~density of snow~~ snow density, ( $\rho$ ), which  
31 simplifies the computation. One consequence of this simplification ~~This simplification is that~~

1 ~~our modeled e-folding depths are independent of snow density, which we acknowledge is not~~  
2 ~~realistic (Chan et al., 2015).has no impact on the optical behavior of the snowpack because it is~~  
3 ~~assumed to be independent on the nitrate fractions.~~

4 ~~Assuming that t-However,~~ the snow density ~~being-is~~ constant means that the snowpack does  
5 not undergo densification. For simplicity, we also hypothesize that no sublimation, wind  
6 redistribution, melt nor flow occur and that the surface of the snowpack is assumed to be flat  
7 and insensitive to erosion.

## 8 **2.4 Parameterization of chemical processes**

9 Figure ~~2-3~~ provides an overview of the physical and chemical processes included in TRANSITS  
10 as well as the parameters and input variables of interest for each process. Table ~~2-2~~ lists the  
11 chemical and physical processes included or not in the model. A description of the  
12 parameterization of each process is given below.

### 13 **2.4.1 Nitrate UV-photolysis**

14 Nitrate photolysis is at the core of the model. At each time step, the photolyzed nitrate mass in  
15 a layer equals  $e^{-J\Delta t} \times m$ , where  $m$  is the initial nitrate mass in the layer and  $J$ , the photolysis  
16 rate constant of  $\text{NO}_3^-$  (Eq. (1)). The UV actinic fluxes ( $I$ ) required for the calculation of  $J$  have  
17 been computed in the 280–350 nm range using offline runs of the TUV-snow radiative-transfer  
18 model (Lee-Taylor and Madronich, 2004). TUV-snow has been run for the DC location and  
19 snowpack for various dates (i.e. solar zenith angle,  $\theta$ ), assuming a clear aerosols-free sky and  
20 using the extraterrestrial irradiance from Chance and Kurucz (2010) and a constant Earth-Sun  
21 distance as that of 27 December 2010. Ozone profiles from 25 to 500 DU with a resolution of  
22 25 DU have been used to run the radiative transfer model. Next, we denote  $k$  the “photic zone  
23 compression factor”, which represents variations of depth of the photic zone under the effect of  
24 changes in physical properties of the snowpack due to snow metamorphism or in chemical  
25 properties. In Eq. (1), the term “ $z$ ” is therefore replaced by “ $z/k$ ”. A typical Dome C snowpack  
26 is represented by  $k$  value of 1. Lower  $k$  values mean that the UV radiation is extinguished more  
27 rapidly with depth. Last, we denote  $q$  the “actinic flux enhancement factor”, which accounts  
28 for variations in the actinic flux received at the snow surface and hence at depth. This parameter  
29 represents changes in the actinic flux emitted from the Sun or changes in the Earth-Sun distance  
30 due to variations in the Earth’s orbit. In Eq. (1), the term “ $I$ ” is therefore replaced by “ $q \times I$ ”. In  
31 the modern DC case,  $q$  is set to 1.

1 Another key control on  $J$  is the quantum yield ( $\Phi$ ), a parameter which is strongly governed by  
2 nitrate location in the snow ice matrix and which corresponds to nitrate availability to  
3 photolysis. Nitrate is assumed to deposit to the snow under the form of  $\text{HNO}_3$  but its adsorption  
4 and/or dissociation to  $\text{NO}_3^- + \text{H}^+$  are not explicitly represented. Indeed, modeling nitrate  
5 location in the snow is well beyond the scope of the present study and a recent molecular  
6 dynamic study demonstrated the fast ionization of  $\text{HNO}_3$  (picosecond time scale) at the ice  
7 interface (Riikonen, Parkkinen, Halonen, & Gerber, 2014). For the sake of simplicity, we  
8 assume that nitrate location in the snow ice matrix is constant. Therefore,  $\Phi$  is set to a constant  
9 value.

10 Nitrate photolysis is assumed to only produce  $\text{NO}_2$ . We acknowledge that other volatile nitrogen  
11 species such as  $\text{NO}$  or  $\text{HONO}$  may be produced. However, the photolysis of  $\text{HONO}$  in the  
12 atmosphere would rapidly produce  $\text{NO}_2$  which would contribute to the  $\text{NO}/\text{NO}_2$  cycle and hence  
13 have a nil impact in terms of N mass balance.

14 In the model,  $^{15}\epsilon_{\text{pho}}$  is explicitly calculated at each time step and in each snow layer using Eq.  
15 (3). Because the layering of the physical properties of snow is fixed,  $^{15}\epsilon_{\text{pho}}$  is constant with time.

16 ~~Earlier, we have hypothesized that the scattering and absorption properties of each layer of the~~  
17 ~~snowpack are kept constant in the 280–350 nm range. In the UV-spectral range (280–350 nm),~~  
18 ~~we have earlier assumed that e-folding depth is constant with wavelength; therefore, even~~  
19 ~~though  $\rho$  modulates the e-folding depth,  $^{15}\epsilon_{\text{pho}}$  is independent of  $\rho$  as well as of depth. This~~  
20 ~~results in the independency of  $^{15}\epsilon_{\text{pho}}$  with depth,~~ in agreement with the laboratory study of  
21 Berhanu et al. (2014a) and the field study of Berhanu et al. (2014b). ~~Therefore~~ As a  
22 consequence, the modeled  $^{15}\epsilon_{\text{pho}}$  is entirely determined by the spectral distribution of the UV  
23 radiation received at the surface of the snowpack. The Rayleigh fractionation model applied to  
24 nitrate photolysis allows calculating the  $\delta^{15}\text{N}$  in the photolyzed ~~and the remaining nitrate-nitrate~~  
25 applying Eqs. (4) ~~and (5)~~ with the use of  $^{15}\epsilon_{\text{pho}}$  and  $\delta^{15}\text{N}$  in the remaining nitrate by simple  
26 mass balance. Nitrate photolysis is assumed to be a mass dependent process so that the  $\delta^{17}\text{O}$  in  
27 the initial, photolyzed and remaining nitrate is ~~the kept the~~ same.

#### 28 2.4.2 Cage effect

29 A constant fraction of the photolyzed nitrate (denoted  $f_{\text{cage}}$ ) is assumed to undergo cage  
30 recombination so that the photo-fragment  $\text{NO}_2$  reacts back with  $\text{OH}$  to re-form  $\text{HNO}_3$ . ~~This~~  
31 ~~results in an apparent remaining nitrate mass fraction denoted  $f_{\text{app}}$  which writes:  $f_{\text{app}} = f + f_{\text{cage}}$~~   
32 ~~(1 -  $f$ ) and, consequently, to a lower apparent quantum yield. In the cage effect process,  $\text{OH}$  is~~

Code de champ modifié

Mis en forme : Anglais (États-Unis), Ne pas vérifier l'orthographe ou la grammaire

Mis en forme : Non Exposant/ Indice



1 assumed to undergo an isotopic exchange with the water molecules of the ice lattice, so that the  
2 recombined HNO<sub>3</sub> contains an oxygen atom originating from H<sub>2</sub>O and featuring  $\Delta^{17}\text{O}(\text{H}_2\text{O}) =$   
3 0 ‰ (McCabe et al., 2005).

### 5 2.4.3 Emission of NO<sub>2</sub> and photochemical steady-state

6 The total photolytic flux (*FP*) represents the potential emission of NO<sub>2</sub> from the snow to the  
7 atmosphere [in accordance with the terminology used in France et al. \(2011\)](#) and is the sum of  
8 the photolytic fluxes [originating](#) from each snow layer. A simple isotopic mass balance is  
9 applied to calculate the  $\delta^{15}\text{N}$  and  $\Delta^{17}\text{O}$  of the photolytic loss flux *FP*. The extraction of NO<sub>2</sub>  
10 from the snowpack is assumed to preserve its chemical and isotopic integrity, i.e. it does not  
11 undergo any chemical reaction or any isotopic fractionation [in the snowpack](#). ~~*FP* represents the  
12 potential flux of NO<sub>2</sub> in accordance with the terminology used in France et al. (2011).~~

~~13 Before its conversion to HNO<sub>3</sub>, NO<sub>2</sub> originating from the snowpack undergoes numerous  
14 photolytic destruction and reformation (Fig. 1). We assume that summer conditions prevail  
15 during the whole sunlit season.~~ Atmospheric chemistry is not explicitly ~~simulated~~ modeled but  
16 only conceptually represented.  $\Delta^{17}\text{O}(\text{NO}_2)$  is calculated following the approach of Morin et al.  
17 (2011), i.e. assuming ~~photochemical~~ [Photochemical steady-state](#) (PSS) of NO<sub>x</sub>  
18 (when the [photolytic](#) lifetime of NO<sub>x</sub> is shorter than 10 minutes), an assumption which is valid  
19 for most of the sunlit season ( $\tau(\text{NO}_2) < 10$  minutes from September 27 to March 7, [Frey et al.](#)  
20 [\(2013, 2014\)](#)). We therefore denote  $\Delta^{17}\text{O}(\text{NO}_2, \text{PSS})$ , the  $\Delta^{17}\text{O}$  value harbored by NO<sub>2</sub> after its  
21 local cycling, which is represented by (Morin et al., 2008, 2011):

$$22 \Delta^{17}\text{O}(\text{NO}_2, \text{PSS}) = \alpha \times \Delta^{17}\text{O}_{\text{O}_3+\text{NO}}(\text{NO}_2) \quad (97)$$

23 with  $\alpha$ , a variable which accounts for the perturbation of the Leighton cycle by various radicals  
24 such as peroxy radicals (RO<sub>2</sub>) and halogen oxides. For simplicity, we only consider BrO, HO<sub>2</sub>  
25 and CH<sub>3</sub>O<sub>2</sub> as the species perturbing the Leighton cycle. The  $\alpha$  variable is calculated at each  
26 time step as in Eq. ~~(498)~~ assuming  $\Delta^{17}\text{O}(\text{HO}_2) = \Delta^{17}\text{O}(\text{CH}_3\text{O}_2) = 0$  ‰ (Morin et al., 2011).  
27 Recent observations at DC seem to support the assumption  $\Delta^{17}\text{O}(\text{CH}_3\text{O}_2) = 0$  ‰ because CH<sub>3</sub>O<sub>2</sub>  
28 may entirely originate from the reaction R + O<sub>2</sub> or photolysis of species (CH<sub>3</sub>CHO) featuring  
29  $\Delta^{17}\text{O} = 0$  ‰ (Kukui et al., 2014). The assumption  $\Delta^{17}\text{O}(\text{HO}_2) = 0$  ‰ is also supported by the  
30 same observations although 5 % of HO<sub>2</sub> originate from the reaction O<sub>3</sub> + OH which leads to  
31  $\Delta^{17}\text{O}(\text{HO}_2) > 0$  ‰. For simplicity, we stick to the assumption  $\Delta^{17}\text{O}(\text{HO}_2) = 0$  ‰.

$$\alpha = \frac{k_{\text{O}_3+\text{NO}}[\text{O}_3] + k_{\text{BrO}+\text{NO}}[\text{BrO}]}{k_{\text{O}_3+\text{NO}}[\text{O}_3] + k_{\text{HO}_2+\text{NO}}[\text{HO}_2] + k_{\text{CH}_3\text{O}_2+\text{NO}}[\text{CH}_3\text{O}_2] + k_{\text{BrO}+\text{NO}}[\text{BrO}]} \quad (408)$$

with temperature- and pressure-dependent kinetic rate constants from Atkinson et al. (2004, 2006, 2007) and the mixing ratios of O<sub>3</sub>, BrO, HO<sub>2</sub> and CH<sub>3</sub>O<sub>2</sub> at ~~ground~~the surface. Savarino et al. (2008) have measured that O<sub>3</sub> preferentially transfers one of its terminal O atom when oxidizing NO with a probability of 92 % which translates in the following equation:

$$\Delta^{17}\text{O}_{\text{O}_3+\text{NO}}(\text{NO}_2) \times 10^3 = 1.18 \times \Delta^{17}\text{O}(\text{O}_3)_{\text{bulk}} \times 10^3 + 6.6 \times 10^{-3} \quad (419)$$

with  $\Delta^{17}\text{O}(\text{O}_3)_{\text{bulk}}$ , the isotopic anomaly of local bulk ozone. The O atom in BrO originates from the terminal oxygen atom of ozone through its reaction with bromine (Morin et al., 2007 and references therein). For simplicity, we assume that the O atom transferred during the NO oxidation by O<sub>3</sub> and BrO is identical.

#### 2.4.4 Local oxidation of NO<sub>2</sub>

NO<sub>2</sub> is directly converted to HNO<sub>3</sub> with the preservation of the N atom. However, a local additional oxygen atom is incorporated. This is a reasonable assumption given the short chemical lifetime of NO<sub>x</sub> with respect to NO<sub>2</sub> + OH (in the order of hours) in comparison with the approximately one-week time step used in the model. The  $\Delta^{17}\text{O}$  of HNO<sub>3</sub> is given by Eq. (4210).

$$\Delta^{17}\text{O}(\text{HNO}_3) = \frac{2}{3}\Delta^{17}\text{O}(\text{NO}_2) + \frac{1}{3}\Delta^{17}\text{O}(\text{add O}) \quad (4210)$$

Similarly to the local cycling of NO<sub>2</sub>, the local oxidation of this species is only conceptually represented. For simplicity, we assume that the formation of HNO<sub>3</sub> only occurs through the pure daytime channel, i.e. the reaction of NO<sub>2</sub> and OH:  $\Delta^{17}\text{O}(\text{add. O}) = \Delta^{17}\text{O}(\text{OH})$ .

In the framework of the OPALE campaign,  $\Delta^{17}\text{O}(\text{OH})$  has been discussed in a submitted paper (Savarino et al., in prep. submitted). The results of this study show that  $\Delta^{17}\text{O}(\text{OH})$  varies in a narrow range, between 1 and 3 ‰, around summer solstice 2011-2012. As a result, we set  $\Delta^{17}\text{O}(\text{OH}) = 3\text{‰}$  throughout the entire sunlit season. According to Kukui et al. (2014), the photolysis of HONO accounts for 56 % of the total atmospheric primary radical production at Dome C. The other two main OH production channels are HO<sub>2</sub> + NO (33 %) and H<sub>2</sub>O<sub>2</sub>

Mis en forme : Non Surlignage

Mis en forme : Non Surlignage

Mis en forme : Non Surlignage

Mis en forme : Non Surlignage

Mis en forme : Non Surlignage

Mis en forme : Non Surlignage

1 photolysis (7 %) (Kukui et al., 2014), both of which can be considered to lead to OH with a nil  
2  $^{17}\text{O}$  excess given the fact that  $\Delta^{17}\text{O}(\text{HO}_2) = 0 \text{ ‰}$  and  $\Delta^{17}\text{O}(\text{H}_2\text{O}_2) = \Delta^{17}\text{O}(\text{HO}_2)$  (Morin et al.,  
3 2011). Reaction channels involving ozone in the formation of OH represent less than 4 %. For  
4 simplicity, we assume that 60 % of OH is produced by HONO photolysis and that the other 40  
5 % lead to  $\Delta^{17}\text{O}(\text{OH}) = 0 \text{ ‰}$ . The  $\Delta^{17}\text{O}$  of OH therefore writes:

$$\Delta^{17}\text{O}(\text{OH}) = 0.6 \cdot \Delta^{17}\text{O}(\text{HONO}) \quad (13)$$

7 with  $\Delta^{17}\text{O}(\text{HONO}) = \Delta^{17}\text{O}(\text{NO}_2^-) = \Delta^{17}\text{O}(\text{photo. NO}_3^-)$  where  $\text{NO}_2^-$  is one of the product of  $\text{NO}_3^-$   
8 photolysis.

## 10 2.5 Parameterization of physical processes

### 11 2.5.1 Snow accumulation

12 The snow accumulation thickness depends on the snow accumulation rate ( $A$ ) as well as on  
13 snow density ( $\rho$ ). Older layers are buried, preserving their nitrate mass and isotopic  
14 composition. Immediately after snow accumulation, the modeled snowpack is resampled at a  
15 1-mm resolution ( $\Delta z = 1 \text{ mm}$ ).

### 17 2.5.2 Nitrate horizontal export

18 The export flux ( $FE$ ) is modeled as a constant fraction of all incoming nitrate fluxes to the  
19 atmosphere  $FE = f_{\text{exp}} \times (FP + FS + FT)$ , assuming that  $\text{NO}_x$  conversion to  $\text{HNO}_3$  is instantaneous  
20 and that nitrate is homogeneous in the atmospheric box, at the chosen time step.

### 21 2.5.2.5.3 Nitrate deposition to the snow

22  
23 The deposited flux ( $FD$ ) and its isotopic composition ( $\Delta^{17}\text{O}(FD)$  and  $\delta^{15}\text{N}(FD)$ ) are obtained  
24 by solving Eqs. (64) to (86) (Fig. 2-3). For the sake of simplicity, the downward deposition flux  
25 is modeled assuming a pure physical deposition diffusion of  $\text{HNO}_3$  ~~in-on~~ the top layer of the  
26 snowpack. The deposition process is assumed to preserve  $\Delta^{17}\text{O}$ . This process is associated with  
27 a  $^{15}\text{N}/^{14}\text{N}$  fractionation constant ( $^{15}\epsilon_{\text{dep}}$ ).

Mis en forme : Hiérarchisation + Niveau : 3 + Style de numérotation : 1, 2, 3, ... + Commencer à : 1 + Alignement : Gauche + Alignement : 1 cm + Tabulation après : 2,27 cm + Retrait : 2,27 cm

## 2.5.32.5.4 Nitrate diffusion in the snowpack

Nitrate diffusion in the snowpack leads to changes in nitrate mass fraction and isotope profiles in the snowpack, and it is represented by the use of a diffusivity coefficient denoted  $D$  and by a zero-flux boundary condition at the top and at the bottom of the snowpack ( $z = 1$  m) :

$$\begin{cases} \frac{\partial \omega(z,t)}{\partial t} = D \frac{\partial^2 \omega(z,t)}{\partial z^2} \\ \frac{\partial \omega(\text{top},t)}{\partial z} = 0 \\ \frac{\partial \omega(\text{bot},t)}{\partial z} = 0 \end{cases} \quad (411)$$

with  $\omega(z, t)$ , the nitrate mass fraction in each layer and,  $z$  and  $t$  the space and time ~~variables and~~  $\frac{\partial \omega(0,t)}{\partial z}$  and  $\frac{\partial \omega(1,t)}{\partial z}$  the nitrate concentration at the top and bottom of the snowpack, respectively.

Given the assumption of a constant snow density and a uniform mesh grid, Eq. (411) also applies to the snow mass in the layer ( $m$ ). Equation (411) is solved at a time step of 3.4 hours (i.e. 50 times shorter than the main time step of the model), which must respect the following:

$\frac{(\Delta z)^2}{3.4 \text{ h}} \ll D$ . Space and time derivatives are approximated by the finite difference method.

### 3 Model ~~setup, runs and~~ evaluation

#### 3.1 Method: observational constraints, model setup and runs

To evaluate the model, we study its ability to reproduce ~~at best~~ the present-day observations at Dome C and across East Antarctica. To this end, a realistic simulation of TRANSITS is compared to the data observed at the air-snow interface at Dome C and in the top 50 cm of snow in East Antarctica.

##### 3.1.1 ~~Field~~ Observational constraints

~~In this section, we briefly describe the observed data used to evaluate the model.~~ Most of the observed data originate from Erbland et al. (2013). Atmospheric nitrate concentration and isotopic measurements were measured 2-m above ground at Dome C during the years 2007-2008 (Frey et al., 2009) and 2009-2010 (Erbland et al., 2013). In this second study, nitrate mass fraction and isotopic composition have also been measured in the skin layer (the  $(4 \pm 2)$  mm of top snow) and for the 2009-2010 period. Nitrate mass fractions and isotopic profiles are

1 available from three 50-cm snow pits sampled at Dome C during the austral summers 2007-  
2 2008 and 2009-2010 (Frey et al., 2009, Erbland et al., 2013). ~~From these snow pits data and~~  
3 ~~from the DC mean snow density profile given by Libois et al. (2014), we calculate  $m_{50\text{cm}}(\text{NO}_3^-)$ ,~~  
4  ~~$\delta^{15}\text{N}(\text{NO}_3^-)$  and  $\Delta^{17}\text{O}(\text{NO}_3^-)$ , the integrated nitrate mass and isotopic composition per unit~~  
5 ~~horizontal surface area in the top 50 cm of the snowpack.~~  $\text{NO}_x$  emission fluxes were measured  
6 at Dome C from 22 December 2009 to 28 January 2010 (Frey et al., 2013).

7 Forty-five 50-cm deep snow profiles were collected at DC from February 2010 to February  
8 2014 and nitrate mass fractions were measured as in Erbland et al. (2013). These previously  
9 unpublished profiles have been collected approximately every month by the DC overwintering  
10 team. From the fifty-one 50-cm snow pits collected at DC (45 unpublished and 6 published in  
11 Röthlisberger et al., 2000, Frey et al., 2009, France et al., 2011 and Erbland et al., 2013), we  
12 ~~use the nitrate mass fraction profiles to also~~ calculate  $m_{50\text{cm}}(\text{NO}_3^-)$ ,  $\delta^{15}\text{N}(\text{NO}_3^-)$  and  $\Delta^{17}\text{O}(\text{NO}_3^-)$   
13 ~~, the total mass of nitrate in the top 50 cm of a 1 m<sup>2</sup> section of the snowpack. The calculation~~  
14 ~~of  $m_{50\text{cm}}(\text{NO}_3^-)$  is given in the Supplementary Information (SI).~~

15 In East Antarctica, nitrate isotopic and mass fraction measurements are available from twenty-  
16 one 50-cm depth snow pits including the 3 DC snow pits presented above (Erbland et al., 2013).  
17 They were sampled along two transects which link D10 (a location in the immediate vicinity of  
18 the French Dumont d'Urville station) to DC and DC to Vostok. The samples collection and  
19 analysis as well as the data reduction are described in Erbland et al. (2013). Reduced data  
20 include the asymptotic mass fraction ( $\omega(\text{as.})$ ) and isotopic composition ( $\delta^{15}\text{N}(\text{as.})$  and  
21  $\Delta^{17}\text{O}(\text{as.})$ ) which represent nitrate below the zone of active nitrate mass loss in the top  
22 decimeters of snow, and  $^{15}\epsilon_{\text{app}}$  and  $^{17}E_{\text{app}}$  apparent fractionation constants.

### 23 3.1.2 TRANSITS simulations

#### 24 Simulation at the air-snow interface at Dome C

25 Table 3-3 gives a summary of the parameters and variables used for the TRANSITS DC realistic  
26 simulation. Below, we discuss their choice. Note that the adjustment parameters ( $\Phi$ ,  $f_{\text{exp}}$ ,  $f_{\text{cage}}$ ,  
27  $D$  and  $^{15}\epsilon_{\text{dep}}$ ) were adjusted manually and not set by an error minimizing procedure.

28 The thickness of the atmospheric boundary layer is set to a constant value of 50 meters, a value  
29 which ~~is sits between the close to the~~ median wintertime value (ca. 30 m) simulated by Swain  
30 and Gallée (2006) ~~and the mean value simulated around 27 December 2012. The larger value~~  
31 ~~chosen accounts for the larger boundary layer thickness found during summer~~ (Gallée et al.,

1 2014). The time series of the nitrate concentration in the atmospheric box was obtained by  
2 smoothing the atmospheric measurements performed at Dome C in 2009-2010 (Erbland et al.,  
3 2013).

4 Stratospheric denitrification is responsible for the input of an estimated nitrogen mass of  $(6.3 \pm$   
5  $2.6) \times 10^7$  kgN per year (Muscari and de Zafra, 2003), a value three times higher than the  
6 estimate of Wolff et al. (2008). Taking into account the area inside the Antarctic vortex where  
7 intense denitrification occurs ( $(15.4 \pm 3.0) \times 10^6$  km<sup>2</sup>, Muscari and de Zafra, 2003), this gives  
8 a flux of  $FS = (4.1 \pm 2.5) \times 10^{-6}$  kgN m<sup>-2</sup> a<sup>-1</sup>. The modeled stratospheric flux is set to occur  
9 constantly for a duration of 12 weeks (approx. 3 months) from June 21 to September 13, the  
10 period when the mean air temperature at 50 mb allows the formation of PSCs of type I ( $T < -$   
11 78 °C) (NOAA observations in 2008, available at  
12 <http://www.cpc.ncep.noaa.gov/products/stratosphere/polar/polar.shtml>). Transitions before  
13 and after the twelve-week  $FS(t)$  plateau are assumed to be linear and last 4 weeks (Fig. 4a). The  
14  $\delta^{15}\text{N}(FS)$  value is set to 19 ‰ as estimated by Savarino et al. (2007) based on computations  
15 from chemical mechanisms, fractionation factors, and isotopic measurements. ~~This value is~~  
16 ~~consistent with the value retrieved at 15 km above South Pole and at summer solstice ( $21 \pm 4$ )~~  
17 ~~‰ based on measurements of the atmospheric  $\text{H}^{15}\text{NO}_3/\text{H}^{14}\text{NO}_3$  isotope ratio profile by the Earth~~  
18 ~~observation instrument MIDAS operated onboard of the Environmental Satellite (ENVISAT)~~  
19 ~~(Brizzi et al., 2009).~~ No direct measurement of  $\Delta^{17}\text{O}$  in stratospheric nitrate exists. Savarino et  
20 al. (2007) estimated that  $\Delta^{17}\text{O}$  is higher than 40 ‰ and we set  $\Delta^{17}\text{O}(FS)$  to 42 ‰.

21 There is no estimate of the nitrogen mass flux received on the Antarctic continent by long range  
22 transport ( $FT$ ). In the absence of such information and for simplicity, we assume that, annually,  
23  $FS/FPI = 50$  ‰. This means that the annual fluxes  $FT$  and  $FS$  are equal. We also assume a  
24 ~~constant repartition~~ uniform distribution of  $FT$  throughout the year. We agree that this  
25 hypothesis is debatable given that air mass movement into the Antarctic plateau may be  
26 hampered at times when the polar vortex is strongest. As for the flux, the  $\delta^{15}\text{N}$  and  $\Delta^{17}\text{O}$  of this  
27 nitrate source are not known. However, we assume that it features  $\delta^{15}\text{N}(FT) = 0$  ‰ and  
28  $\Delta^{17}\text{O}(FT) = 30$  ‰, which represent averaged values for tropospheric nitrate in pristine areas in  
29 low/middle latitudes (Morin et al., 2009).

30 ~~The fraction of nitrate fluxes which is horizontally exported from the atmospheric box is set to~~  
31 ~~a constant value of  $f_{\text{exp}} = 20$  ‰.~~

1 During the OPALE experiment, the first measurements of  $\Delta^{17}\text{O}(\text{O}_3)_{\text{bulk}}$  in the Antarctic  
2 troposphere have been performed (Savarino et al, submitted).  $\Delta^{17}\text{O}(\text{O}_3)_{\text{bulk}}$  is therefore set to  
3 25.2 ‰ which represents the mean summertime value observed at Dome C.

4  
5  
6 Annual snow accumulation rates measured at Dome C vary considerably at the inter-annual  
7 timescale as a result of snow redistribution by the wind (Libois et al., 2014). For example, years  
8 with net ablation are as frequent as 15 %. The same process also affects the ~~repartition~~  
9 distribution of snow accumulation rates at a sub-annual timescale. For the sake of simplicity,  
10 the annual snow accumulation rate is set to a constant value of  $28 \text{ kg m}^{-2} \text{ a}^{-1}$  (93 mm of snow  
11 per year for  $\rho = 300 \text{ kg m}^{-3}$ ) which is representative of the Dome C site (Frezzotti et al., 2004,  
12 Libois et al., 2014). We also assumed a ~~constant repartition~~ uniform distribution of snow  
13 accumulation within the computed year. Snow densities also vary considerably at the  
14 decimeter-scale both horizontally and vertically (Libois et al., 2014). To simplify, the snow  
15 density has been set to  $300 \text{ kg m}^{-3}$ , the average value found for the snow top layers at Dome C  
16 (France et al., 2011). This value is close to the average value ( $316 \text{ kg m}^{-3}$ ) observed in a mean  
17 25-cm depth DC profile (Libois et al., 2014). We note that our choice of snow density for the  
18 nitrate mass and isotopic calculations is consistent with that used for the optical calculations in  
19 the soft windpack layer at the surface, where most of the action occurs.

20 The adjustment parameter  $^{15}\epsilon_{\text{dep}}$  (representing the  $^{15}\text{N}/^{14}\text{N}$  fractionation associated with  $\text{HNO}_3$   
21 deposition) is set to a value of +10 ‰ in order to ~~reproduce-match at best~~ the shift in  $\delta^{15}\text{N}$  ~~in~~  
22 ~~the between~~ observed atmospheric and skin layer nitrate (Erbland et al., 2013). The diffusivity  
23 coefficient is ~~calculated as in Thibert and Domine (1998) with the mean summertime DC~~  
24 ~~temperature (i.e. 237 K in Nov-Dec-Jan).  $D$  is therefore set to  $1.0\text{-}3 \cdot 10^{-11}\text{-}11 \text{ cm}^2 \text{ s}^{-1}$ . The~~  
25 fraction of nitrate fluxes which is horizontally exported from the atmospheric box is set adjusted  
26 to a constant value of  $f_{\text{exp}} = 20 \%$ .

27  
28 The parameter  $\Phi$  is ~~set adjusted~~ to a constant value of 0.026 ~~and th-e magnitude of the cage~~  
29 effect is adjusted using a constant parameter of  $f_{\text{cage}} = 0.15$ , which means that 15 % of the  
30 photolyzed nitrate undergoes cage recombination and isotopic exchange with water. The  
31 magnitude of the cage effect is adjusted using a constant parameter of  $f_{\text{cage}} = 0.15$ , which means

~~1 that 15 % of the photolyzed nitrate undergoes cage recombination and isotopic exchange with  
2 water. Given the choice of a modeled cage effect of 15 %, we obtain an apparent modeled  
3 quantum yield (denoted  $\phi^*$ ) of  $0.85 \times 0.026 \approx 0.022$ , a value smaller than the mean value for  
4 buried nitrate (0.05) but higher than the smallest value observed for this domain (0.003)  
5 (Meusinger et al., 2014).~~

6 We used absorption cross sections of  $^{14}\text{NO}_3^-$  and  $^{15}\text{NO}_3^-$  in snow recommended by Berhanu et  
7 al. (2014a). The TUV-snow model used to model the actinic flux in the DC snowpack was run  
8 using constant  $k$  and  $q$  parameters set to 1. An additional input is the ozone column and we used  
9 the measurements at Dome C over the 2000-2009 period. The 2000-2005 data were derived  
10 from the measurements made by the Earth Probe Total Ozone Mapping Spectrometer  
11 (EP/TOMS) and processed by the NASA (data obtained at <http://ozoneaq.gsfc.nasa.gov/>). The  
12 2007-2009 data were obtained from the “Système d’Analyse par Observation Zénithale”  
13 (SAOZ) observation network at ground (data obtained at <http://saoz.obs.uvsq.fr/index.html>).  
14 Weekly averages have been calculated over the 2000-2009 period and converted to obtain the  
15 same resolution (25 DU) than that used for the offline runs of the TUV-snow model (Fig. 3-4).

16 The variable  $\alpha$  has been calculated from Eq. (408) using weekly average mixing ratios of  $\text{O}_3$   
17 measured at Dome C in 2007-2008 (Legrand et al., 2009). During the OPALE campaign, Frey  
18 et al. (2014) have measured BrO mixing ratios of 2–3 pptv. We assume that [BrO] is constant  
19 throughout the year and equal to 2.5 pptv. Air temperatures and pressures at each time step  
20 were calculated from the 3-hours observations from the Concordia Automatic Weather Station  
21 (AWS 8989) in 2009-2010 (University of Wisconsin-Madison, data available at  
22 <ftp://amrc.ssec.wisc.edu/pub/aws/q3h/>, accessed July 4 2013). Mixing ratios of  $\text{HO}_2$  and  $\text{CH}_3\text{O}_2$   
23 were deduced from those of  $\text{RO}_2$  assuming  $\text{RO}_2 = \text{HO}_2 + \text{CH}_3\text{O}_2$  and  $[\text{HO}_2] / [\text{RO}_2] = 0.7$  (Kukui  
24 et al., 2014). Mixing ratios of  $\text{RO}_2$  were estimated from their linear relationship with  $J(\text{NO}_2)$ :  
25  $[\text{RO}_2] / (\text{molecule cm}^{-3}) = 7.25 \times 10^9 \cdot 10^{15} \times (J(\text{NO}_2) / \text{s}^{-1})$  (Figure 3b in Kukui et al., 2014). The  
26 time series of  $J(\text{NO}_2)$  was calculated with the TUV model for the appropriate solar zenith angle.

~~27 There is a lack of measurements of  $\delta^{17}\text{O}(\text{O}_3)_{\text{bulk}}$  in the Antarctic troposphere. Therefore, we  
28 used the constant value of  $\delta^{17}\text{O}(\text{O}_3)_{\text{bulk}} = 25.2 \%$  which represents the mean value observed in  
29 the Southern Hemisphere and measured during an Atlantic cruise in April/May 2012 (Viears  
30 and Savarino, 2014).~~

31 We note that Frey et al. (2014) have measured high  $[\text{NO}_2]/[\text{NO}]$  ratios which are not consistent  
32 with other measurements available at Dome C. The authors suggest that an unknown



1 mechanism which converts NO into NO<sub>2</sub> or interferences in the NO<sub>x</sub> measurements are  
2 responsible for the discrepancy observed. Given that the oxidant budget is not yet fully resolved  
3 at DC, we stick to our simple parameterization of the local resetting of the oxygen isotopic  
4 composition of NO<sub>2</sub> ~~(Eq (7))~~. We recall that we have made various simplifications in the  
5 description of the local cycling and oxidation of NO<sub>2</sub>. These assumptions include:  $\Delta^{17}\text{O}(\text{HO}_2)$   
6 = 0 ‰, ~~the simplified description of the neglected activity of O<sub>3</sub> when calculating  $\Delta^{17}\text{O}(\text{OH})$ ,~~  
7 ~~the simplified more complex NO to NO<sub>2</sub> conversion reaction scheme (and the potential greater~~  
8 ~~influence of with a O<sub>3</sub> could potentially have a greater influence of O<sub>3</sub>)~~ and, eventually, the  
9 neglected nighttime NO<sub>2</sub> oxidation pathway at the beginning and end of the sunlit season  
10 ~~(which, again, involves involving O<sub>3</sub>). For these reasons, w~~We therefore anticipate that the  $\Delta^{17}\text{O}$   
11 values simulated by TRANSITS at DC will represent the lower bound ~~to of~~ the observations,  
12 ~~because O<sub>3</sub>-dominated oxidation will imply larger  $\Delta^{17}\text{O}$  values.~~

Mis en forme : Indice

Mis en forme : Indice

### 13 Simulations across East Antarctica

14 Sampled sites on the D10-DC-Vostok route are characterized by a wide range of annual snow  
15 accumulation rates which gradually drop from 558 kg m<sup>-2</sup> a<sup>-1</sup> close to the coast (D10) to 20 kg  
16 m<sup>-2</sup> a<sup>-1</sup> high on the plateau (around Vostok) (Erbland et al., 2013). The simulation of nitrate in  
17 East Antarctic snowpacks and the investigation of TRANSITS's ability to reproduce such wide  
18 snow accumulation conditions, we consider 10 test sites whose snow accumulation rates are  
19 [20, 25, 30, 40, 50, 75, 100, 200, 300, 600] kg m<sup>-2</sup> a<sup>-1</sup>, respectively. For simplicity, we consider  
20 that  $A$  is the sole variable used to characterize different sites from the coast to the plateau in  
21 East Antarctica. All the other parameters and variables are kept the same of those for DC.  
22 TRANSITS is therefore run in the DC realistic configuration described above. This means that  
23 we do not consider changes in latitude, elevation or ozone column conditions which would  
24 impact the TUV-modeled actinic fluxes. Also, the physical, optical and chemical properties of  
25 the snowpacks are considered constant. No changes in ~~atmospheric temperature (which would~~  
26 ~~affect  $D$ ) and~~ local atmospheric chemistry ~~is~~ ~~are~~ taken into account and the horizontal export of  
27 nitrogen from locations on the plateau to those close to the coast is not modeled. Last, we  
28 hypothesize that the time series of atmospheric nitrate concentrations are the same than that  
29 measured at DC. This assumption is supported by the observation of Savarino et al. (2007) who  
30 show comparable atmospheric nitrate concentration time series at the coastal Dumont d'Urville  
31 station and at DC.

Mis en forme : Police :Italique

1 The parameters and variables used for the DC realistic simulation as well as those used for the  
2 simulations across East Antarctica are given in Table [3-3](#).

### 3 **3.1.3 Model initialization and output data**

4 The 1-m snowpack is initialized with a constant nitrate profile of  $\omega(\text{NO}_3^-) = 50 \text{ ngNO}_3^- \text{ g}^{-1}$ ,  
5  $\Delta^{17}\text{O}(\text{NO}_3^-) = 30 \text{ ‰}$  and  $\delta^{15}\text{N}(\text{NO}_3^-) = 50 \text{ ‰}$ . The atmosphere box is initialized with  $\gamma(\text{NO}_3^-) =$   
6  $5 \text{ ngNO}_3^- \text{ m}^{-3}$  and  $\Delta^{17}\text{O}$  and  $\delta^{15}\text{N}$  values of 30 ‰ and 5 ‰, respectively.

7 The model is run for a time sufficiently long to allow it to converge (e.g. 25 years for DC  
8 conditions). Raw data generated by the model are processed to obtain the time series of  
9 concentration and isotopic composition of atmospheric nitrate and in a top skin layer of 4 mm,  
10 the depth profiles of mass fraction,  $\delta^{15}\text{N}$  and  $\Delta^{17}\text{O}$  in snow nitrate and the time series of the  $\text{NO}_2$   
11 flux from the snow to the atmosphere.

12 From the simulated profiles of nitrate mass and isotopic composition in snow, we calculate the  
13 apparent fraction constants ( $^{15}\epsilon_{\text{app}}$  and  $^{17}E_{\text{app}}$ ) as in Erbland et al. (2013). Also, the nitrate mass  
14 and isotopic composition in the top 50 cm are calculated. We recall that the model also  
15 computes the simulated mass fraction and isotopic composition in the archived nitrate, which  
16 can be compared to the observed asymptotic values.

17 **[Sections 3.2 and 3.3 below were completely reorganized.]**

## 18 **3.2 Results**

19 In this section, we briefly describe the simulated results. A comparison between the model  
20 results and the observations data will be given in the “evaluation and discussion” section. We  
21 note that the model results are insensitive to the values used for the model’s initialization.

### 22 **3.2.1 Simulation results at the DC air-snow interface**

23 Figure 4 gives the results at the air-snow interface for the DC-like realistic simulation: simulated  
24 nitrate concentrations,  $\delta^{15}\text{N}$  and  $\Delta^{17}\text{O}$  in both the atmospheric and skin layer compartments as  
25 well as the simulated fluxes ( $FD$ ,  $FE$ ,  $FP$ ) together with the observations at Dome C in 2007-  
26 2008 and 2009-2010. Table 4 gives a summary of averages and minimum/maximum of the  
27 simulated values in the atmosphere and skin layer.

28 In the atmospheric compartment, the average nitrate concentration is  $32 \text{ ng m}^{-3}$  which represents  
29 an average mass of  $3.6 \times 10^{-4} \text{ mgN m}^{-2}$ . Atmospheric concentrations start to rise by the

1 beginning of August and peak at 110 ng m<sup>-3</sup> at the end of November to get back to winter  
2 background values (5 ng m<sup>-3</sup>) in March. The simulated annual weighted  $\delta^{15}\text{N}$  value is +0.2 ‰.  
3 Simulated atmospheric  $\delta^{15}\text{N}$  values first show a 20 ‰ decrease in spring from the winter mean  
4 value of approx. +10 ‰, which concurs with the beginning of the increase in atmospheric  
5 concentrations (mid-Aug. to mid-Oct.) and then an increase at a rate of approx. 10 ‰ per month.  
6 The highest atmospheric  $\delta^{15}\text{N}$  value is approx. +20 ‰ and is simulated in early February. The  
7 simulated annual weighted  $\Delta^{17}\text{O}$  value is 23.7 ‰. The highest atmospheric  $\Delta^{17}\text{O}$  values are  
8 simulated in winter (39.3 ‰ in Jul.-Aug.). They rapidly decrease by 18 ‰ from mid-Aug. to  
9 October, remain stable around 22 ‰ throughout the summer and slowly start to rise in February  
10 to reach winter values in July.

11 In the skin layer compartment, the average nitrate mass fraction is 3074 ng g<sup>-1</sup>, which represents  
12 an average mass of 0.8 mgN m<sup>-2</sup>. Skin layer mass fractions start to rise in June when the  
13 stratospheric nitrate input occurs and peak at 5706 ng g<sup>-1</sup> at the end of December to gradually  
14 get back to winter background values (700 ng g<sup>-1</sup>) in June. The simulated annual weighted  $\delta^{15}\text{N}$   
15 value is +34.9 ‰. Simulated atmospheric  $\delta^{15}\text{N}$  values in the skin layer and atmosphere show  
16 similar variations:  $\delta^{15}\text{N}$  values in the skin layer are stable in winter (+20 ‰), decrease by 5 ‰  
17 in spring, increase at a rate of approx. 20 ‰ per month in summer, reach a maximum value of  
18 +60 ‰ in early February before decreasing at a rate of ca. 10 ‰ per month in winter. The  
19 simulated annual weighted  $\Delta^{17}\text{O}$  value is 25.5 ‰. Here, simulated atmospheric  $\Delta^{17}\text{O}$  values in  
20 the skin layer and atmosphere show similar variations: maximum  $\Delta^{17}\text{O}$  values in skin layer are  
21 simulated in winter (38.9 ‰ in Jul.-Aug.), rapidly decrease by 18 ‰ from mid-Sep. to October  
22 and remain stable around 21 ‰ throughout the summer and slowly start to rise in February to  
23 reach winter values in July.

24 The comparison of those two compartments shows that the average nitrate mass in the skin  
25 layer compartment is 2300 times higher than that in the atmospheric compartment. Also, we  
26 observe that nitrate mass fractions in the skin layer start to rise two months earlier than  
27 atmospheric concentrations do and that the summer maxima is simulated one month later.  
28 Annual weighted  $\delta^{15}\text{N}$  and  $\Delta^{17}\text{O}$  values in the skin layer are shifted by +34.7 ‰ and +1.7 ‰,  
29 respectively, compared to the atmospheric value. Variations in  $\delta^{15}\text{N}$  in both compartments are  
30 in phase, however, the spring decrease in  $\delta^{15}\text{N}$  values is smaller in the skin layer than in the  
31 atmosphere and the increasing rate in summer is two times higher. Consequently, the difference  
32 between  $\delta^{15}\text{N}$  values in skin layer and atmospheric nitrate varies from +10 ‰ in winter to 38

1 %<sub>o</sub> in summer. Variations in  $\Delta^{17}\text{O}$  values in both compartments are almost in phase. The  
2 difference between  $\Delta^{17}\text{O}$  in skin layer and atmospheric nitrate is variable and negative in winter,  
3 increases in spring to reach +8 ‰ and is stable and slightly negative (-1 ‰) in summer.

4 Figure 5 and Table 5 give the snowpack results for the DC-like realistic simulation: simulated  
5 nitrate mass fraction and isotopic composition in the top 50 cm of snow and in the archived flux  
6 as well as the simulated apparent fractionation constants. The simulated nitrate mass in the top  
7 50 cm (Fig.5a) shows an average value of  $(8.1 \pm 1.6) \text{ mgN m}^{-2}$  (mean  $\pm 1 \sigma$ ). The simulated  
8  $m_{50\text{cm}}(\text{NO}_3^-)$  varies in the range 6.2–11.0  $\text{mgN m}^{-2}$  with its maximum reached by the end of  
9 September and its minimum reached by the end of January. The simulated isotopic composition  
10 of nitrate in the top 50 cm shows weighted averages of +100.5 ‰ and 23.3 ‰ for  $\delta^{15}\text{N}$  and  
11  $\Delta^{17}\text{O}$ , respectively (Figs.5c and 5f). The two time series also show cycles with variations  
12 respectively in anti-phase and in phase with variations of  $m_{50\text{cm}}(\text{NO}_3^-)$ ,  $\delta^{15}\text{N}_{50\text{cm}}(\text{NO}_3^-)$  and  
13  $\Delta^{17}\text{O}_{50\text{cm}}(\text{NO}_3^-)$  respectively vary in the 77.4–127 ‰ and 20.0–27.4 ‰ ranges.

14 The simulated  $^{15}\text{N}/^{14}\text{N}$  apparent fractionation constant shows an annual average of  $(-49.5 \pm 3.7)$   
15 ‰ with weak annual variations (from -43.0 to -53.6 ‰) (Fig.5d). The annually averaged  $^{15}\epsilon_{\text{app}}$   
16 value is slightly higher than the annual weighted mean  $^{15}\epsilon_{\text{pho}}$  value (-55.1 ‰). Compared to  
17  $^{15}\epsilon_{\text{app}}$ ,  $^{17}\epsilon_{\text{app}}$  shows variations of greater relative amplitude (from 0.7 to 2.4 ‰) with an annual  
18 average of  $(1.4 \pm 0.6)$  ‰.

19 Figure 6 shows the specific case of the simulated snow nitrate for the week of December 24 in  
20 the case of the DC realistic simulation. Simulated nitrate mass fractions decrease by more than  
21 two orders of magnitude in the top 15 cm and  $\delta^{15}\text{N}$  and  $\Delta^{17}\text{O}$  values increase and decrease with  
22 depth from 40 ‰ to a mean background value above 290 ‰ and from 21 ‰ to a mean  
23 background value below 18 ‰ at around 20-30 cm depth, respectively. The simulated profiles  
24 are smooth and a small secondary peak can be observed in the mass fraction profile at around  
25 9 cm depth, a depth which corresponds to one year of snow accumulation.

26 Table 6 gives the simulated nitrate mass fluxes and their isotopic composition in the case of the  
27 DC realistic simulation. The  $FA/FPI$  ratio for the DC-like simulation is 1.8 ‰, which means  
28 that a small fraction of the primary input flux of nitrate is archived below one meter. The  
29 remaining fraction ( $FE/FPI = 1 - FA/FPI = 98.2$  ‰) is exported outside the atmospheric box.  
30 The photolytic, deposition and export fluxes show a peak whose timing follows the sunlit  
31 season (Fig. 4a). The annual photolytic flux is  $32.1 \times 10^{-6} \text{ kgN m}^{-2} \text{ a}^{-1}$  and is compensated by  
32 an annual deposition flux of  $32.2 \times 10^{-6} \text{ kgN m}^{-2} \text{ a}^{-1}$ . Annually, the simulated  $FD$  and  $FP$  fluxes

1 represent four times the primary input flux of nitrate ( $FD \approx FP \approx 4 \times FPI$ ). In the archived  
2 nitrate, the simulated mass fraction,  $\delta^{15}\text{N}$  and  $\Delta^{17}\text{O}$  values are constant throughout the season:  
3 23.0 ng g<sup>-1</sup>, 318 ‰ and 17.8 ‰, respectively (Fig. 5, Tab. 6).

### 5 **3.2.2 Simulation results across East Antarctica**

6 Figure 7 shows the results for the TRANSITS simulations across East Antarctica in which only  
7 the snow accumulation rate is varied. The simulated  $^{15}\text{N}/^{14}\text{N}$  apparent fractionation constants  
8 are low ( $-46.1 \pm 2.2$ ) ‰,  $n = 4$ ) for East Antarctic plateau sites ( $A \leq 50 \text{ kg m}^{-2} \text{ a}^{-1}$ , Erbland et  
9 al., 2013) and close to zero ( $-10.3 \pm 9.0$ ) ‰,  $n = 3$ ) for coastal sites ( $A \geq 200 \text{ kg m}^{-2} \text{ a}^{-1}$ . Also,  
10 simulated plateau sites feature an average  $^{17}E_{\text{app}}$  value, which is significantly positive ( $+1.0 \pm$   
11 0.3) ‰, Fig. 7b). The simulated archived flux ( $FA$ ) and  $\Delta^{17}\text{O}(FA)$  both decrease with increasing  
12  $1/A$  (Figs. 7e and 7d). Simulated  $\delta^{15}\text{N}(FA)$  values monotonically increase with increasing  $1/A$ .  
13 Figure 8 presents the same results in a different way. Panel a is a “modified Rayleigh plot”  
14 where  $\ln(\delta^{15}\text{N}(FA) + 1)$  is represented as a function of  $\ln(FA)$  (which equals  $\ln(\omega(FA) \times A)$   
15 instead of  $\ln(\omega(FA))$ ). In this representation, we observe that the simulated data fall on a line  
16 whose slope is  $-0.064$ . Fig.8b shows that  $\Delta^{17}\text{O}(FA)$  and  $\delta^{15}\text{N}(FA)$  (Fig.8b) are negatively  
17 correlated.

### 19 **3.3 Evaluation and discussion**

20 In this section, we evaluate the model results in light of the observational constraints described  
21 above. In particular, we attempt to state clearly the observations, which are well reproduced by  
22 the model and those which are not. In the sections below, we also discuss the choice of the  
23 adjustment parameters which were made to run TRANSITS.

#### 25 **3.3.1 Validation of the mass loss, diffusion and $^{15}\text{N}/^{14}\text{N}$ fractionation** 26 **process**

27 The nitrate mass loss is quantitatively represented in the TRANSITS model. Indeed, Fig.6a  
28 shows that nitrate mass fractions decrease by a factor 10 in the top 10 cm of the snowpack in  
29 agreement with observations. Also, the simulated archived nitrate mass fractions values are

1 consistent with the observations (Fig.5). This means that the nitrate mass fraction lost by  
2 photolysis (1-f) and calculated from the photolytic rate constant (J, Eq. (1)) is quantitatively  
3 simulated by TRANSITS model runs.

4 Nitrate- $\delta^{15}\text{N}$  isotopic profiles in snow also show that the  $^{15}\text{N}/^{14}\text{N}$  fractionation associated with  
5 nitrate photolysis is quantitatively represented within the uncertainties. Indeed, the DC realistic  
6 simulation reproduces well the depth profile of  $\delta^{15}\text{N}$  in snow nitrate as observed on Fig.6b with  
7 simulated  $\delta^{15}\text{N}$  values as high as 150 ‰ at 10 cm depth. First, the simulated  $^{15}\text{N}/^{14}\text{N}$  apparent  
8 fractionation constants are consistent with the observations at Dome C (Fig. 5d) and for plateau  
9 sites ( $A \leq 50 \text{ kg m}^{-2} \text{ a}^{-1}$ , Fig. 7a). This means that the absorption cross sections used for  $^{14}\text{NO}_3^-$   
10 and  $^{15}\text{NO}_3^-$  (Berhanu et al., 2014a) and the variables used in the TUV-snow model ( $\text{O}_3$  column)  
11 allow a quantitative description of the  $^{15}\text{N}/^{14}\text{N}$  fractionation constant associated with nitrate  
12 photolysis ( $^{15}\epsilon_{\text{photo}}$ , Eq. (3)). Secondly, the  $\delta^{15}\text{N}$  values in the archived nitrate is well reproduced  
13 by the model: the simulated  $\delta^{15}\text{N}(\text{FA})$  value (318 ‰) compares well with the observations (from  
14 275 to 300 ‰, Fig. 5f). This is a further evidence that the nitrate mass fraction lost by photolysis  
15 (1-f) are quantitatively simulated by TRANSITS model runs. Indeed, using ~~the same~~ a quantum  
16 yield of  $2.1 \times 10^{-3}$  at 246 K as in France et al. (2011) ( ~~$2.1 \times 10^{-3}$  at 246 K~~) not only leads to  
17 unrealistic FA/FPI ratio (71 %) and  $\omega(\text{FA})$  value (917  $\text{ng g}^{-1}$ ) but also to a very small  $\delta^{15}\text{N}(\text{FA})$   
18 value (+20.3 ‰), which clearly reflects a weak recycling and an ~~important trapping~~  
19 overestimate of primary nitrate trapped in snow. The adjusted photolytic quantum yield of  $\Phi =$   
20 0.026 allows computing a consistent variation range of  $\delta^{15}\text{N}$  in nitrate archived at depth. Given  
21 the choice of a modeled cage effect of  $f_{\text{cage}} = 0.15$ , we obtain an apparent modeled quantum  
22 yield of  $0.85 \times 0.026 \approx 0.022$ , a value smaller than the mean value for buried nitrate (0.05) but  
23 higher than the smallest value observed for this domain (0.003) (Meusinger et al., 2014).

24 Additionally, we observe from Fig. 6a that the simulated profiles are smooth and that a small  
25 secondary peak can be observed in the simulated mass fraction profile at around 9 cm depth,  
26 consistently with ~~these~~ observations. Such smooth profiles can only be simulated because  
27 nitrate diffusion was taken into account and turning this process off leads to simulated mass  
28 fraction and isotope profiles in the snow showing unrealistic spiky seasonal variations similar  
29 as those simulated by Wolff et al. (2002) and France et al. (2011). The secondary peak observed  
30 in simulated nitrate mass fraction profiles (at 9 cm depth, which corresponds to one year of  
31 snow accumulation) represents nitrate residual from the previous year's skin layer. This is  
32 consistent with secondary peaks observed in some snow pits on the Antarctic plateau, e.g. snow

Mis en forme : Police :Gras

Code de champ modifié

Mis en forme : Police :Gras

Code de champ modifié

Mis en forme : Police :Gras

1 pits (e.g. DC07-2, S21 (at 10 cm depth), S2 (at 7 and 17 cm depth) and S3 (around 10 cm  
2 depth) in Supplementary Information, Erbland et al. (2013). Since TRANSITS is able to  
3 reproduce such a feature, we conclude that a simplified description of nitrate diffusion (i.e.  
4 constant diffusion coefficient) is not detrimental.

5 The adjusted value used for  $D$  can be compared to the effective diffusivity of nitric acid in snow  
6 (denoted  $D_{\text{eff}}$ ) as calculated in Herbert et al. (2006) and by assuming that the snow layers are  
7 always under-saturated in nitrate. Such approach is followed because  $\text{HNO}_3$  is a sticky gas.  
8 According to Herbert et al. (2006), the  $D_{\text{eff}}$  is a function of the diffusivity of  $\text{HNO}_3$  in the  
9 interstitial air which depends on temperature and pressure (Massmann, 1998). Using a Specific  
10 Surface Area of snow of  $38 \text{ m}^2 \text{ kg}^{-1}$  (Gallet et al., 2011), a snow density of  $300 \text{ kg m}^{-3}$ ,  
11 the median temperature and pressure for DC summer 2012 (Kukui et al., 2014) and a partition  
12 coefficient in the uptake of  $\text{HNO}_3$  on ice (Crowley et al., 2010), we find  $D_{\text{eff}} = 7.3 \times 10^{-12} \text{ m}^2 \text{ s}^{-1}$ .  
13 Our adjusted value for  $D$  ( $1.0 \times 10^{-11} \text{ m}^2 \text{ s}^{-1}$ ) is close to the effective diffusivity of nitric acid  
14 in snow (denoted  $D_{\text{eff}}$ ) and more than three orders of magnitude higher than the diffusion  
15 coefficient of nitrate ion in a single monocrystal of ice calculated at the same temperature ( $2.6$   
16  $\times 10^{-15} \text{ m}^2 \text{ s}^{-1}$ , Thibert and Dominé, 1998), which means that the macroscopic mobility of nitrate  
17 in the snowpack is mostly the consequence of  $\text{HNO}_3$  mobility in the interstitial air. We recall  
18 that our description of nitrate diffusion in the snowpack is basic and that the picture may well  
19 be more complicated with, e.g. wind pumping effects and temperature gradients in snow.

Mis en forme : Exposant

### 21 **3.3.2 Validation of the cage effects**

22 The choice of a non-zero value for  $f_{\text{cage}}$  allows generating decreasing  $\Delta^{17}\text{O}$  profiles in snow in  
23 accordance with the observations in three snow pits from DC (Fig.6c). On this figure, the  
24 decreasing trend in the data overlaps with additional variability in  $\Delta^{17}\text{O}$ . A better metric to  
25 evaluate the changes in  $\Delta^{17}\text{O}$  associated with depth, i.e. with the loss of nitrate, is the apparent  
26  $^{17}\text{O}$ -excess fractionation constant,  $^{17}E_{\text{app}}$ . Fig.5g shows that the simulated  $^{17}E_{\text{app}}$  values at DC  
27 are positive, consistently with the observations, confirming the decreasing contribution of cage  
28 recombination effects to  $\Delta^{17}\text{O}(\text{NO}_3^-)$  (McCabe et al., 2005, Frey et al., 2009). The simulation  
29 across East Antarctica confirms the ability of the model to reproduce the sensitivity of  $\Delta^{17}\text{O}$  to  
30 the nitrate mass loss (Fig.7). Indeed, for sites with  $A \leq 50 \text{ kg m}^{-2} \text{ a}^{-1}$ , the model calculates a  
31 mean  $^{17}E_{\text{app}}$  value of  $(+1.0 \pm 0.3) \text{ ‰}$  for the December/January period while the observed

1 average value is  $(+2.0 \pm 1.2) \%$  (mean  $\pm 1 \sigma$ ,  $n = 10$ ). We observe that an  $f_{\text{cage}}$  parameter set to  
2 0 would have led to a mean December/January  $^{17}E_{\text{app}}$  value almost nil:  $(+0.3 \pm 0.2) \%$ .

### 4 **3.3.3 Validation of the macroscopic fluxes**

5 The primary input flux of nitrate to the air-snow system ( $FPI$ ) derived from Muscari and de  
6 Zafra (2003) (and from our assumption  $FT = FS$ ) is realistic. Indeed, simulated and observed  
7 East Antarctica data almost fall on the same line of slope -0.065 in the modified Rayleigh plot  
8 (Fig.8a). In this representation, changing  $FPI$  leads to the horizontal shift of the simulated data  
9 thus confirming the realistic value of  $FPI = 8.2 \times 10^{-6} \text{ kgN m}^{-2} \text{ a}^{-1}$ . We note that our simulation  
10 in East Antarctica is very simple because it only takes into account changes in snow  
11 accumulation rates, which are large on the D10–DC–Vostok route. A more sophisticated  
12 simulation along this line is beyond the scope of the present study because it would require  
13 including a radiative transfer model such as TUV-snow (or such as TARTES, Libois et al.,  
14 2014) in TRANSITS in order to deal with latitudinal and elevation changes. Also, the  
15 simulation should take into account boxes from Vostok to D10 with the exchange of nitrate  
16 horizontally exported from the center of the continent towards the coast, basically changing our  
17 1-D model into a 2-D model.

18 The maximum value of the photolytic flux ( $FP$ ) simulated for DC is  $3.27 \times 10^{-12} \text{ kgN m}^{-2} \text{ s}^{-1}$   
19 (Fig. 4a, Tab. 6), a value around 40 times higher than that obtained by France et al. (2011). This  
20 difference is not surprising since we are using a quantum yield 12 times higher than France et  
21 al. (2011). The different scaling may be explained by the differences in the complexities of the  
22 two models (TRANSITS includes recycling and a net export). The observed median  $\text{NO}_x$   
23 emission fluxes are  $1.6 \times 10^{-13} \text{ kgN m}^{-2} \text{ s}^{-1}$  and  $3.7 \times 10^{-13} \text{ kgN m}^{-2} \text{ s}^{-1}$  over the 22 December  
24 2009 to 28 January 2010 period (Frey et al., 2013) and the 1 December 2011 to 12 January 2012  
25 period (Frey et al., 2014), respectively. Our computed median  $\text{NO}_2$  fluxes over the same periods  
26 are  $2.8 \times 10^{-12} \text{ kgN m}^{-2} \text{ s}^{-1}$  and  $3.3 \times 10^{-12} \text{ kgN m}^{-2} \text{ s}^{-1}$ , i.e. values respectively 18 and 9 times  
27 higher than in the observations by Frey et al. (2013, 2014).

28 The discrepancy between simulated and observed  $FP$  values may be explained by the fact that  
29  $FP$  represents the potential flux of  $\text{NO}_2$  emitted from the snow to the atmosphere, i.e. an upper  
30 limit when comparing to the observed  $\text{NO}_2$  flux. TRANSITS does not take into account various  
31 potential processes affecting  $\text{NO}_x$  emission from snow, such as gas-phase diffusion or chemical



1 conversion prior to emission and forced ventilation from the snowpack (France et al., 2011;  
2 Frey et al., 2013; Meusinger et al., 2014). Future improvements of the model could include an  
3 explicit representation of the vertical transport of NO<sub>2</sub> within and outside the snowpack with  
4 the following processes: NO<sub>x</sub> diffusion, wind pumping, ~~mixing~~, chemical conversion and  
5 deposition prior to the net emission from the snow, the latter depending on oxidant levels in  
6 firn air (HO<sub>x</sub>, O<sub>3</sub>, and maybe halogens, Zatzko et al., 2013). Another improvement could be the  
7 modeling of two nitrate domains (photolabile and buried nitrate, Meusinger et al., 2014).

8 We note that if HONO production is greater than assumed at Dome C, following the recent  
9 laboratory study of Scharko et al. (2014), this will not change the main conclusions of this  
10 study. Indeed, the photolytically produced HONO will be photolyzed to form NO in the  
11 atmosphere and this NO would simply enter the NO/NO<sub>2</sub> cycles where oxygen isotopes are  
12 reset.

13 The parameterization of HNO<sub>3</sub> deposition is simplistic since it solves the mass balance equation  
14 (Eq. (4)) in order to reproduce the nitrate concentration in the atmosphere. A sensitivity test of  
15 TRANSITS has been run using nitrate atmospheric concentrations 10 times higher than the  
16 ideal DC time series used for the DC realistic simulation. The higher nitrate concentration in  
17 the atmosphere had no significant impact on any of the nitrate reservoirs both in terms of mass  
18 and isotopic composition. Indeed, in the case of the DC realistic simulation, the atmospheric  
19 nitrate mass represent a 1/2300<sup>th</sup> and a 1/22500<sup>th</sup> of nitrate mass in the skin layer and in the top  
20 50 cm, respectively. Future improvements of the model could use a physical description of the  
21 deposition of HNO<sub>3</sub> using for example a vertical deposition velocity.

22 Hereafter, the ratio  $FA/FPI$  is termed the “nitrate trapping efficiency” because it reflects the  
23 fraction of nitrate that is trapped below the photic zone. In the DC realistic simulation, the  
24 nitrate trapping efficiency is 1.8 % (Tab. 6), which means that only a small fraction of the  
25 primary nitrate is archived. Consequently, the next export of nitrate is ~~important~~ significant ( $FE$   
26 = 98.2 % of the nitrate of primary origin =  $8.05 \times 10^{-6}$  kgN m<sup>-2</sup> a<sup>-1</sup>, Tab. 6) and reflects the  
27 chosen adjusted value of  $f_{exp}$  (0.2). To the best of our knowledge, there is no observation that  
28 could independently corroborate this  $FE$  value because it would require the direct measurement  
29 of this flux. We however point out that a non-zero  $f_{exp}$  parameter is necessary to reproduce  
30 realistic  $\delta^{15}N$  values both in the atmosphere and skin layer. Indeed, when running the model  
31 with  $f_{exp} = 0$ ,  $\delta^{15}N$  values in those compartments become highly negative ( $\leq -120$  ‰) which is  
32 clearly not realistic when compared to the observations (Figs. 4e and 4h) and seen in Frey et al.

1 (2009). Also, in such conditions, the model does not converge within a reasonable time and  
2 simulated nitrate endlessly builds up in the photic zone.

3 The parameter  $f_{\text{exp}}$  can however be related to physical variables. Indeed, it represents the  
4 competition between the export of NO<sub>y</sub> (NO<sub>2</sub> or HNO<sub>3</sub>) and the deposition of (to make it  
5 simple) HNO<sub>3</sub>. Let us consider atmospheric NO<sub>2</sub> and HNO<sub>3</sub> at steady-state. The deposition of  
6 NO<sub>2</sub> is neglected because it is a factor  $8.0 \pm 3.2$  slower than that of HNO<sub>3</sub> (Zhang, et al., 2009).  
7 Also, oxidation by OH is considered to be the only channel of NO<sub>2</sub> oxidation (an assumption  
8 valid in summer). Following the approach of Jacob (1999), a summertime value for  $f_{\text{exp}}$  can be  
9 approached by considering the chemical lifetime of NO<sub>2</sub> with respect to its oxidation by OH,  
10 the residence time of atmospheric NO<sub>2</sub> against horizontal export and that of atmospheric HNO<sub>3</sub>  
11 against deposition and horizontal export processes. Using kinetic rate constants from Atkinson  
12 et al. (2004), *T, P*, wind speeds and OH mixing ratios for mean summertime conditions at DC  
13 (Kukui, et al., 2014), HNO<sub>3</sub> dry deposition velocity from Huey et al. (2004), and vertical and  
14 horizontal characteristic dimensions of 100 m (average summertime boundary layer height,  
15 Gallée et al., 2014) and 400 km (Antarctic plateau width), respectively, we obtain  $f_{\text{exp}} = 0.20$ , a  
16 value which equals the value used to adjust the model but which is rather fortuitous. Indeed, we  
17 acknowledge that this calculation suffers from a number of uncertainties, e.g. using kinetic rate  
18 constants of NO<sub>2</sub> + OH from Sander et al. (2006), we obtain  $f_{\text{exp}} = 0.36$ . Future improvements  
19 of the model could aim at a physical parameterization of the nitrate export.

Mis en forme : Anglais (États-Unis), Ne pas vérifier l'orthographe ou la grammaire

### 21 3.3.4 Validation of the residence time in the photic zone and calculation of 22 the average number of recyclings

23 Results from the East Antarctica simulations show that the observed linear  $\delta^{15}\text{N}(FA)$  versus  $1/A$   
24 relationship (Freyer et al., 1996, Erbland et al., 2013) is very well reproduced (Fig. 7c). This  
25 demonstrates that the residence time of nitrate in the snowpack zone of active photochemistry  
26 is treated in a realistic manner in the model, ~~as a result of the correct description of snow~~  
27 ~~accumulation and nitrate photochemistry at depth.~~ When snow accumulation rates get very low  
28 ( $A < 20 \text{ kg m}^{-2} \text{ a}^{-1}$ ), simulated  $\delta^{15}\text{N}(FA)$  values do not seem to reach an asymptotic value as  
29 observed in the field where  $\delta^{15}\text{N}(\text{as.})$  seems to reach a plateau not exceeding 360 ‰ (Fig.7c).  
30 This observed feature could be the result of the different nitrate locations on snow grains, with  
31 buried nitrate (Meusinger et al., 2014) whose photolysis is, constituting a lower limit in the  
32 photolysis loss process.

1 Nitrate recycling at the air-snow interface at DC is observed and illustrated by the simulated  
2 macroscopic photolytic and deposition fluxes at the snowpack surface. Indeed,  $FP$  and  $FD$   
3 almost equilibrate and these annual fluxes are 4 times higher than the annual primary input of  
4 nitrate ( $FPI$ , Tab. 6).

5 Here, our main focus is on nitrate which is archived below the zone of active photochemistry  
6 because only this one that is ultimately archived in ice cores. One key question is to determine  
7 the “Yearly Average Number of Recyclings” which was undergone by the archived nitrate  
8 (hereafter denoted  $YANR(FA)$ ). To this end, a new tracer, denoted  $CYCL$ , has been introduced  
9 in the TRANSITS model. In a given box (snow layer or atmosphere),  $CYCL$  represents the  
10 average number of recyclings undergone by nitrate in the considered box. The  $CYCL$  variable  
11 follows a numerical treatment comparable to that of  $\delta^{15}N$  and  $A^{17}O$ , i.e. a “recycling” (instead  
12 of an isotopic) mass balances, diffusion and the calculation of  $CYCL$  values in the macroscopic  
13 fluxes ( $FP$ ,  $FD$ ,  $FE$ ,  $FA$ ). The  $CYCL$  value for primary nitrate is set to 0 and  $CYCL$  variables in  
14 the boxes are incremented by 1 each time  $NO_2$  molecules cross the air-snow interface.  
15  $YANR(FA)$  is calculated as a mass-weighted average of the  $CYCL$  values of the 52 snow layers  
16 which are archived below 1 m over the course of one year.

17 Following the above approach for the Dome C simulation, we obtain  $YANR(FA) = 4.0$  for the  
18 last layer before leaving the photic zone which means that, on average, the archived nitrate at  
19 Dome C has undergone 4.0 recyclings (i.e. loss, local oxidation, deposition). We recall that this  
20 number of recyclings represents an average value for the archive nitrate. Considering individual  
21 ions in the archived nitrate, the range of number of recyclings must be wide since some ions  
22 may well have travelled through the entire snowpack zone of active photochemistry without  
23 been recycled while some did undergo many recyclings.

24 Figure 7g shows the  $YANR(FA)$  values calculated for the 10 simulated sites in East Antarctica.  
25 We observe that  $YANR(FA)$  is proportional to  $1/A$  for  $A \geq 50 \text{ kg m}^{-2} \text{ a}^{-1}$  which means that the  
26 burial of nitrate (i.e. the residence time of nitrate in the photic zone) determines the  $YANR(FA)$   
27 value. On the Antarctic plateau, where snow accumulations rates are below this threshold value,  
28  $YANR(FA)$  reaches a plateau on the order of 4 recyclings. Concurrently, we observe that  $FP$   
29 remains constant at  $32.8 \times 10^{-6} \text{ kgN m}^{-2} \text{ a}^{-1}$  (data not shown) because increasing residence time  
30 of nitrate in the photic zone with decreasing snow accumulation rates lead to a nitrate mass  
31 fraction profile in snow which becomes more asymmetric with most of nitrate getting confined  
32 in a thinner layer at the top. As a result,  $FP$  levels off due to the negative feedback of the

1 decreasing nitrate mass fractions at depth. Figure 7g clearly shows the following relationship  
2 between that  $YANR(FA)$  is linked to and  $FP$  and the exact expression is:  $YANR(FA) = \frac{FP}{-FP}$ . This  
3 finding represents an independent confirmation of the definition given by Davis et al. (2008)  
4 on the basis of the macroscopic yearly primary and photolytic fluxes: the “Nitrogen Recycling  
5 Factor”, NRF = ratio of nitrogen emission and nitrogen deposition. While we are satisfied to  
6 end up with the Davis et al. (2008) expression for  $YANR(FA)$  using our independent model-  
7 based tracer experiment, it must be noted that we define  $YANR$  as the average number of  
8 recyclings undergone by the archived nitrate while Davis et al (2008) define it as the “nitrogen  
9 recycling factor within a photochemical season”.

### 11 **3.3.5 Validation of the nitrate mass in each compartment**

12 Nitrate mass in the different compartments is reasonably well reproduced by the model. Indeed,  
13 the simulated average nitrate mass in the atmospheric compartment represents a 1/22500<sup>th</sup> of  
14 that in the top 50 cm of snow and this is consistent with observations in 2009-2010 where this  
15 ratio is 1/8300 (Tables 4 and 5, considering a constant boundary layer height of 50 m). Also,  
16 the annual variations in nitrate mass fractions in the skin layer are well reproduced by the model:  
17 deviations from the winter background values occur during the sunlit season to reach a  
18 maximum in December (Fig. 4g). We however note that the period of high values above  
19 background is longer (September to April) for the simulation than in the observations  
20 (October/February). Lastly, simulated nitrate mass in the top 50 cm of snow has been shown to  
21 increase in winter and to decrease during the sunlit season (Fig.5a), similarly to the observed  
22 data: the average winter  $m_{50\text{cm}}(\text{NO}_3^-)$  value ( $3.6 \pm 0.5$  mgN m<sup>-2</sup>, May to Nov.) is higher than  
23 the average summer value ( $3.2 \pm 1.2$  mgN m<sup>-2</sup>, Dec. to Apr.). In winter, the input and output  
24 to the nitrate reservoir in the top 50 cm of snow are the deposition and archiving fluxes,  
25 respectively. During this season, the deposition flux is greater than the archiving flux which  
26 leads to an increase in  $m_{50\text{cm}}(\text{NO}_3^-)$ . When the sunlit season starts, the additional photolysis  
27 output flux starts, leading the sum  $FA + FP$  to exceed  $FD$  and thus decreasing  $m_{50\text{cm}}(\text{NO}_3^-)$ .

28 Additionally, the simulated average mass ratio between the skin layer and the top 50 cm of  
29 snow is 10 % (Tables 4 and 5), a value approx. 3 times higher than the 2009-2010 observed  
30 value (3 %, considering a snow density of 300 kg m<sup>-3</sup> for the skin layer snow). This discrepancy  
31 is accompanied by a factor 2.4 between simulated and observed annual average  $m_{50\text{cm}}(\text{NO}_3^-)$

1 values ( $8.1 \pm 1.6$ ) mgN m<sup>-2</sup> versus ( $3.4 \pm 1.0$ ) mgN m<sup>-2</sup>, Fig. 5a) and by a factor 7.9 between  
2 simulated and observed annual average mass fractions in the skin layer (3074 ng g<sup>-1</sup> versus 390  
3 ng g<sup>-1</sup>, Fig. 4g). Nitrate mass in the top 50 cm and in the skin layer are therefore higher in the  
4 DC simulation than in the observations and nitrate in the skin layer is more concentrated in the  
5 simulation.

6 Fully resolving these discrepancies is beyond the scope of this paper. However, we first note  
7 that lower observed skin layer mass fractions could be linked to heterogeneities in sampling the  
8 skin layer (whose thickness is  $4 \pm 2$  mm, Erbland et al., 2013), especially when considering  
9 that different overwintering people were involved in this task. For instance, sampling 6 mm  
10 instead of 4 mm could lead to the sampling of a more diluted skin layer. However, we  
11 acknowledge that this sampling issue would have a limited impact on the observed skin layer  
12 mass fractions. Secondly, higher simulated annual  $m_{50\text{cm}}(\text{NO}_3^-)$  values could be the result of the  
13 time-response of the modeled snowpack to past changes in primary input fluxes. Indeed, when  
14 run in the DC realistic simulation with a multiplication of *FPI* by a factor 10 after 25 years of  
15 simulation, TRANSITS shows a time-response of approximately 21 years. This means that the  
16 snowpack requires 21 years to reach stable  $m_{50\text{cm}}(\text{NO}_3^-)$  values again. As a consequence, the  
17 different  $m_{50\text{cm}}(\text{NO}_3^-)$  value observed today at Dome C could reflect changes in primary input  
18 flux conditions as far back as one or two decades in the past. A third explanation involves the  
19 absence of a snow erosion process during which wind blows away a significant fraction of the  
20 non-cohesive skin layer. This process would decrease nitrate mass fractions in the skin layer as  
21 observed in the field around 10 January 2010 (Erbland et al., 2013) and, in turn, decrease nitrate  
22 mass fractions in the snow layers below.

### 23

### 24 **3.3.6 Validation of the $\delta^{15}\text{N}$ values in each compartment**

25 In section 3.2.1, we have seen that the simulated  $\delta^{15}\text{N}$  profiles in snow are consistent with the  
26 observations. In particular, apparent  $^{15}\text{N}/^{14}\text{N}$  fractionation constants are well reproduced  
27 leading the simulation of realistic  $\delta^{15}\text{N}(\text{FA})$  values. In this section, we compare the simulated  
28 and observed time series of  $\delta^{15}\text{N}$  in the atmospheric and skin layer nitrate.

29 Overall, the annual variations of  $\delta^{15}\text{N}$  values in skin layer and atmospheric nitrate are generally  
30 well reproduced by the model although some discrepancies can be noted Figs. 4e and 4h). For  
31 example, the winter observed  $\delta^{15}\text{N}$  values and 10 ‰ shift between atmosphere and snow are

1 well simulated supporting the choice of the  $^{15}\text{N}/^{14}\text{N}$  fractionation constant associated with the  
2 deposition of nitric acid (+10 ‰), the positive sign of  $^{15}\epsilon_{\text{dep}}$  being consistent with a dry  
3 deposition of  $\text{HNO}_3$ . Also, the spring variations and timing of atmospheric  $\delta^{15}\text{N}$  are well  
4 reproduced. Indeed, the lowest  $\delta^{15}\text{N}$  values in the atmospheric nitrate occur in October  
5 (simulated: -25.3 ‰, observed: -17.0 ‰, Fig. 4e) when the stratospheric input has stopped and  
6 when the UV radiation becomes significant to encourage the production of isotopically depleted  
7  $\text{NO}_x$  from the snowpack. The return to positive atmospheric  $\delta^{15}\text{N}(\text{NO}_3^-)$  values in summer is  
8 faster at Dome C than it has been observed at DDU and this feature has been attributed to the  
9 longer exposure time of nitrate at the snow surface at Dome C (Savarino et al., 2007; Frey et  
10 al., 2009). TRANSITS confirms this suggestion when run with the higher snow accumulation  
11 rate which characterizes DDU (data not shown). At Dome C, shortly after the decrease,  $\delta^{15}\text{N}$   
12 values rapidly start to rise again because the nitrate in snow becomes more enriched in  $^{15}\text{N}$  and  
13 the extracted  $\text{NO}_2$  has rising  $\delta^{15}\text{N}$  values as well. With large  $\theta$  values at the end of the summer,  
14 the apparent ozone column crossed by the UV rays is more important and the photolytic  
15 fractionation constant ( $^{15}\epsilon_{\text{pho}}$ ) becomes more negative (Fig. 5d). This leads to decreasing  $\delta^{15}\text{N}$   
16 values extracted from the snowpack even if the enrichment does not stop there. Finally,  
17 wintertime values of  $\delta^{15}\text{N}$  are reached back by the end of April/beginning of May when the  
18 nitrate photolysis stops.

19 The simulated annual variation of skin layer  $\delta^{15}\text{N}$  is also consistent with the observations.  
20 However, the spring decrease observed in 2009-2010 is more marked than the simulation one  
21 (25 ‰ and 5 ‰, respectively, Fig. 4h). One reason is that the simulated  $\delta^{15}\text{N}$  values in skin  
22 layer start to rise 1.5 months earlier than in the observations (Fig. 4h). Although simulated  $\delta^{15}\text{N}$   
23 values start to rise earlier, we note that the summer increasing rate in skin layer  $\delta^{15}\text{N}$  values is  
24 similar in the simulations and in the observations (approx. +20 ‰ per month). One consequence  
25 of the 1.5 month delay between simulated and observed skin layer  $\delta^{15}\text{N}$  values is that the  $\delta^{15}\text{N}$   
26 difference between skin layer and atmospheric nitrate at the end of the summer is greater in the  
27 simulation than it is for the observation (approx. +40 ‰ versus +20 ‰). Focusing on the  
28 beginning of the skin layer,  $\delta^{15}\text{N}$  records (Fig. 4h) shows that the end of summer 2008-09 was  
29 different than the next year, with differences up to 40 ‰ between the simulation and  
30 observation. In particular, the large observed variations which lead to skin layer  $\delta^{15}\text{N}$  values as  
31 high as +60 ‰ (Erbland et al., 2013) are not reproduced by the model. This could be the result  
32 of snow sampling effects (i.e. local spatial heterogeneity or different sampling of the operator  
33 in the field).

### 3.3.7 Photolytically-driven dynamic equilibrium at the air-snow interface

The simulated variations of  $\Delta^{17}\text{O}$  in the atmospheric and skin layer compartments are consistent with the observations, i.e.  $\Delta^{17}\text{O}$  decreases from high winter values to the lowest values in the middle of summer (Figs. 4f and 4i). The model also reproduces well the small negative difference between the atmospheric and skin layer annual weighted  $\Delta^{17}\text{O}$  values (simulated: -1.2 ‰, observed: -2.3 ‰). When considering the annual variability of the difference in  $\Delta^{17}\text{O}$  in the atmosphere and skin layer, the model reproduces well the important shift in early October (simulated: -8 ‰, observed: -7 ‰) as well as the small negative shift by the end of the summer (simulated: approx. -2 ‰, observed: approx. -2 ‰).

The above observations show that TRANSITS is able to qualitatively reproduce the  $\Delta^{17}\text{O}$  variations in nitrate for each compartment. Concurrent variations in  $\Delta^{17}\text{O}$  in atmospheric and skin layer nitrate indicate equilibrium at the air-snow interface. The simulated and observed differences between  $\Delta^{17}\text{O}$  in the atmosphere and skin layer are the result of their respective nitrate reservoirs and indicate that the isotopic equilibrium is dynamic. Another evidence for the different size reservoir is that the (oxygen and nitrogen) isotope time series in the skin layer are smoother than in the atmosphere (Fig.4).

The photolytic and deposition fluxes in summer show that there is an intense nitrate recycling at the air-snow interface at this season (Fig.4a), a feature which is confirmed by our calculation of the average number of recyclings undergone by the archived nitrate ( $YANR(FA) = 4.0$ ). The local signature of  $\text{NO}_2$  cycling and oxidation harbored by  $\Delta^{17}\text{O}$  is therefore incorporated in skin layer nitrate. Given the good qualitative agreement between the simulated and observed  $\Delta^{17}\text{O}$  in skin layer nitrate throughout the year, we conclude that TRANSITS has a realistic representation of the local cycling and oxidation of  $\text{NO}_2$  in the atmosphere.

We also observe that TRANSITS reproduces well the  $\Delta^{17}\text{O}(FA)/\delta^{15}\text{N}(FA)$  anti-correlation and general trend in the case of the simulation across East Antarctica (Fig.8c). This anti-correlation is partly the result of the cage recombination effects but some of it is also due to the greater incorporation of the summertime isotopic signature of the local cycling and oxidation of the photolytically produced  $\text{NO}_2$ . On the same figure, the observations show a large scattering of approx. 5 ‰ when compared to data simulated by TRANSITS. One reason for that is the inability of the model to reproduce variations of  $\Delta^{17}\text{O}$  in nitrate below 20 cm which can be as

1 high as 5 ‰ (Fig.6c). Such variations may be linked to variability in ozone column, snow  
2 accumulation, local atmospheric chemistry, primary inputs of nitrate from one year to another  
3 which are not accounted for by TRANSITS. McCabe et al. (2007) first observed such 2–3 years  
4 period cycles in a 6-m snow pit from South Pole and attributed these cycles to variability in the  
5 stratospheric ozone column or to stratospheric nitrate import; the same periodicity in  $\Delta^{17}\text{O}$  is  
6 found in DC surface snow (Frey et al., 2009, Erbland et al., 2013). Future work should  
7 investigate the impact of the variations in the ozone column on the  $\Delta^{17}\text{O}$  in the archived nitrate.  
8 Quantitatively speaking,  $\Delta^{17}\text{O}$  values in the atmosphere, skin layer, in the top 50 cm of snow  
9 and in the archived nitrate are not well reproduced. Indeed, the simulated annual weighted  $\Delta^{17}\text{O}$   
10 values in the atmosphere and skin layer are approx. 6 ‰ lower than in the observations (23.7  
11 ‰ versus 29.4 ‰ and 25.5 ‰ versus 31.7 ‰, respectively). The same is observed for simulated  
12  $\Delta^{17}\text{O}_{50\text{cm}}(\text{NO}_3^-)$  and  $\Delta^{17}\text{O}(\text{FA})$  values (Figs. 5f and 5h). From Figs.4f and 4I, we observe that  
13 wintertime  $\Delta^{17}\text{O}$  values in atmospheric and skin layer nitrate are reasonably well reproduced  
14 while most of the discrepancies are observed in summer.

### 16 **3.3.8 On the discrepancies between simulated and observed $\Delta^{17}\text{O}$ values**

17 In the previous section, we have shown that the model reproduces well the winter  $\Delta^{17}\text{O}$  values  
18 as well as the variations in  $\Delta^{17}\text{O}$  values in the different compartments. However, a quantitative  
19 transcription of the information harbored by the oxygen isotopes is not achieved yet by  
20 TRANSITS. In particular, the summer  $\Delta^{17}\text{O}$  values are 8 to 10 ‰ lower in the simulations than  
21 in the observations (Fig.4). We recall that a number of simplifications have been made in the  
22 description of the local cycling and oxidation of  $\text{NO}_2$ , thus leading to the simulation of  $\Delta^{17}\text{O}$   
23 values which must be considered as lower bounds.

24 First, the local oxidation of  $\text{NO}_2$  has been assumed to only occur through the daytime channel,  
25 i.e. through the oxidation by OH. In order to verify this hypothesis, we calculate  $r(\text{OH vs O}_3)$   
26  $= v(\text{OH}) / (v(\text{OH}) + v(\text{O}_3))$ , the relative apportioning of the daytime and nighttime  $\text{NO}_2$   
27 oxidation channel, with the assumption that the latter occurs through  $\text{NO}_2 + \text{O}_3$ . For the  
28 calculation of  $r(\text{OH vs O}_3)$ , we use kinetic rate constants from Atkinson et al. (2004), ozone  
29 mixing ratios from Legrand et al. (2009) and OH mixing ratios are extrapolated from  $J(\text{NO}_2)$   
30 calculated by TRANSITS and using the relationship  $[\text{OH}]/(\text{molecule m}^{-3}) = 2.5 \times 10^{14} \times$   
31  $J(\text{NO}_2)/\text{s}^{-1}$  (Kukui et al., 2014). For the realistic DC simulation,  $r(\text{OH vs O}_3)$  is higher than 0.95



1 from the fourth week after sunrise to the second week before sunset, i.e. for more than 90 % of  
2 the sunlit season. We also note that for the periods when  $r(\text{OH vs O}_3) < 0.95$ , the actinic flux is  
3 at maximum 6 % of the maximum actinic flux calculated for summer solstice. The calculation  
4 of a *FP*-weighted average of  $r(\text{OH vs O}_3)$  gives 99 % which means that over the sunlit season,  
5 the daytime oxidation channel of  $\text{NO}_2$  is almost 100 times faster than the nighttime oxidation  
6 channel. This result supports our choice of the simple representation of  $\text{NO}_2$  oxidation (by OH  
7 only) in TRANSITS and cannot explain the discrepancy in the  $\Delta^{17}\text{O}$  values simulated in  
8 summer. However, we acknowledge that species such as halogen oxides (denoted XO) could  
9 compete with OH in the oxidation of  $\text{NO}_2$ , thus importing high  $\Delta^{17}\text{O}$  values (Savarino et al.,  
10 submitted).

11 Secondly, the calculation of  $\Delta^{17}\text{O}(\text{OH})$  has been simplified by assuming a constant value  
12 throughout the entire sunlit season. Given the low temperatures at the beginning and end of the  
13 sunlit season, we acknowledge that  $\Delta^{17}\text{O}(\text{OH})$  values may be higher at these periods because of  
14 the less efficient isotopic exchange in the removal of the  $\Delta^{17}\text{O}$  by OH inherited during its  
15 formation and because of the potential higher contribution of ozone photolysis in its production  
16 (Morin et al., 2011).

17 Thirdly, the cycling of  $\text{NO}_2$  is assumed to be in photochemical-steady state and ~~thus~~  
18 ~~that~~ therefore  $\Delta^{17}\text{O}(\text{NO}_2, \text{PSS})$  can be calculated following Eq. (7). For the DC realistic  
19 simulation, the computed  $\alpha$  variable varies in the range 0.80–1 with the minimum value  
20 calculated a few weeks after summer solstice when  $\text{O}_3$  mixing ratio reach its minimum (Legrand  
21 et al., 2009), and the maximum value calculated at the beginning and at the end of the sunlit  
22 season. The *FP*-weighted annual average value of  $\alpha$  is 0.86, which shows that the Leighton  
23 cycle is significantly perturbed by  $\text{HO}_2$  and  $\text{CH}_3\text{O}_2$  and the transfer of the  $^{17}\text{O}$ -excess harbored  
24 by ozone to  $\text{NO}_2$  is not 100 % efficient. The hypothesis of an annually constant BrO mixing  
25 ratio of 2.5 pptv is crude because it must be lower at the beginning and end of the sunlit season.  
26 However, we observe that BrO marginally contributes to  $\alpha$  at these periods. Also, while a  
27 TRANSITS simulation with  $\alpha$  set to 1 allows a better agreement with the observations, the  
28 simulated  $\Delta^{17}\text{O}$  values are still too low (e.g. in this case, the minimum summertime  $\Delta^{17}\text{O}$  values  
29 in skin layer, atmospheric and archived nitrate are 24.3 ‰, 25.4 ‰ and 20.0 ‰, respectively).  
30 This small experiment indicates that our current knowledge of the  $\text{NO}_x$  processing at Dome C  
31 is not complete and that some of our hypothesis should not be valid. In particular, the hypothesis  
32 of the photochemical steady-state of  $\text{NO}_x$  could be questioned. Indeed, we recall that the

1 NO<sub>x</sub>/HO<sub>x</sub> chemistry at Dome C is not yet completely understood (Kukui et al., 2014 and  
2 OPALE special issue) and a nitrogen species (HNO<sub>4</sub> or unknown species) is expected to disturb  
3 the NO<sub>x</sub> photochemical cycle leading to the high NO<sub>2</sub>/NO ratio observed by Frey et al., 2014  
4 and/or to participate in the oxidation of NO<sub>2</sub> (via e.g. XO, Savarino et al., submitted).

5 Fourthly, the  $\Delta^{17}\text{O}$  value associated with the stratospheric flux of nitrate could be higher than  
6 the 42 ‰ value used in our simulations and initially suggested by Savarino et al. (2007). In  
7 particular, it could explain the 2–3 years period observed in  $\Delta^{17}\text{O}(\text{NO}_3^-)$  from snow pits at South  
8 Pole (McCabe et al., 2007) and at Dome C (Frey et al., 2009; Erbland et al., 2013). Also, the  
9 model would benefit from a better description of the timing of the long-distance transport flux  
10 of nitrate and the time series of the  $\Delta^{17}\text{O}$  value associated with it both of which were set constant  
11 throughout the season in our simulations.

12 While a number of isotopic information are still required to produce more realistic simulations  
13 at Dome C, we acknowledge that the most critical requirement is a better understanding of the  
14 NO<sub>x</sub> chemistry on the Antarctic plateau. Integrating a more realistic chemistry in TRANSITS  
15 will probably amplify the intense NO/NO<sub>2</sub> cycling in the atmosphere and not fundamentally  
16 change the nature of the processes at play at the air-snow interface of DC. However, we  
17 anticipate that the type of archived information below the photic zone will not change, mostly  
18 because the seasonal  $\Delta^{17}\text{O}$  variations in atmospheric and skin layer nitrate are well reproduced.

#### 21 **4 A framework for the interpretation of nitrate isotope records in ice cores**

22 In section 3, we have run a DC realistic simulation as well as simulations representing various  
23 sites in East Antarctica. We have shown that the model reproduced reasonably well the  
24 available mass and isotopic observations. While a quantitative reproduction of  $\Delta^{17}\text{O}$  values in  
25 atmospheric and skin layer nitrate could not be achieved (mostly because of a lack of  
26 understanding of the NO<sub>x</sub> chemistry at Dome C), we have shown that variations in  $\Delta^{17}\text{O}$  values  
27 in these compartments were well reproduced.

28 ~~Potentially measurable quantities in ice cores are  $\delta(\text{FA})$ ,  $\delta^{15}\text{N}(\text{FA})$  and  $\Delta^{17}\text{O}(\text{FA})$  (e.g. Hastings~~  
29 ~~et al., 2005, Frey et al., 2009). Given snow accumulation rates derived independently, one can~~  
30 ~~also obtain  $\text{FA} = \delta(\text{FA}) \times A$ . In this section, we develop a framework for the interpretation of~~  
31 nitrate records in ice cores in the case where Dome C conditions apply. To this end, a larger

1 number of sensitivity tests of the TRANSITS model were run. Potentially measurable quantities  
2 in ice cores are  $\omega(FA)$ ,  $\delta^{15}N(FA)$  and  $\Delta^{17}O(FA)$  (e.g. Hastings et al., 2005, Frey et al., 2009).  
3 Given snow accumulation rates derived independently, one can also obtain  $FA = \omega(FA) \times A$ .

#### 4 4.1 Parameters and variables controlling $FA$ and $\delta^{15}N(FA)$

##### 5 4.1.1 Sensitivity tests: description and results

6 The sensitivity of the model is tested in simple cases where single variables and parameters are  
7 changed. For each simulation, the model was run for 25 years (i.e. until convergence). The  
8 realistic simulation for DC is used as the reference simulation. Tab. 5-7 provides an overview  
9 the variations imposed on the tested variables and parameters. The ~~four~~ five following variables  
10 and parameters have been set to 0 (Tab. 5-7):  $^{15}\epsilon_{dep}$ ,  $\Delta^{17}O(FS)$ ,  $\Delta^{17}O(FT)$ ,  $\Delta^{17}O(OH)$  and  
11  $\Delta^{17}O(O_3)_{bulk}$ . The  $\delta^{15}N(FS)$  and  $\delta^{15}N(FT)$  parameters have been changed to 119 ‰ and 100 ‰,  
12 respectively. The parameters  $FPI$  and  $h_{AT}$  were multiplied by a factor 10. The mixing ratios of  
13  $[BrO]$ ,  $[O_3]$ ,  $[HO_2]$  and  $[CH_3O_2]$  were multiplied by a factor 2. The nine following variables  
14 and parameters have been changed by +20 %:  $FS/FPI$ ,  $f_{cage}$ ,  $f_{exp}$ ,  $A$ ,  $\rho$ ,  $k$ ,  $q$ ,  $\Phi$  and  $D$ . The  
15 sensitivity to the snow accumulation ~~repartition-distribution~~ in the year has been tested by  
16 running the model with summer snow accumulation rates two times higher than the winter ~~ones~~  
17 rates and ~~conversely vice versa~~. The sensitivity to  $T$  has been tested by shifting the observed  
18 atmospheric temperature time series by -10 K. The model sensitivity to the ozone column has  
19 been run for four simulations: with constant ozone columns of 100 DU, 300 DU and 500 DU  
20 as well as with an ozone hole of 100 DU from Aug. to Nov. and an ozone column of 300 DU  
21 the rest of the time. Last, the sensitivity of the model to the atmospheric nitrate concentrations  
22 has been tested by running it with concentrations ten times higher than in the realistic DC  
23 simulation. The total number of simulations is then ~~3031~~, which includes the reference  
24 simulation.

25 For each test, the following outputs ( $FA$ ,  $FA/FPI$ ,  $\delta^{15}N(FA)$  and  $\Delta^{17}O(FA)$ ) were calculated.  
26 The description and results of the tests scenarios are given in Tab. 5-7. As an example and a  
27 guideline to read Tab. 5-7, we describe the result for the test where the snow accumulation rate  
28 was changed. The value used in the reference simulation is  $28 \text{ kg m}^{-2} \text{ a}^{-1}$  and that of the tested  
29 scenario is 20 % greater (i.e.  $33.6 \text{ kg m}^{-2} \text{ a}^{-1}$ ). Tab. 5-7 indicates that such an increase in  $A$  leads  
30 to an increase of the archived nitrate mass flux from ~~21.04-77~~ % to ~~43.32-90~~ % of the primary

1 nitrate mass flux.  $\Delta^{17}\text{O}$  in the archived nitrate is increased by 0.9-8 ‰. Conversely,  $\delta^{15}\text{N}$  in the  
2 archived nitrate is decreased by 4853.7-8 ‰ from 287317.4-7 ‰ to 238263.7-9 ‰.

3 Table 5-7 shows that ~~three-two~~ parameters and variables have no impact at all on the archived  
4  $h_{\text{AT}}$  and  $\gamma(\text{NO}_3^-)$  and  $^{15}\epsilon_{\text{dep}}$ . The reason ~~for these observations~~ is that the nitrate mass in the  
5 atmospheric box is negligible when compared to the nitrate reservoir in snow as discussed  
6 previously (section 3.3.5.3.3.7). The parameter  $FPI$  is the only one affecting  $FA$ , while  $FA$  and  
7  $FPI$  are linearly linked (i.e.  $FA/FPI$  remains constant), but this does not modify  $\delta^{15}\text{N}(FA)$ . The  
8  $\delta^{15}\text{N}$  signatures in the primary nitrate sources ( $\delta^{15}\text{N}(FS)$  and  $\delta^{15}\text{N}(FT)$  ~~and the  $^{15}\text{N}/^{14}\text{N}$~~   
9 ~~fractionation constant associated with deposition ( $^{15}\epsilon_{\text{dep}}$ )~~ have an impact on  $\delta^{15}\text{N}(FA)$ . ~~In~~  
10 ~~contrast~~ Likewise, some parameters only impact  $\Delta^{17}\text{O}(FA)$  such as the  $\Delta^{17}\text{O}$  signature in the  
11 primary nitrate sources ( $\Delta^{17}\text{O}(FS)$  and  $\Delta^{17}\text{O}(FT)$ ),  $\Delta^{17}\text{O}$  of bulk ozone,  $\Delta^{17}\text{O}$  of OH and  
12 parameters and variables driving the local cycling and oxidation of  $\text{NO}_2$ :  $[\text{O}_3]$ ,  $[\text{BrO}]$ ,  $[\text{HO}_2]$ ,  
13  $[\text{CH}_3\text{O}_2]$  and  $T$ .

14 The other parameters and variables impact at the same time  $FA$ ,  $FA/FPI$ ,  $\delta^{15}\text{N}(FA)$  and  
15  $\Delta^{17}\text{O}(FA)$ . These are:  $f_{\text{cage}}$ ,  $f_{\text{exp}}$ ,  $A$ ,  $\rho$ ,  $k$ ,  $q$ ,  $\Phi$ ,  $D$ ,  $FS/FPI$ , the snow accumulation ~~repartition~~  
16 ~~distribution~~ and the  $\text{O}_3$  column.

#### 17 4.1.2 Modified Rayleigh plots

18 From ice cores, one can measure  $\delta^{15}\text{N}(FA)$ ,  $\Delta^{17}\text{O}(FA)$ ,  $\omega(FA)$  and the annual snow  
19 accumulation rates ( $A$ ) thus allowing the calculation of  $FA = \omega(FA) \times A$ . In this section and the  
20 following, we attempt to provide an interpretation for  $\delta^{15}\text{N}(FA)$  values measured from ice cores.  
21 To this end, we use a data representation which we term “modified Rayleigh plot” where  
22  $\ln(\delta^{15}\text{N}(FA) + 1)$  is plotted against  $\ln(FA)$  rather than  $\ln(\omega(FA))$ , since it includes the variability  
23 in  $A$  in contrast to  $\omega(FA)$ . Fig. 940 summarizes the results obtained for most of the sensitivity  
24 which impact  $FA/FPI$ ,  $FA$  and  $\delta^{15}\text{N}(FA)$ , i.e. tests where the following variables are changed :  
25  $\Phi$ ,  $A$ ,  $\rho$ ,  $k$ ,  $q$ ,  $f_{\text{cage}}$ ,  $f_{\text{exp}}$ ,  $D$ ,  $FS/FPI$ ,  $FPI$ ,  $\text{O}_3$  column and the snow accumulation ~~repartition~~  
26 ~~distribution~~ in the year. The thick black dashed curve in Fig. 940 represents the DC realistic  
27 simulation in which  $\Phi$  is varied to obtain changes in  $FA$  and  $\delta^{15}\text{N}(FA)$ . The curve is almost  
28 linear with a slope of -0.061-064 passing through the “starting point” whose coordinates are  
29  $(\ln(FPI), \ln(\delta^{15}\text{N}(FPI) + 1))$ . For instance, this means that a decrease in the archived flux ( $FA$ ,  
30 i.e. changes in  $FA/FPI$ ) corresponds to an increase in  $\delta^{15}\text{N}(FA)$ .

Mis en forme : Non Exposit/ Indice

Mis en forme : Non Exposit/ Indice

Mis en forme : Exposit

Mis en forme : Exposit

Mis en forme : Police :12 pt

1 Most of the sensitivity simulation outputs fall on the thick black dashed curve, which represents  
2 the DC realistic simulation. We also observe from Fig. 940 that some simulations fall on curves  
3 which have different slopes or which have the same slope but different starting points. The  
4 parameters and variables are therefore sorted in 3 groups: those which control the “starting  
5 point”, those which control the slope in the modified Rayleigh plot and those which control the  
6 horizontal and vertical distances from the starting point, i.e. the final position on the curve.

#### 7 4.1.3 Controls on the “starting point”

8 Fig. 940 shows that the starting point is determined by  $FPI$  and  $\delta^{15}N(FT)$  and  $\delta^{15}N(FS)$ . On one  
9 hand, changes in  $FPI$  lead to a horizontal shift of the starting point (green star in Fig. 940) and,  
10 other things being equal, to a horizontal shift of the entire line in this plot. On the other hand,  
11 changes in the  $\delta^{15}N$  value in the primary input ( $\delta^{15}N(FT)$  and  $\delta^{15}N(FS)$ ) lead to a vertical shift  
12 of the starting point and the entire curve. Changes in the  $f_{exp}$  also result in a slight horizontal  
13 shift of the simulated “archived point”. Indeed,  $f_{exp}$  sets the net horizontal export of nitrate from  
14 the atmospheric box, which results in more or less of the primary input flux lost through this  
15 process. In the case of an increasing  $f_{exp}$  parameter, the “apparent”  $FPI$  is therefore shifted to  
16 lower  $FPI$  values.

17 Sensitivity tests where  $\delta^{15}N(FT)$  and  $\delta^{15}N(FS)$  were shifted by +100 ‰ show that significant  
18 amounts of the nitrogen signatures of the primary nitrate inputs are preserved (72-71 ‰ and 56  
19 58 ‰, respectively, Tab. 5-7), even if the recycling of nitrate has led to a 270-300 ‰ increase in  
20  $\delta^{15}N(FA)$ . Therefore,  $\delta^{15}N(FA)$  harbours harbors a fraction of the nitrogen isotopic signature of  
21 the primary inputs of nitrate but we note that it remains almost insignificant given the observed  
22 low variability of  $\delta^{15}N(FS)$  ([+20, +30] ‰, Brizzi et al., 2009) and  $\delta^{15}N(FT)$  ([-10, +10] ‰,  
23 Morin et al., 2009).

#### 24 4.1.4 Controls on the slope

25 Figure 9 shows that only the ozone column controls the slope of the curve (Fig. 940). The  
26 distribution of the actinic flux determines the  $^{15}N/^{14}N$  fractionation constant associated with  
27 nitrate photolysis ( $^{15}\epsilon_{pho}$ ) (Frey et al., 2009) and hence the slope of the curve. In the case of the  
28 DC reference simulation, a yearly mean apparent fractionation constant ( $^{15}\epsilon_{app}$ ) of -55.1 ‰ was  
29 calculated for  $^{15}\epsilon_{pho}$  ranging from -52.9 to -78.8 ‰ (Tab. 6-5). The variability of the curvature  
30 the thick back curve representing the DC reference simulation in Fig. 940 is linked to the greater  
31 incorporation of the summertime value of  $^{15}\epsilon_{pho}$  (Fig. 56d): when  $FA/FPI$  increases,  $^{15}\epsilon_{pho}$

1 less negative and the curvature decreases. Therefore, the slope of the thick dashed lines in the  
2 modified Rayleigh plots is slightly more negative ( $-0.064$  =  $-6.4$ ‰) than  $^{15}\epsilon_{app}$ .  
3 Lower ozone columns have a strong impact on  $FA$  and  $\delta^{15}N(FA)$ :  $FA$  is lower while  $\delta^{15}N(FA)$   
4 is higher (Fig. 940). The first effect is explained by higher amounts of UV radiations which  
5 the ground and so higher increase the photolytic photolysis rates. The second effect is linked  
6 to the fact that a lower ozone column leads to higher less negative  $^{15}\epsilon_{pho}$  values of the  
7 fractionation constant, as observed in spring during the ozone hole period (Figs. 3 and 56d).  
8 Indeed, a lower ozone column allows UV radiations of shorter wavelengths in the 280–350 nm  
9 range to reach the ground, i.e. a shift to the blue of the UV spectra, therefore resulting in less  
10 negative higher  $^{15}\epsilon_{pho}$  values (Frey et al., 2009). Referring to Eq. (24), and to our sensitivity  
11 tests reveals that changes in the ozone column result in changes in UV flux (i.e. in  $f$ ) which  
12 overweights the changes effect due to the in-UV spectra shift (i.e. in  $^{15}\epsilon_{pho}$ ). From our sensitivity  
13 tests, we also observe that an ozone hole in late winter/spring (Aug. to Nov.) significantly  
14 imprints  $\delta^{15}N(FA)$  (Fig. 940). Therefore, we suggest that  $\delta^{15}N(FA)$  archived over the last  
15 at Dome C and other East Antarctic plateau sites could potentially be imprinted by changes in  
16 the ozone column, especially in Spring when stratospheric ozone destruction processes are at  
17 play occur.

#### 18 4.1.5 Controls on the distance from the starting point and along the slope

19 Hereafter, the ratio  $FA/FPI$  is termed the “nitrate trapping efficiency” because it reflects the  
20 fraction of nitrate which is trapped below the photic zone.

21 In the modified Rayleigh plot, the horizontal distance from the starting point is  $\ln(FA/FPI) =$   
22  $\ln(FA) - \ln(FPI) = \ln(FA/FPI)$ , i.e. the horizontal distance from the starting point is directly  
23 linked to the trapping efficiency. This quantity is therefore equivalent to the  $f$  term used in Eq.  
24 (42) because it reflects the nitrate fraction remaining in snow below the photic zone. The  
25 trapping efficiency and the intensity of the photolysis are linked because a more intense  
26 photolysis is necessary to lead to a lower nitrate trapping efficiency.

27 In the modified Rayleigh plot, the vertical distance from the starting point is  $\ln(\delta^{15}N(FA) + 1)$   
28  $- \ln(\delta^{15}N(FPI) + 1)$ . Fig. 940 shows that, at first order, the vertical and horizontal distance from  
29 the starting point are linked by the slope. This means that at a given slope in the modified  
30 Rayleigh plot, i.e. at a given spectral distribution of the actinic flux,  $\ln(\delta^{15}N(FA) + 1)$  is linearly  
31 linked with  $\ln(FA/FPI)$ , i.e.  $\delta^{15}N(FA)$  is linked with the trapping efficiency.

1 Our sensitivity tests have shown that the nitrate trapping efficiency is controlled by  $\Phi$ ,  $A$ ,  $\rho$ ,  $k$ ,  
2  $q$ ,  $f_{\text{cage}}$ ,  $f_{\text{exp}}$ ,  $D$ ,  $FS/FPI$ ,  $O_3$  column and the snow accumulation ~~repartition-distribution~~ in the  
3 year. Indeed,  $\Phi$ ,  $f_{\text{cage}}$ ,  $q$  and  $O_3$  column are key parameters and variables in controlling the  
4 photolytic mass loss while  $A$ ,  $\rho$ ,  $k$ ,  $D$  and the seasonality in snow accumulation determine nitrate  
5 exposure time to the actinic flux. Considering the seasonality of snow accumulation, we observe  
6 that it plays a minor role in setting  $FA/FPI$  and hence  $\delta^{15}N(FA)$ . The reason is that, in DC  
7 conditions, nitrate residence time in the photic zone is very long and set by the other parameters  
8 and variables at play in the photolytic process. The same applies to the  $FS/FPI$  ratio: the impact  
9 on nitrate trapping efficiency is small.

10 The case of the export flux parameter,  $f_{\text{exp}}$ , is different. Indeed, it does not impact the residence  
11 time of nitrate in the photic zone, nor does it impact its photolytic loss. However, an increase  
12 in  $f_{\text{exp}}$  results in a greater export of atmospheric nitrate, which is depleted in  $^{15}N$  with respect to  
13 nitrate in snow (data not shown in Tab. ~~5-7~~). In fact, the increase in  $f_{\text{exp}}$  also leads to higher  
14  $\delta^{15}N(FA)$  and  $\delta^{15}N(FE)$  values. In the two simulations tested,  $\delta^{15}N(FE)$  is always smaller than  
15  $\delta^{15}N(FPI)$ , which means that the “removal” of nitrate featuring  $\delta^{15}N(FE) \leq \delta^{15}N(FPI)$  is  
16 compensated by the increase of  $\delta^{15}N$  in the archived nitrate. This increase in  $\delta^{15}N(FA)$  is  
17 therefore not due to an increased photolysis intensity but to the isotopic mass balance.

18 The parameters and variables  $\Phi$ ,  $k$ ,  $A$ ,  $\rho$  and  $q$  have the largest impact on the nitrate trapping  
19 efficiency ( $FA/FPI$ ), ~~with-which~~ mostly ~~equivalent~~ impacts ~~on~~  $\delta^{15}N(FA)$ . ~~The fact that~~ they  
20 control  $FA/FPI$  and  $\delta^{15}N(FA)$  to a similar extent is not surprising since  $k$ ,  $A$ ,  $\rho$  and  $q$  are  
21 intimately linked together in determining the residence time in the photic layer and so the  
22 exposure time of nitrate to near-surface conditions.

23 In this paper, the model does not aim at representing the counter ion of nitrate. However, we  
24 acknowledge that the diffusion of nitrate may be different depending on the nature of its counter  
25 ion ( $H^+$  or, e.g.  $Ca^{2+}$ ), especially when glacial conditions are considered (Röthlisberger et al.,  
26 2000).

#### 27 **4.1.6 Method to interpret $FA$ and $\delta^{15}N(FA)$ measured in ice cores**

28 In this section we summarize our recommended approach to interpret nitrate isotope records in  
29 ice cores. The approach is valid provided that pieces of evidence show that the nitrate recycling  
30 (i.e. loss, local oxidation and deposition) observed today has also occurred in the past. The

1 measurement of elevated  $\delta^{15}\text{N}(FA)$  values could be ~~such a piece of an~~ evidence for a photolytic  
2 nitrate removal from snow.

3 Information potentially accessible from ice cores are  $\omega(FA)$  and  $\delta^{15}\text{N}(FA)$ . Knowledge on the  
4 past snow accumulation rates (~~assumed or~~ deduced from other proxies) allow the calculation of  
5  $FA = \omega(FA) \times A$ . If  $FA$  and  $\delta^{15}\text{N}(FA)$  data align in the modified Rayleigh plot, ~~the previous~~  
6 ~~sections have shown that it is possible to retrieve information on the ozone column, In this case~~  
7 one can deduce that the ozone column is likely to have remained constant through time and its  
8 value can be inferred from the slope of the curve (e.g. lower right panel in Fig. ~~940~~). In this  
9 as well,  $FPI$  is likely to have remained constant through time and its value can be retrieved,  
10 provided that  $\delta^{15}\text{N}(FPI)$  have remained constant as well and that one can assume its value. If  
11 the data do not align in the modified Rayleigh plot, it is likely that either or both the ozone  
12 column and  $FPI$  have varied over time. If an assumption on the ozone column can be made or  
13 if this information can be obtained from other considerations, one can determine past changes  
14 in  $FPI$  provided that an assumption on  $\delta^{15}\text{N}(FPI)$  can be made. Fig. ~~4211~~ gives a schematic of  
15 the method to determine  $FPI$  from the measurement of  $\omega(FA)$  and  $\delta^{15}\text{N}(FA)$  in ice cores. As  
16 discussed above, a ~~portion fraction~~ of  $\delta^{15}\text{N}(FT)$  and  $\delta^{15}\text{N}(FS)$  is left in  $\delta^{15}\text{N}(FA)$ . However,  
17  $\delta^{15}\text{N}(FT)$  and  $\delta^{15}\text{N}(FS)$  are small when compared to the ca. 250+ ‰ added under the effect of  
18 nitrate recycling at the air-snow interface, thereby erasing information on  $\delta^{15}\text{N}(FT)$  and  
19  $\delta^{15}\text{N}(FS)$ . In other words,  $\delta^{15}\text{N}(FA)$  is almost insensitive to change of  $\delta^{15}\text{N}(FT)$  and  $\delta^{15}\text{N}(FS)$ .

## 20 4.2 Parameters and variables controlling $\Delta^{17}\text{O}(FA)$

21 The parameters and variables controlling  $\Delta^{17}\text{O}(FA)$  can be sorted in four groups:

- 22 -  $f_{\text{cage}}$ , which controls the cage effects,
- 23 - those which impact  $FA/FPI$ , which sets the magnitude of loss and hence the  
24 magnitude of the cage effects,
- 25 -  $\Delta^{17}\text{O}(FT)$  and  $\Delta^{17}\text{O}(FS)$ , which set  $\Delta^{17}\text{O}$  in the primary source of nitrate
- 26 -  $\Delta^{17}\text{O}(\text{O}_3)_{\text{bulk}}$ ,  $\Delta^{17}\text{O}(\text{OH})$ ,  $[\text{BrO}]$ ,  $[\text{HO}_2]$ ,  $[\text{CH}_3\text{O}_2]$ ,  $[\text{O}_3]$  and  $T$  which set  $\Delta^{17}\text{O}$  in the  
27 secondary source of nitrate in the atmosphere (i.e.  $\text{NO}_2$  which is cycled in the  
28 atmosphere),  $\Delta^{17}\text{O}(\text{NO}_2, \text{PSS})$

### 29 4.2.1 Correction of the reduction in $\Delta^{17}\text{O}(FA)$ imposed by cage effects

30 We have shown that cage recombination effects following nitrate photolysis in snow lead to  
31 positive simulated  $^{17}E_{\text{app}}$  values in snow. For instance, for DC realistic conditions (i.e. for  $f_{\text{cage}}$



1 = 0.15 and  $FA/FPI = 21.0-8\%$ ,  $\Delta^{17}O(FA)$  is reduced by  $\approx 7-6\%$  because of cage effects (Fig.  
2 To calculate the reduction in  $\Delta^{17}O(FA)$  as a result of cage recombination effects, we have run  
3 TRANSITS in the DC realistic simulation by varying  $\Phi$  from 0 to 0.036 and with an  $f_{\text{cage}}$   
4 parameter set to 0 and 0.15 in order to switch the cage effects on and off, respectively.

5 We denote  $\Delta^{17}O(FA, \text{corr.})$ , the  $\Delta^{17}O(FA)$  value corrected from cage effects, which was  
6 estimated here by setting  $f_{\text{cage}} = 0$ . Figure 1110dc shows that for  $\ln(FA/FPI) < -1.22$  (i.e.,  $FA/FPI$   
7  $< 30-14\%$ ), the  $\Delta^{17}O(FA, \text{corr.})/\Delta^{17}O(FA)$  ratio is linear with  $\ln(FA/FPI)$ :  $\Delta^{17}O(FA,$   
8  $\text{corr.})/\Delta^{17}O(FA) = -0.066-063 \times \ln(FA/FPI) + 1.076052$ . In section 4.1.6, we have shown that  
9 ratio can be retrieved from the measurement of  $\delta^{15}N(FA)$  given an hypothesis on the  $O_3$  column  
10 and  $\delta^{15}N(FPI)$ . Using this approach,  $\Delta^{17}O(FA)$  is corrected from the cage effect.

11 From Figure 1044be, we observe that  $\Delta^{17}O(FA, \text{corr.})$  reaches a plateau at around  $27-23.5\%$  for  
12 nitrate trapping efficiencies ( $\ln(FA/FPI) < -3$ , i.e.  $FA/FPI < 5\%$ ). Although we anticipate that,  
13  $\Delta^{17}O(FA, \text{corr.})$  is mostly controlled by the local cycling and oxidation of  $NO_2$  (as previously  
14 observed from sensitivity tests), there is still the need to separate the  $\Delta^{17}O$  impact of local  
15 cycling and oxidation of  $NO_2$  from those of  $\Delta^{17}O(FT)$  and  $\Delta^{17}O(FS)$ .

#### 16 4.2.2 Contributors to $\Delta^{17}O(FA, \text{corr.})$

17 In this section, we consider  $\Delta^{17}O(FT)$ ,  $\Delta^{17}O(FS)$ ,  $\Delta^{17}O(NO_2, \text{PSS})$  and  $\Delta^{17}O(\text{add. O})$ , which  
18 impact  $\Delta^{17}O(FA, \text{corr.})$ . To determine the scaled contributions of the variable  $\Delta^{17}O(X)$ , we have  
19 run the TRANSITS model with this variable set to 0. We denote  $\overline{\Delta^{17}O(FA)}$  the  $\Delta^{17}O(FA)$  value  
20 obtained when  $\Delta^{17}O(X)$  has been set to 0. From the previous section, we can calculate  
21  $\overline{\Delta^{17}O(FA, \text{corr.})}$  based on the computed  $FA/FPI$  value. For  $\Delta^{17}O(X)$ , we calculate the scaled  
22 contribution to  $\Delta^{17}O(FA, \text{corr.})$  as  $(\Delta^{17}O(FA, \text{corr.}) - \overline{\Delta^{17}O(FA, \text{corr.})}) / \Delta^{17}O(X)$ .

23 Figure 1044ed shows the obtained scaled contributions to  $\Delta^{17}O(FA, \text{corr.})$ . For example, for  
24  $\ln(FA/FPI) < -23$ , we observe that the statistical contribution of the variable  $\Delta^{17}O(NO_2, \text{PSS})$   
25 contributes to the budget of  $\Delta^{17}O(FA, \text{corr.})$  by is 62-55 % of  $\Delta^{17}O(NO_2, \text{PSS})$ , which means  
26 that if  $\Delta^{17}O(NO_2, \text{PSS}) = 20\%$ , then this variable will contribute to  $\Delta^{17}O(FA, \text{corr.})$  by as much  
27 as  $0.62-55 \times 20 = 112.4\%$ . For the same nitrate trapping efficiency,  $\Delta^{17}O(FT)$  contributes  
28 much less, i.e. by  $46-13\%$  of  $\Delta^{17}O(FT)$ , which is to say by  $43.8-9\%$  for  $\Delta^{17}O(FT) = 30\%$ .

29 -From the same panel Fig. 044e, we observe that for  $\ln(FA/FPI) < -1.22$ , the scaled contributions  
30 of  $\Delta^{17}O(NO_2, \text{PSS})$  and  $\Delta^{17}O(\text{add. O})$  to  $\Delta^{17}O(FA, \text{corr.})$  is higher-greater than  $56-50\%$  of  
31  $\Delta^{17}O(NO_2, \text{PSS})$  and 25 % of their respective values, i.e. a sum which is more the twice-three

Mis en forme : Surlignage

1 ~~times the sum of those the scaled contributions~~ of  $\Delta^{17}\text{O}(FT)$  and  $\Delta^{17}\text{O}(FS)$ , which contribute to  
 2 ~~less than ( $< 20-14\%$  and of  $\Delta^{17}\text{O}(FT)$ ) and  $\Delta^{17}\text{O}(FS)$  ( $< 5-11\%$  of  $\Delta^{17}\text{O}(FS)$ )~~ their respective  
 3 ~~values~~. This means that, in the conditions tested (i.e. low trapping efficiencies which  
 4 characterize the Antarctic plateau),  $\Delta^{17}\text{O}(FA, \text{corr.})$  is poorly controlled by  $\Delta^{17}\text{O}(FS)$  and  
 5  $\Delta^{17}\text{O}(FT)$  and dominated by local cycling and oxidation of  $\text{NO}_2$ . We note that, for very low  
 6 nitrate trapping efficiencies ( $\ln(FA/FPI) < -3$ ), the sum of the scaled contributions of  $\Delta^{17}\text{O}(\text{NO}_2,$   
 7  $\text{PSS}) + \Delta^{17}\text{O}(\text{add. O})$  and of the sum of those of  $\Delta^{17}\text{O}(FS)$  and  $-\Delta^{17}\text{O}(FT)$  reach a plateaus at  
 8 65-82% of  $\Delta^{17}\text{O}(\text{NO}_2, \text{PSS})$  and 22% of  $\Delta^{17}\text{O}(FS)$  and  $\Delta^{17}\text{O}(FT)$  and 18%, respectively. From  
 9 Fig. 1044ba, we observe that these plateaus are consistent with YANR(FA) values ( $\approx$  that of the  
 10 ratio  $FD/FPI$ ) at a value of around 4, i.e. the archived nitrate has been recycled 4 times on  
 11 average and is therefore mostly secondary nitrate which has been locally reformed~~primary~~  
 12 ~~inputs of nitrate only annually contribute to 1/4 of the deposited flux, the rest being the~~  
 13 ~~deposition of locally recycled nitrate (secondary inputs of nitrate). This is consistent with the~~  
 14 ~~3:1 ratio in the scaled contributions of  $\Delta^{17}\text{O}(\text{NO}_2, \text{PSS})$  and the sum of those of  $\Delta^{17}\text{O}(FS)$  and~~  
 15  ~~$\Delta^{17}\text{O}(FT)$ .~~

16 For low nitrate trapping efficiencies, we also observe that the scaled contribution of  $\Delta^{17}\text{O}(FT)$   
 17 increases while that of  $\Delta^{17}\text{O}(FS)$  decreases. This is linked to the preferential incorporation, yet  
 18 small, of the local  $\Delta^{17}\text{O}$  signature on the summertime primary source of nitrate.

19 Figure 1044fe represents an application of what precedes in the case of Dome C, i.e. using  
 20  $\Delta^{17}\text{O}(FT) = 30\%$ ,  $\Delta^{17}\text{O}(FS) = 42\%$  ~~and~~  $\Delta^{17}\text{O}(\text{NO}_2, \text{PSS}) = 31.3\%$  ~~and~~  $\Delta^{17}\text{O}(\text{add. O}) = 3\%$ .

21 Figure 1044gf reproduces the relationship between  $\delta^{15}\text{N}(FA)$  and  $FA/FPI$  as a function of ozone  
 22 column. In the case of the present-day DC conditions (realistic DC  $\text{O}_3$  column and  $\delta^{15}\text{N}(FA)$  in  
 23 range [151, 334] = 287%, Fig. 7c), we find that the relative contribution of  $\Delta^{17}\text{O}(\text{NO}_2, \text{PSS})$ ,  
 24  $\Delta^{17}\text{O}(\text{add. O})$ ,  $\Delta^{17}\text{O}(FT)$  and  $\Delta^{17}\text{O}(FS)$  to  $\Delta^{17}\text{O}(FA, \text{corr.})$  are in the following ranges: 63-52,  
 25 551%, 126, 281%, 27-11, 131% and 40-5, 91%, respectively. In DC conditions,  $\Delta^{17}\text{O}(FA,$   
 26  $\text{corr.})$  therefore harbors almost two third of the oxygen isotope signature of the local cycling  
 27 and oxidation of  $\text{NO}_2$  and the remaining signature of primary inputs of nitrate is small. This is  
 28 such because the archived nitrate has undergoes more than  $\approx 150-40$  cycles (defined as the  
 29 ratio  $FP/FA$ ) before being ultimately trapped in snow below the photic zone (Fig. 1044a).

30  
 31

Mis en forme : Police :Non Italique

Mis en forme : Police :Non Italique

Mis en forme : Police :Non Italique

Mis en forme : Police :Italique

Mis en forme : Police :Italique, Non souligné

Mis en forme : Police :Non Italique

Mis en forme : Police :Non Italique

Mis en forme : Non Surlignage

Mis en forme : Non Surlignage

Mis en forme : Non Surlignage

Mis en forme : Non Surlignage

### 4.2.3 Method to interpret $\Delta^{17}\text{O}(\text{FA}, \text{corr.})$ derived from ice cores measurements

~~In this section, we suggest a method to interpret  $\Delta^{17}\text{O}(\text{FA})$  values measured from ice cores. In section 4.2.1, we have provided a method to correct  $\Delta^{17}\text{O}(\text{FA})$  from cage effects from the knowledge of the variations in nitrate trapping efficiency. From section 4.1.6, we provided a framework for the interpretation of  $\omega(\text{FA})$  and  $\delta^{15}\text{N}(\text{FA})$  which can be measured from ice cores. The variation in nitrate trapping efficiency ( $\text{FA}/\text{FPI}$ ) which, we recall, can ~~could~~ be determined from  $\delta^{15}\text{N}(\text{FA})$  values and hypothesis on past variations in  $\delta^{15}\text{N}(\text{FPI})$  and in the ozone column (see also Fig. 1121). Knowledge of the variations in nitrate trapping efficiency allows to~~ which is only influenced by past changes in  $\Delta^{17}\text{O}(\text{NO}_2, \text{PSS})$ ,  $\Delta^{17}\text{O}(\text{add. O})$ ,  $\Delta^{17}\text{O}(\text{FT})$  and  $\Delta^{17}\text{O}(\text{FS})$  and that of their scaled contributions, as shown in the previous section.

To determine the variations in the scaled contributions of  $\Delta^{17}\text{O}(\text{NO}_2, \text{PSS})$ ,  $\Delta^{17}\text{O}(\text{add. O})$ ,  $\Delta^{17}\text{O}(\text{FT})$  and  $\Delta^{17}\text{O}(\text{FS})$ , we use the nitrate trapping efficiency determined in section 4.1.6. Assumptions or evidences on past changes in one or several of two of the three-four variables controlling  $\Delta^{17}\text{O}(\text{FA}, \text{corr.})$  (i.e.  $\Delta^{17}\text{O}(\text{NO}_2, \text{PSS})$ ,  $\Delta^{17}\text{O}(\text{add. O})$ ,  $\Delta^{17}\text{O}(\text{FT})$  and  $\Delta^{17}\text{O}(\text{FS})$ ) allow to determine past changes in the ~~last one~~ other ones. For instance, assuming that  $\Delta^{17}\text{O}(\text{add. O})$ ,  $\Delta^{17}\text{O}(\text{FT})$  and  $\Delta^{17}\text{O}(\text{FS})$  have remained constant over time allows to determine past changes in the local cycling of  $\text{NO}_2$  above the East Antarctic plateau.

Fig. ~~1112~~ gives a schematic of the method to determine  $\Delta^{17}\text{O}(\text{FA}, \text{corr.})$  as well as in the scaled contributions of  $\Delta^{17}\text{O}(\text{NO}_2, \text{PSS})$ ,  $\Delta^{17}\text{O}(\text{add. O})$ ,  $\Delta^{17}\text{O}(\text{FT})$  and  $\Delta^{17}\text{O}(\text{FS})$  from the measurement of  $\omega(\text{FA})$ , A.  $\delta^{15}\text{N}(\text{FA})$  and  $\Delta^{17}\text{O}(\text{FA})$  in ice cores.

If we assume that modern conditions in East Antarctica have prevailed in the past, we anticipate from Fig. ~~1044~~ that almost two third of the variations  $\Delta^{17}\text{O}(\text{FA}, \text{corr.})$  are the result of variations in  $\Delta^{17}\text{O}(\text{NO}_2, \text{PSS})$  and  $\Delta^{17}\text{O}(\text{add. O})$ . In this case, the potential for  $\Delta^{17}\text{O}(\text{FA}, \text{corr.})$  to trace past changes in atmospheric oxidation at the global scale is weak. However, in such conditions,  $\Delta^{17}\text{O}(\text{FA}, \text{corr.})$  would rather hold information about we would have in this case a tool to document past changes in the local and summertime atmospheric oxidation above the East Antarctic plateau.

## 1 5 Summary and conclusions

2 The TRANSITS model is a conceptual, multi-layer, 1-D isotopic model which represents the  
3 air-snow transfer of nitrate and its isotopic composition on the Antarctic plateau at around a  
4 one-week time resolution. It rests on the conceptual model initially proposed by Davis et al.  
5 (2008) and on the fact that nitrate photolysis is the process dominating nitrate mass loss at the  
6 low accumulation sites which characterize the Antarctic plateau (Frey et al., 2013; Erbland et  
7 al., 2013). The particularity of TRANSITS is its representation of the isotopic composition of  
8 nitrate ( $\delta^{15}\text{N}$  and  $\Delta^{17}\text{O}$ ).

9 When using a realistic scenario representing the Dome C conditions, the model reproduces well  
10 the variations in concentrations and isotopic time series observed in the atmospheric and skin  
11 layer compartments, thus supporting the theory of Davis et al. (2008). While the nitrogen  
12 isotope ratio is well reproduced by the model, the simulated  $\Delta^{17}\text{O}$  data in the air-snow interface  
13 are lower than the observations. This has been attributed to simplifications in the description of  
14 the local cycling and oxidation of  $\text{NO}_2$ . One consequence is that simulated  $\Delta^{17}\text{O}$  values in the  
15 snowpack and in the archived nitrate are lower than the observations—as well. Nevertheless,  
16 However, cage recombination effects occurring in snow are well reproduced by the model as  
17 shown by the agreement between the simulated and observed values of the apparent  
18 fractionation constant ( $^{17}E_{\text{app}}$ ). The representation of nitrate diffusion within the snowpack  
19 allows simulating nitrate mass fraction and isotope depth profiles, which are consistent with  
20 observations. Under the DC realistic simulation conditions, the quantum yield imposed value  
21 ( $\phi = 0.026$ ) which is necessary to to reproduce the observations (0.026) transcripts means is  
22 compatible with the idea that nitrate lies in two different domains in or on the snow-ice matrix  
23 (Meusinger et al., 2014). The comparison of the simulated and observed  $\text{NO}_2$  fluxes shows that  
24 the simulated  $\text{NO}_2$  fluxion is 9 to 18 times higher than the observed  $\text{NO}_2$ -flux at Dome C in  
25 2009-2010 and 2011-2012. This discrepancy could result from the simplifications made in the  
26 model regarding the fates of the nitrate photolysis products., which could be due to simplifying  
27 assumptions made in the model regarding the product of nitrate photolysis.

28 TRANSITS has been used to investigate the spatial variability in the mass and isotopic  
29 composition of the nitrate archived from the Antarctic coast to the plateau (Dome C to Vostok)  
30 obtained from 21 snow pits collected from 2007 to 2010 (Erbland et al., 2013). Using the  
31 realistic simulation and the snow accumulation rates varying in a range observed on the zone  
32 of interest (from 20 to 600  $\text{kg m}^{-2} \text{a}^{-1}$ ), we have shown that, in present-day conditions, changes

1 in snow accumulation rates ~~are enough~~ are sufficient to explain the first order variations ~~in the~~ of  
2  $\delta^{15}\text{N}$  in the archived nitrate. This suggests that ~~functioning the~~ principles at the ~~base-heart~~ of  
3 the model (~~the principles o.i.e.f~~ photolytic mass loss, isotopic fractionation and exposure time  
4 of nitrate) are ~~realistic~~ adequate. Moreover, the use of a nitrate primary input flux of  $8.2 \times 10^{-6}$   
5  $\text{kgN m}^{-2} \text{a}^{-1}$  is consistent with ~~the~~ the observations.

6 ~~The model has shown a 21 years response time to changes in the primary input flux of nitrate,~~  
7 ~~which could explain the difference between the observed and simulated nitrate mass in the top~~  
8 ~~50 cm of snow. Such a response time is the result of the important number of recycling cycles~~  
9 ~~undergone by nitrate at the air snow interface of DC (> 150 (4.0 cycles). This effect must be~~  
10 ~~taken into account for future analysis of firn and ice cores. Also, combination of photolysis and~~  
11 ~~diffusion which delay nitrate ions.~~

Mis en forme : Surlignage

Mis en forme : Surlignage

Mis en forme : Surlignage

Mis en forme : Surlignage

12 We proposed some improvements and guidelines for future work on the TRANSITS model.  
13 First, the model requires that NO<sub>x</sub> chemistry at Dome C should be fully understood, in  
14 particular the high NO<sub>2</sub>/NO ratio observed (Frey et al., 2014). Then, For example, the model  
15 would will benefit from the measurement of  $\Delta^{17}\text{O}(\text{O}_3)_{\text{bulk}}$  on the East Antarctic plateau (Viears  
16 and Savarino, 2014) as well as the measurements of  $\Delta^{17}\text{O}(\text{NO})$ ,  $\Delta^{17}\text{O}(\text{NO}_2)$  or  $\Delta^{17}\text{O}$  in other key  
17 species participating in the oxidation scheme (HO<sub>2</sub>, RO<sub>2</sub>, BrO). Additional processes or  
18 mechanisms could be implemented, such as nitrate pools featuring different photolytic  
19 capacities/availabilities, modeled by different quantum yield that would vary in space and time  
20 that could be modeled using a quantum yield which would vary with space and time. Some  
21 additional parameters could also be taken into account such as the latitude of the simulated site  
22 to better represent plateau sites other than Dome C. The radiative transfer model TARTES  
23 (Libois et al., 2013) could be explicitly incorporated into TRANSITS. This would allow the  
24 modeling of the e-folding attenuation depth dependence with respect to the physical and  
25 chemical properties of the snowpack. The explicit representation of the export and depositions  
26 fluxes (using horizontal and vertical air mass velocities, respectively) could also be explored as  
27 well as the explicit description of the erosion of the snow surface by the wind. ~~This would allow~~  
28 ~~the modeling of the e-folding attenuation depth dependence to the vertical profile of the physical~~  
29 ~~properties and the impurity content of the snowpack. The explicit representation of the export~~  
30 ~~and depositions fluxes (using horizontal and vertical air mass velocities, respectively) could~~  
31 ~~also be also explored as well as the explicit description of the erosion of the snow surface by~~  
32 ~~the wind.~~

Mis en forme : Indice

1 A framework for the interpretation of nitrate isotope records in ice cores ~~has been~~ proposed.  
2 From ice cores, the following data are ~~measurable~~accessible:  $\omega(FA)$ ,  $\delta^{15}N(FA)$  ~~and~~  $\Delta^{17}O(FA)$   
3 and the annual snow accumulation rates. The interpretation framework described in this paper  
4 will be applicable to ice core records which display proofs of significant nitrate recycling, e. g.  
5 on the basis of elevated  $\delta^{15}N(FA)$  values. In this case, sensitivity tests have shown that  $\delta^{15}N(FA)$   
6 is the result of a  $^{15}N/^{14}N$  fractionation constant which is set by the ~~spectral repartition of the~~ UV  
7 radiation spectrum (i.e. set by the ozone column above the site of interest). Indeed, the ozone  
8 column controls the slope in the “modified Rayleigh plot” introduced in this study. At a given  
9 ozone column,  $\delta^{15}N(FA)$  is ~~at last~~ controlled by:

- 10 1. the nitrate trapping efficiency (i.e. the ratio of the archived flux versus the primary  
11 nitrate inputs,  $FA/FPI$ ) which determines the exposure time of nitrate and thus the  
12 intensity of nitrate recycling.
- 13 2. ~~the nitrate trapping efficiency (i.e. the ratio of the archived flux versus the primary nitrate~~  
14 ~~inputs,  $FA/FPI$ ) which is determined by the exposure time of nitrate and the intensity of~~  
15 ~~nitrate recycling, and, at a lesser extent, the  $\delta^{15}N$  of the primary sources of nitrate whose~~  
16 ~~variations are negligible in comparison to the change produced by the photolysis loss.~~

17 ~~and the  $\delta^{15}N$  in the primary inputs of nitrate whose variations are negligible when compared to~~  
18 ~~the  $\delta^{15}N$  imprinted by nitrate recycling.~~ We have observed that the major controls on  $FA/FPI$   
19 are the photolytic quantum yield ( $\Phi$ ), the annual snow accumulation rate ( $A$ ), the snow density  
20 ( $\rho$ ), the photic zone compression factor ( $k$ ) and the actinic flux enhancement factor ( $q$ ), with  
21 equivalent relative impacts.

22 Given a constant ~~spectral repartition of the~~ actinic flux spectrum, the archived flux ( $FA$ ) is  
23 primarily controlled by the primary input flux and the trapping efficiency. Therefore, the plot  
24 of  $FA$  versus  $\delta^{15}N(FA)$  in the modified Rayleigh space is a good candidate to track modern or  
25 past changes in the spectral distribution of the UV received at ground, i.e. changes in the ozone  
26 column but also changes in the solar UV spectra. ~~Therefore, the  $(FA, \delta^{15}N(FA))$  couples plotted~~  
27 ~~in the modified Rayleigh plot are good candidates to track modern or past changes in the~~  
28 ~~spectral distribution of the UV received at ground, i.e. changes in the ozone column but also~~  
29 ~~changes in the solar UV spectra.~~ At a given spectral distribution of the actinic flux, past  
30 variations in  $FPI$  can be reconstructed from  $FA$  and  $\delta^{15}N(FA)$  if  $\delta^{15}N(FPI)$  is known or  
31 assumed. ~~At a given spectral distribution of the actinic flux, past variations in  $FPI$  can be~~  
32 ~~reconstructed from  $(FA, \delta^{15}N(FA))$  data and an assumption on variations in  $\delta^{15}N(FPI)$ .~~

Mis en forme : Anglais (États-Unis)

Mis en forme : Paragraphe de liste, Interligne : 1,5 ligne,  
Numéros + Niveau : 1 + Style de numérotation : 1, 2, 3, ... +  
Commencer à : 1 + Alignement : Gauche + Alignement : 0,63  
cm + Retrait : 1,27 cm

Mis en forme : Anglais (États-Unis)

1 From the nitrate trapping efficiency ( $FA/FPI$ ), we have shown that we can deduce  $\Delta^{17}O(FA,$   
2 corr.) which represents the  $\Delta^{17}O$  value in the archived flux corrected from the cage  
3 recombination effects. To achieve this correction, the potential impact of nitrate speciation  
4 (association to  $H^+$  or, e.g.,  $Ca^{2+}$ ) on the cage effect should be considered (e.g. during glacial  
5 conditions). The variable  $\Delta^{17}O(FA, \text{corr.})$  is controlled by  $\Delta^{17}O(NO_2, \text{PSS}), \Delta^{17}O(\text{add. O}),$   
6  $\Delta^{17}O(FT)$  and  $\Delta^{17}O(FS)$  and the scaled contributions of each of these four variables has been  
7 determined as a function of  $FA/FPI$ . We have shown that these contributions are independent  
8 of the ozone column. Under the modern DC conditions, we have shown that the isotope mass  
9 balance of  $\Delta^{17}O(FA, \text{corr.})$  can be written as  $[52, 55] \% \times \Delta^{17}O(NO_2, \text{PSS}) + [26, 28] \% \times$   
10  $\Delta^{17}O(\text{add. O}) + [11, 13] \% \times \Delta^{17}O(FT) + [5, 9] \% \times \Delta^{17}O(FS)$ . These proportions result from  
11 the intense recycling cycles (on average, 4.0) present at low accumulation sites. As a  
12 consequence,  $\Delta^{17}O(FA, \text{corr.})$  is mostly driven by the  $\Delta^{17}O$  signature acquired during the  
13 summertime and local processing of  $NO_2$  in the DC atmosphere and only weakly by the  $\Delta^{17}O$   
14 signature of the primary nitrate fluxes ( $FT$  and  $FS$ ).

15 If the modern DC conditions applied to the past as well (i.e. important loss by photolysis  
16 followed by the local recycling of nitrate),  $\Delta^{17}O(FA, \text{corr.})$  obtained from ice cores drilled on  
17 the East Antarctic plateau is expected to deliver information about the oxidative chemistry  
18 occurring at the local and summertime scale rather than at the global scale. The reverse should  
19 therefore also be true. High accumulation sites with limited photolytic loss should deliver  
20 information about the oxidative chemistry of  $NO_x$  at the remote scale.

21 ~~From the nitrate trapping efficiency ( $FA/FPI$ ), we have shown that we can deduce  $\Delta^{17}O(FA,$   
22 ~~corr.) which represents the  $\Delta^{17}O$  value in the archived flux corrected from the cage~~  
23 ~~recombination effects. The variable  $\Delta^{17}O(FA, \text{corr.})$  is controlled by  $\Delta^{17}O(NO_2, \text{PSS}), \Delta^{17}O(FT)$   
24 ~~and  $\Delta^{17}O(FS)$  and the scaled contributions of each of these three variable has been determined~~  
25 ~~as a function of  $FA/FPI$ . We have shown that these contributions are independent of the ozone~~  
26 ~~column. Under the modern DC conditions, we have shown that 63 %, 27 % and 10 % of~~  
27  ~~$\Delta^{17}O(FA, \text{corr.})$  are due to  $\Delta^{17}O(NO_2, \text{PSS}), \Delta^{17}O(FT)$  and  $\Delta^{17}O(FS)$ , respectively. These are~~  
28 ~~the result of the important number of recycling cycles undergone by nitrate at the air-snow~~  
29 ~~interface. Therefore, if the modern DC conditions applied in the past as well (i.e. important loss~~  
30 ~~by photolysis followed by the local recycling of nitrate), the determination of  $\Delta^{17}O(FA, \text{corr.})$~~   
31 ~~from ice cores drilled on the East Antarctic plateau are expected to deliver mostly information~~~~~~

- 1 ~~about the local~~the oxidative chemistry occurring at the local and summertime scale rather than
- 2 at the global scale.



## 1 Acknowledgements

2 This research has received the financial support of the Agence Nationale de la Recherche  
3 (ANR), through the VANISH (contract ANR-07-VULN-013) and OPALE (contract ANR-09-  
4 BLAN-0226) projects (J.E., J.S.). It was partly conducted in the framework of the International  
5 Associated Laboratory (LIA) "Climate and Environments from Ice Archives" 2012-2016  
6 linking several Russian and French laboratories and institutes. J. L. F. and M. D. K. gratefully  
7 acknowledge NERC for support through grants NE/F0004796/1 and NE/F010788, NERC FSF  
8 for support and expertise through grants 555.0608 and 584.0609 and Royal Holloway Earth  
9 Sciences research strategy fund awards. Partial funding has also been received from LICENCE  
10 (LEFE-CHAT), a scientific program of the Institut National des Sciences de l'Univers  
11 (INSU/CNRS), as well as from the IPICS program (CNRS) and from IPEV (program NITEDC  
12 – 1011) (J.E., J.S.). LGGE and CNRM-GAME/CEN are part of LabEx OSUG@2020 (ANR10  
13 LABX56). We thank F. Dominé, G. Picard and D. Voisin for helpful discussions on light  
14 penetration in snow and modeling. ~~The authors are grateful to;~~ C. Carmagnola, G. Picard, F.  
15 Dupont and N. Champollion who shared their knowledge on Python, M. Zatko for discussions  
16 about nitrate diffusion and the number of recyclings-; ~~and J.E. thanks G. Krinner and S. Parouty~~  
17 ~~for providing the snow accumulation data used in this work. Last, we thank~~ the overwintering  
18 people ~~(S. Lafont, I. Bourgeois, S. Aubin, A. Barbero and C. Lenormant)~~, for the samples  
19 collection at Concordia – Dome C from 2010 to 2013. Last, we thank the reviewers for their  
20 help in improving the manuscript. Eric Wolff is deeply acknowledged from his fundamental  
21 contribution to calculate the recycling effect.  
22 The authors encourage the use of the TRANSITS model. It is available upon request from the  
23 correspondence author.

24

## 25 References to add

- 26 ~~Herbert 2006~~
- 27 ~~Massmann 1998~~
- 28 ~~Gallet 2011~~
- 29 ~~Crowley 2010~~

30

## 1 **References**

- 2 Alexander, B., Hastings, M. G., Allman, D. J., Dachs, J., Thornton, J. A., and Kunasek, S. A.:  
3 Quantifying atmospheric nitrate formation pathways based on a global model of the oxygen  
4 isotopic composition ( $\delta^{17}\text{O}$ ) of atmospheric nitrate, *Atmos. Chem. Phys.*, 9, 5043-5056,  
5 doi:10.5194/acp-9-5043-2009, 2009.
- 6 Atkinson, R., Baulch, D. L., Cox, R. A., Crowley, J. N., Hampson, R. F., Hynes, R. G., Jenkin,  
7 M. E., Rossi, M. J., and Troe, J.: Evaluated kinetic and photochemical data for atmospheric  
8 chemistry: Volume I – gas phase reactions of  $\text{O}_x$ ,  $\text{HO}_x$ ,  $\text{NO}_x$  and  $\text{SO}_x$  species, *Atmos. Chem.*  
9 *Phys.*, 4, 1461–1738, 2004.
- 10 Atkinson, R., Baulch, D. L., Cox, R. A., Crowley, J. N., Hampson, R. F., Hynes, R. G., Jenkin,  
11 M. E., Rossi, M. J., and Troe, J.: Evaluated kinetic and photochemical data for atmospheric  
12 chemistry: Volume II – gas phase reactions of organic species, *Atmos. Chem. Phys.*, 6, 3625–  
13 4055, 2006.
- 14 Atkinson, R., Baulch, D. L., Cox, R. A., Crowley, J. N., Hampson, R. F., Hynes, R. G., Jenkin,  
15 M. E., Rossi, M. J., and Troe, J.: Evaluated kinetic and photochemical data for atmospheric  
16 chemistry: Volume III – gas phase reactions of inorganic halogens, *Atmos. Chem. Phys.*, 7,  
17 981–1191, 2007.
- 18 Berhanu, T. A., Meusinger, C., Erbland, J., Jost, R., Bhattacharya, S. K., Johnson, M. S. and  
19 Savarino, J.: Laboratory study of nitrate photolysis in Antarctic snow. II. Isotope effects and  
20 wavelength dependence, *J. Chem. Phys.*, 140, 244306, doi: 10.1063/1.4882899, 2014a.
- 21 Berhanu, T. A., Savarino, J., Erbland, J., Vicars, W. C., Preunkert, S., Martins, J. F., and  
22 Johnson, M. S.: Isotopic effects of nitrate photochemistry in snow: a field study at Dome C,  
23 Antarctica, *Atmos. Chem. Phys. Discuss.*, 14, 33045-33088, doi:10.5194/acpd-14-33045-2014,  
24 2014b.
- 25 Blunier, T., Floch, G. L., Jacobi, H.-W., and Quansah, E.: Isotopic view on nitrate loss in  
26 Antarctic surface snow, *Geophys. Res. Lett.*, 32 (L13501), doi:10.1029/2005GL023011, 2005.
- 27 Boxe, C. S. and Saiz-Lopez, A.: Multiphase modeling of nitrate photochemistry in the quasi-  
28 liquid layer (QLL): implications for  $\text{NO}_x$  release from the Arctic and coastal Antarctic  
29 snowpack, *Atmos. Chem. Phys.*, 8, 4855 – 4864, 2008.

- 1 [Chan, H. G., King, M. D., and Frey, M. M.: The impact of parameterising light penetration into](#)  
2 [snow on the photochemical production of NO<sub>x</sub> and OH radicals in snow, \*Atmos. Chem. Phys.\*](#)  
3 [Discuss., 15, 8609-8646, doi:10.5194/acpd-15-8609-2015, 2015.](#)
- 4 ~~[Brizzi, G., Arnone, E., Carlotti, M., Dinelli, B. M., Flaud, J. M., Papandrea, E., Perrin, A., and](#)  
5 [Ridolfi, M.: Retrieval of atmospheric H<sup>15</sup>NO<sub>3</sub>/H<sup>14</sup>NO<sub>3</sub> isotope ratio profile from](#)  
6 [MIPAS/ENVISAT limb scanning measurements, \*J. Geophys. Res.\*, 114, D16301,](#)  
7 [doi:10.1029/2008JD011504, 2009.](#)~~
- 8 Chance, K. and Kurucz, R. L.: An improved high-resolution solar reference spectrum for  
9 Earth's atmosphere measurements in the ultraviolet, visible, and near infrared, *J. Quant.*  
10 *Spectrosc. Ra.*, 111, 1289–1295, 2010.
- 11 Chu, L. and Anastasio, C.: Quantum yields of hydroxyl radical and nitrogen dioxide from the  
12 photolysis of nitrate on ice, *J. Phys. Chem.*, 107, 9594–9602, 2003.
- 13 Chu, L. and Anastasio, C.: Temperature and wavelength dependence of nitrite photolysis in  
14 frozen and aqueous solutions, *Environ. Sci Technol.*, 41(10), 3626–3632, 2007.
- 15 [Crowley, J. N., Ammann, M., Cox, R. A., Hynes, R. G., Jenkin, M. E., Mellouki, A.,](#)  
16 [Rossi, M. J., Troe, J., and Wallington, T. J.: Evaluated kinetic and photochemical data for](#)  
17 [atmospheric chemistry: Volume V – heterogeneous reactions on solid substrates, \*Atmos. Chem.\*](#)  
18 [Phys., 10, 9059-9223, doi:10.5194/acp-10-9059-2010, 2010.](#)
- 19 Davis, D. D., Seelig, J., Huey, G., Crawford, J., Chen, G., Wang, Y., Buhr, M., Helmig, D.,  
20 Neff, W., Arimoto, D. B. R., and Eisele, F.: A reassessment of Antarctic plateau reactive  
21 nitrogen based on ANTCI 2003 airborne and ground based measurements, *Atmos. Environ.*,  
22 42, 2831 – 2848, doi:10.1016/j.atmosenv.2007.07.039, 2008.
- 23 Dominé, F. and Shepson, P. B.: Air-snow interactions and atmospheric chemistry, *Science*, 297,  
24 1506 – 1510, 2002.
- 25 Dominé, F., Taillandier, A.-S., Houdier, S., Parrenin, F., Simpson, W. R., and Douglas, T. A.:  
26 Interactions between snow metamorphism and climate physical and chemical aspects, in:  
27 *Physics and Chemistry of Ice*, edited by Kuhs, W. F., pp. 27 – 46, Royal Society of Chemistry,  
28 Cambridge, UK, 2007.

1 ~~Dominé, F., Albert, M., Huthwelker, T., Jacobi, H. W., Kokhanovsky, A. A., Lehning, M.,~~  
2 ~~Picard, G., and Simpson, W. R.: Snow physics as relevant to snow photochemistry, Atmos-~~  
3 ~~Chem. Phys., 8, 171–208, 2008.~~

4 EPICA community members: Eight glacial cycles from an Antarctic ice core, *Nature*, 429, 623–  
5 628, doi:10.1038/nature02599, 2004.

6 Erbland, J., Vicars, W. C., Savarino, J., Morin, S., Frey, M. M., Frosini, D., Vince, E., and  
7 Martins, J. M. F.: Air–snow transfer of nitrate on the East Antarctic Plateau – Part 1: Isotopic  
8 evidence for a photolytically driven dynamic equilibrium in summer, *Atmos. Chem. Phys.*, 13,  
9 6403–6419, doi:10.5194/acp-13-6403-2013, 2013.

10 France, J. L., King, M. D., Frey, M. M., Erbland, J., Picard, G., Preunkert, S., MacArthur, A.,  
11 and Savarino, J.: Snow optical properties at Dome C (Concordia), Antarctica; implications for  
12 snow emissions and snow chemistry of reactive nitrogen, *Atm. Chem. Phys.*, 11, 9787–9801,  
13 doi:10.5194/acp-11-9787-2011, 2011.

14 Frey, M. M., Savarino, J., Morin, S., Erbland, J., and Martins, J. M. F.: Photolytic imprint in  
15 the nitrate stable isotope signal in snow and atmosphere of East Antarctica and implications for  
16 reactive nitrogen cycling, *Atmos. Chem. Phys.*, 9, 8681 – 8696, doi:10.5194/acp-9-8681-2009,  
17 2009.

18 Frey, M. M., Brough, N., France, J. L., Anderson, P. S., Traulle, O., King, M. D., Jones, A. E.,  
19 Wolff, E. W., and Savarino, J.: The diurnal variability of atmospheric nitrogen oxides (NO and  
20 NO<sub>2</sub>) above the Antarctic Plateau driven by atmospheric stability and snow emissions, *Atmos.*  
21 *Chem. Phys.*, 13, 3045–3062, doi:10.5194/acp-13-3045-2013, 2013.

22 Frey, M. M., Roscoe, H. K., Kukui, A., Savarino, J., France, J. L., King, M. D., Legrand, M.,  
23 and Preunkert, S.: Atmospheric nitrogen oxides (NO and NO<sub>2</sub>) at Dome C, East Antarctica,  
24 during the OPALE campaign, *Atmos. Chem. Phys. Discuss.*, 14, 31281–31317,  
25 doi:10.5194/acpd-14-31281-2014, 2014.

26 Freyer, H. D., Kobel, K., Delmas, R. J., Kley, D., and Legrand, M. R.: First results of <sup>15</sup>N/<sup>14</sup>N  
27 ratios in nitrate from alpine and polar ice cores, *Tellus*, 48B, 93–105, 1996.

28 Frezzotti, M., Pourchet, M., Flora, O., Gandolfi, S., Gay, M., Urbini, S., Vincent, C., Becagli,  
29 S., Gagnani, R., Proposito, M., Severi, M., Traversi, R., Udisti, R., and Fily, M.: New  
30 estimations of precipitation and surface sublimation in East Antarctica from snow accumulation  
31 measurements, *Climate Dynamics*, 23, 803–813, 10.1007/s00382-004-0462-5, 2004.

1 Gallée, H., Preunkert, S., Argentini, S., Frey, M. M., Genthon, C., Jourdain, B., Pietroni, I.,  
2 Casasanta, G., Barral, H., Vignon, E., and Legrand, M.: Characterization of the boundary layer  
3 at Dome C (East Antarctica) during the OPALE summer campaign, *Atmos. Chem. Phys.*  
4 *Discuss.*, 14, 33089-33116, doi:10.5194/acpd-14-33089-2014, 2014.

5 [Gallet, J.-C., Domine, F., Arnaud, L., Picard, G., and Savarino, J.: Vertical profile of the specific](#)  
6 [surface area and density of the snow at Dome C and on a transect to Dumont D'Urville.](#)  
7 [Antarctica – albedo calculations and comparison to remote sensing products, \*The Cryosphere\*,](#)  
8 [5, 631-649, doi:10.5194/tc-5-631-2011, 2011.](#)

9 [Grannas, A. M., Jones, A. E., Dibb, J., et al.: An overview of snow photochemistry: evidence,](#)  
10 [mechanisms and impacts, \*Atmos. Chem. Phys.\*, 7, 4329–4373, doi:10.5194/acp-7-4329-2007,](#)  
11 [2007.](#)

12 Hastings, M. G., Sigman, D. M. and Steig, E. J.: Glacial/Interglacial changes in the isotopes of  
13 nitrate from the GISP2 ice core, *Global Biogeochem. Cy.*, 19, GB4024,  
14 doi:10.1029/2005GB002502, 2005.

15 [Herbert, B. M. J., Halsall, C. J., Jones, K. C., and Kallenborn, R.: Field investigation into the](#)  
16 [diffusion of semi-volatile organic compounds into fresh and aged snow, \*Atmos. Environ.\*, 40,](#)  
17 [1385–1393, 2006.](#)

18 Huey, L. G., Tanner, D. J., Slusher, D. L., Dibb, J. E., Arimoto, R., Chen, G., Davis, D., Buhr,  
19 M. P., Nowak, J. B., Mauldin III, R. L., Eisele, F. L., and Kosciuch, E.: CIMS measurements  
20 of HNO<sub>3</sub> and SO<sub>2</sub> at the South Pole during ICAT 2000, *Atmos. Environ.*, 38, 5411 – 5421,  
21 doi:10.1016/j.atmosenv.2004.04.037, 2004.

22 Jacob, D. J.: *Introduction to Atmospheric Chemistry*, Princeton University Press, Princeton, NJ,  
23 USA, 1999.

24 Jarvis, J. C., Steig, E. J., Hastings, M. G. and Kunasek, S. A.: Influence of local photochemistry  
25 on isotopes of nitrate in Greenland snow, *Geophys. Res. Lett.*, 35 (L21804), doi:  
26 10.1029/2008GL035551, 2008.

27 Jarvis, J. C., Hastings, M. G., Steig, E. J. and Kunasek, S. A.: Isotopic ratios in gas-phase HNO<sub>3</sub>  
28 and snow nitrate at Summit, Greenland, *J. Geophys. Res.*, 114, D17301, doi:  
29 10.1029/2009JD012134, 2009.

1 Kaempfer, T. U. and Plapp, M.: Phase-field modeling of dry snow metamorphism, *Physical*  
2 *Review E.*, 79, doi:10.1103/PhysRevE.79.031502, 2009.

3 King, M. D. and Simpson, W. R.: Extinction of UV radiation in Arctic snow at Alert, Canada  
4 (82°N), *Journal of Geophysical Research*, 106, 12 499–12 507, 2001.

5 Kukui, A., Legrand, M., Preunkert, S., Frey, M. M., Loisil, R., Gil Roca, J., Jourdain, B.,  
6 King, M. D., France, J. L., and Ancellet, G.: Measurements of OH and RO<sub>2</sub> radicals at Dome  
7 C, East Antarctica, *Atmos. Chem. Phys.*, 14, 12373-12392, doi:10.5194/acp-14-12373-2014,  
8 2014

9 Kunasek, S. A., Alexander, B., Steig, E. J., Hastings, M. G., Gleason, D. J. and Jarvis, J. C.:  
10 Measurements and modeling of  $\delta^{17}\text{O}$  of nitrate in snowpits from Summit, Greenland, *J.*  
11 *Geophys. Res.*, 113, D24302, doi:10.1029/2008JD010103, 2008.

12 Lee-Taylor, J. and Madronich, S.: Calculation of actinic fluxes with a coupled atmosphere-  
13 snow radiative transfer model, *J. Geophys. Res.*, 107, 4796, doi:10.1029/2002JD002084, 2002.

14 Legrand, M. R. and Delmas, R. J.: Relative contributions of tropospheric and stratospheric  
15 sources to nitrate in Antarctic snow, *Tellus*, 38B(3–4), 236—249, 1986.

16 Legrand, M. R. and Kirchner, S.: Origins and variations of nitrate in South Polar precipitation,  
17 *J. Geophys. Res.*, 95 (D4), 3493–3507, 1990.

18 Legrand, M., Preunkert, S., Jourdain, B., Gallee, H., Goutail, F., Weller, R., and Savarino, J.:  
19 Year-round record of surface ozone at coastal (Dumont d'Urville) and inland (Concordia) sites  
20 in East Antarctica, *J. Geophys. Res.-Atmos.*, 114, D20306, doi:10.1029/2008JD011667, 2009.

21 Liao, W. and Tan, D.: 1-D Air-snowpack modeling of atmospheric nitrous acid at South Pole  
22 during ANTCI 2003, *Atmos. Chem. Phys.*, 8, 7087–7099, doi:10.5194/acp-8-7087-2008, 2008.

23 Libois, Q., Picard, G., France, J. L., Arnaud, L., Dumont, M., Carmagnola, C. M., and King,  
24 M. D.: Influence of grain shape on light penetration in snow, *The Cryosphere*, 7, 1803-1818,  
25 doi:10.5194/tc-7-1803-2013, 2013.

26 Libois, Q., Picard, G., Arnaud, L., Morin, S. and Brun, E.: Modeling the impact of snow drift  
27 on the decameter-scale variability of snow properties on the Antarctic Plateau, *J. Geophys. Res.*  
28 *Atmos.*, 119, doi:10.1002/2014JD022361, 2014.

29 [Massmann, W. J.: A review of the molecular diffusivities of H<sub>2</sub>O, CO<sub>2</sub>, CH<sub>4</sub>, CO, O<sub>3</sub>, O<sub>2</sub>, NH<sub>3</sub>,](#)  
30 [N<sub>2</sub>O, NO and NO<sub>2</sub> in air, O<sub>2</sub> and N<sub>2</sub> near STP, \*Atmos. Environ.\*, 32\(6\), 1111-1127, 1998.](#)

1 McCabe, J. R., Boxe, C. S., Colussi, A. J., Hoffman, M. R., and Thiemens, M. H.: Oxygen  
2 isotopic fractionation in the photochemistry of nitrate in water and ice, *J. Geophys. Res.*, 110,  
3 9 PP., doi:10.1029/2004JD005484, 2005.

4 McCabe, J. R., Thiemens, M. H., and Savarino, J.: A record of ozone variability in South Pole  
5 Antarctic snow: The role of nitrate oxygen isotopes, *J. Geophys. Res.*, 112, D12 303,  
6 doi:10.1029/2006JD007822, 2007.

7 Meusinger, C., Berhanu, T. A., Erbland, J., Savarino, J. and Johnson, M. S.: Laboratory study  
8 of nitrate photolysis in Antarctic snow. I. Observed quantum yield, domain of photolysis, and  
9 secondary chemistry, *J. Chem. Phys.*, 140, 244305, doi: 10.1063/1.4882898, 2014.

10 Michalski, G., Scott, Z., Kabling, M., and Thiemens, M. H.: First measurements and modeling  
11 of  $\delta^{17}\text{O}$  in atmospheric nitrate, *Geophys. Res. Lett.*, 30, 1870, doi:10.1029/2003GL017015,  
12 2003.

13 Morin, S., Savarino, J., Bekki, S., Gong, S., and Bottenheim, J. W.: Signature of Arctic surface  
14 ozone depletion events in the isotope anomaly ( $\delta^{17}\text{O}$ ) of atmospheric nitrate, *Atmos. Chem.*  
15 *Phys.*, 7, 1451 – 1469, 2007.

16 Morin, S., Savarino, J., Frey, M. M., Yan, N., Bekki, S., Bottenheim, J. W., and Martins, J. M.  
17 F.: Tracing the origin and fate of  $\text{NO}_x$  in the Arctic atmosphere using stable isotopes in nitrate,  
18 *Science*, 322, 730 – 732, doi:10.1126/science.1161910, 2008.

19 Morin, S., Savarino, J., Frey, M. M., Dominé, F., Jacobi, H. W., Kaleschke, L., and Martins, J.  
20 M. F.: Comprehensive isotopic composition of atmospheric nitrate in the Atlantic Ocean  
21 boundary layer from 65°S to 79°N, *J. Geophys. Res.*, 114, D05 303,  
22 doi:10.1029/2008JD010696, 2009.

23 Morin, S., Sander, R., and Savarino, J.: Simulation of the diurnal variations of the oxygen  
24 isotope anomaly ( $\delta^{17}\text{O}$ ) of reactive atmospheric species, *Atm. Chem. Phys.*, 11, 3653–3671,  
25 doi:10.5194/acp-11-3653-2011, 2011.

26 Muscari, G. and de Zafra, R. L.: Evolution of the  $\text{NO}_y\text{-N}_2\text{O}$  correlation in the Antarctic  
27 stratosphere during 1993 and 1995, *J. Geophys. Res.*, 108(D14), 4428,  
28 doi:4410.1029/2002JD002871, 2003.

1 Röthlisberger, R., Hutterli, M. A., Sommer, S., Wolff, E. W., and Mulvaney, R.: Factors  
2 controlling nitrate in ice-cores: evidence from the Dome C deep ice core, *J. Geophys. Res.*,  
3 105(D16), 20 565–20 572, 2000.

4 [Sander, S. P., Friedl, R R., Golden, D. M., Kurylo, M. J., Moortgat, G. K., Keller-Rudek, H.,  
5 Wine, P. H., Ravishankara, A. R., Kolb, C. E., Molina, M. J., Finlayson-Pitts, B. J., Huie, R.  
6 E., and Orkin, V. L.: Chemical Kinetics and Photochemical Data for Use in Atmospheric  
7 Studies, Evaluation Number 15, JPL Publication 06-2, Jet Propulsion Laboratory, Pasadena,  
8 CA, 2006.](#)

9 Savarino, J., Kaiser, J., Morin, S., Sigman, D. M., and Thiemens, M. H.: Nitrogen and oxygen  
10 isotopic constraints on the origin of atmospheric nitrate in coastal Antarctica, *Atmos. Chem.  
11 Phys.*, 7, 1925 – 1945, doi:10.5194/acp-7-1925-2007, 2007.

12 Savarino, J., Bhattacharya, S. K., Morin, S., Baroni, M., and Doussin, J.-F.: The NO+O<sub>3</sub>  
13 reaction: a triple oxygen isotope perspective on the reaction dynamics and atmospheric  
14 implications for the transfer of the ozone isotope anomaly, *J. Chem. Phys.*, 128, 194 303,  
15 doi:10.1063/1.2917581, 2008.

16 [Savarino, J., Vicars, W. C., Legrand, M., Preunkert, S., Jourdain, B., Frey, M. M., Kukui, A.,  
17 and Gil Roca, J.: Oxygen isotope mass balance of atmospheric nitrate at Dome C, East  
18 Antarctica, during the OPAL campaign, \*Atmos. Chem. Phys. Discuss.\*, submitted.](#)

19

20 Scharko, N. K., Berke, A. E. and Raff, J. D.: Release of Nitrous Acid and Nitrogen Dioxide  
21 from Nitrate Photolysis in Acidic Aqueous Solutions, *Environ. Sci. Technol.*, 48 (20), 11991-  
22 12001, doi: 10.1021/es503088x, 2014.

23 Seinfeld, J. and Pandis, S.: *Atmospheric Chemistry and Physics*, Wiley Interscience, 1998.

24 Swain, M. R. and Gallée, H.: *Antarctic Boundary Layer Seeing*, Publications of the  
25 Astronomical Society of the Pacific, 118, pp. 1190–1197, 2006.

26 Thibert, E. and Dominé, F.: Thermodynamics and kinetics of the solid solution of HNO<sub>3</sub> in ice,  
27 *J. Phys. Chem. B*, 102, 4432 – 4439, 1998.

28 Thomas, J. L., Stutz, J., Lefer, B., Huey, L. G., Toyota, K., Dibb, J. E., and von Glasow, R.:  
29 Modeling chemistry in and above snow at Summit, Greenland - Part 1: Model description and  
30 results, *Atmos. Chem. Phys.*, 11, 4899–4914, doi:10.5194/acp-11- 4899-2011, 2011.



- 1 Traversi, R., Udisti, R., Frosini, D., Becagli, S., Ciardini, V., Funke, B., Lanconelli, C., Petkov,  
2 B., Scarchilli, C., Severi, M. and Vitale, V.: Insights on nitrate sources at Dome C (East  
3 Antarctic Plateau) from multi-year aerosol and snow records, *Tellus B*, 66, 22550,  
4 <http://dx.doi.org/10.3402/tellusb.v66.22550>, 2014.
- 5 ~~Vicars, W. C. and Savarino, J.: Quantitative constraints on the  $^{17}\text{O}$  excess ( $\Delta^{17}\text{O}$ ) signature of  
6 surface ozone: Ambient measurements from  $50^\circ\text{N}$  to  $50^\circ\text{S}$  using the nitrite-coated filter  
7 technique, *Geochim. Cosmochim. Acta*, 135, pp 270–287, doi:10.1016/j.gca.2014.03.023,  
8 2014.~~
- 9 Wagenbach, D., Graf, W., Minikin, A., Trefzer, U., Kipfstuhl, J., Oerter, H., and Blindow, N.:  
10 Reconnaissance of chemical and isotopic firm properties on top of Berkner Island, Antarctica,  
11 *Ann. Glaciol.*, 20, 307 – 312, 1994.
- 12 Wang, Y., Choi, Y., Zeng, T., Davis, D., Buhr, M., Huey, L. G., and Neff, W.: Assessing the  
13 photochemical impact of snow  $\text{NO}_x$  emissions over Antarctica during ANTCI 2003, *Atmos.*  
14 *Environ.*, 41, 3944 – 3958, doi:10.1016/j.atmosenv.2007.01.056, 2007.
- 15 Wolff, E.: Ice core studies of global biogeochemical cycles, chap. Nitrate in polar ice, pp. 195–  
16 224, Springer-Verlag, New York, 1995.
- 17 Wolff, E. W., Jones, A. E., Martin, T. J., and Grenfell, T. C.: Modelling photochemical  $\text{NO}_x$   
18 production and nitrate loss in the upper snowpack of Antarctica, *Geophys. Res. Lett.*, 29, 1944,  
19 doi:10.1029/2002GL015823, 2002.
- 20 Wolff, E. W., Jones, A. E., Bauguitte, S. J.-B., and Salmon, R. A.: The interpretation of spikes  
21 and trends in concentration of nitrate in polar ice cores, based on evidence from snow and  
22 atmospheric measurements, *Atmos. Chem. Phys.*, 8, 5627 – 5634, 2008.
- 23 Wolff, E.W., Barbante, C., Becagli, S., Bigler, M., Boutron, C. F., Castellano, E., de Angelis,  
24 M., Federer, U., Fischer, H., Fundel, F., Hansson, M., Hutterli, M., Jonsell, U., Karlin, T.,  
25 Kaufmann, P., Lambert, F., Littot, G. C., Mulvaney, R., Röthlisberger, R., Ruth, U., Severi, M.,  
26 Siggaard-Andersen, M. L., Sime, L. C., Steffensen, J. P., Stocker, T. F., Traversi, R., Twarloh,  
27 B., Udisti, R., Wagenbach, D., Wegner, A.: Changes in environment over the last 800 000 years  
28 from chemical analysis of the EPICA Dome C ice core, *Quaternary Science Reviews*, 29, 285–  
29 295, doi:10.1016/j.quascirev.2009.06.013, 2010.
- 30 Zatkan, M. C., Grenfell, T. C., Alexander, B., Doherty, S. J., Thomas, J. L., and Yang, X.: The  
31 influence of snow grain size and impurities on the vertical profiles of actinic flux and associated

1 NO<sub>x</sub> emissions on the Antarctic and Greenland ice sheets, *Atmos. Chem. Phys.*, 13, 3547-3567,  
2 doi:10.5194/acp-13-3547-2013, 2013.

3 [Zhang, L., Vet, R., O'Brien, J. M., Mihele, C., Liang, Z., & Wiebe, A. \(2009\). Dry deposition](#)  
4 [of individual nitrogen species at eight Canadian rural sites. \*J. Geophys. Res.\*, 114\(D02301\).](#)  
5 [doi:10.1029/2008JD010640.](#)  
6

1 **Tables**

2 Table 1. List of the acronyms used in this paper.

Compartment	Acronym	Unit	Definition
Atmosphere	<i>FS</i>	$\text{kgN m}^{-2} \text{a}^{-1}$	Stratospheric input flux
	<i>FT</i>	$\text{kgN m}^{-2} \text{a}^{-1}$	Tropospheric input flux
	<i>FPI</i>	$\text{kgN m}^{-2} \text{a}^{-1}$	Primary input flux ( $FPI = FS + FT$ )
	<i>FE</i>	$\text{kgN m}^{-2} \text{a}^{-1}$	Exported flux ( $FE = FPI - FA$ )
	<i>FA</i>	$\text{kgN m}^{-2} \text{a}^{-1}$	Archived flux
	<i>FD</i>	$\text{kgN m}^{-2} \text{a}^{-1}$	Deposited flux
	<i>FP</i>	$\text{kgN m}^{-2} \text{a}^{-1}$	Photolytic flux
	$\delta^{15}\text{N}(FX)$	‰	$\delta^{15}\text{N}$ in flux <i>FX</i>
	$\Delta^{17}\text{O}(FX)$	‰	$\Delta^{17}\text{O}$ in flux <i>FX</i>
	$\gamma(\text{NO}_3^-)$	$\text{ng m}^{-3}$	Atmospheric nitrate concentration
	$h_{AT}$	$\text{m}$	Height of the ABL
	$f_{\text{exp}}$	Adimensional	Exported fraction of the incoming fluxes to the atmospheric box
	<i>T</i>	$\text{K}$	Near ground atmospheric temperature
	<i>P</i>	$\text{mbar}$	Near ground atmospheric pressure
	$^{15}\epsilon_{\text{dep}}$	‰	$^{15}\text{N}/^{14}\text{N}$ fractionation constant associated with nitrate deposition
	$J(\text{NO}_2)$	$\text{s}^{-1}$	Photolytic rate constant of $\text{NO}_2$
	$\alpha$	Adimensional	Leighton cycle perturbation factor
	$\Delta^{17}\text{O}(\text{O}_3)_{\text{bulk}}$	‰	$^{17}\text{O}$ -excess in bulk ozone
	$\vartheta$	°	Solar zenith angle
	<i>I</i>	$\text{cm}^{-2} \text{s}^{-1} \text{nm}^{-1}$	Actinic flux
<i>q</i>	Adimensional	Actinic flux enhancement factor	
<i>PSS</i>	-	<b>Photochemical Steady State</b>	
Snow	<i>A</i>	$\text{kg m}^{-2} \text{a}^{-1}$	Annual snow accumulation rate
	$\rho$	$\text{kg m}^{-3}$	Snow density
	$f_{\text{cage}}$	Adimensional	Cage effect factor
	<i>D</i>	$\text{m}^2 \text{s}^{-1}$	Diffusion coefficient
	$\omega(\text{NO}_3^-)$	$\text{ng g}^{-1}$	Nitrate mass fraction
	$m_{50\text{cm}}(\text{NO}_3^-)$	$\text{mgN}$	Nitrate mass fraction in the top 50 cm
	$\Delta^{17}\text{O}(50\text{cm})$	‰	$\Delta^{17}\text{O}$ in the top 50 cm
	$\delta^{15}\text{N}(50\text{cm})$	‰	$\delta^{15}\text{N}$ in the top 50 cm
	$\Phi$	Adimensional	Quantum yield in nitrate photolysis
	$\sigma$	$\text{cm}^2$	Absorption cross section of $^{14}\text{NO}_3^-$
	$\sigma'$	$\text{cm}^2$	Absorption cross section of $^{15}\text{NO}_3^-$
	<i>k</i>	Adimensional	Photic zone compression factor
	<i>J</i>	$\text{s}^{-1}$	Photolytic rate constant of $^{14}\text{NO}_3^-$
	<i>J'</i>	$\text{s}^{-1}$	Photolytic rate constant of $^{15}\text{NO}_3^-$
	$\eta$	$\text{m}$	E-folding attenuation depth

$^{15}\epsilon_{app}$	‰	Apparent $^{15}\text{N}/^{14}\text{N}$ fractionation constant
$^{17}\epsilon_{app}$	‰	$^{17}\text{O}$ -excess apparent fractionation constant
$^{15}\epsilon_{pho}$	‰	$^{15}\text{N}/^{14}\text{N}$ fractionation constant associated with nitrate photolysis
<u>CYCL</u>	Adimensional	<u>Average number of recyclings in a box</u>
<u>YANR(FA)</u>	Adimensional	<u>Yearly Average Number of Recyclings undergone by the archived nitrate</u>

Mis en forme : Police :Italique, Non Exposant/ Indice  
 Mis en forme : Non Exposant/ Indice  
 Mis en forme : Non Exposant/ Indice

1  
 2 Table 2. List of the physical and chemical processes included and excluded in TRANSITS.  
 3 Physical and chemical processes are written in straight and italic font, respectively.

	Processes included	Processes excluded
Snow	Snow accumulation	Snow densification
	<u>Macroscopic n</u> Nitrate diffusion	Snow metamorphism (sublimation, melting)
		Snow erosion
		Snowpack ventilation
		<del>Dissociation of the deposited <math>\text{HNO}_3</math></del>
		Nitrate location changes
	Nitrate UV-photolysis	Nitrate saturation
	Cage recombination effects	Physical release of $\text{HNO}_3$
	Nitrate export	Variation of ABL
Atmosphere	Primary nitrate inputs (strato. and tropo.)	
	$\text{HNO}_3$ dry deposition	
	Local cycling of $\text{NO}_2$ (conceptual)	
	Location oxidation of $\text{NO}_2$ by OH (conceptual)	Nitrate wet deposition
		Formal atmospheric chemistry

Mis en forme : Justifié

4  
 5

1  
2 Table 3. Parameters and variables used for the realistic simulation of TRANSITS. Input time-  
3 variables and fixed parameters are written in bold.

Process		Realistic, DC	Realistic, EAP
Snow accumulation	$\rho$ / (kg m <sup>-3</sup> )		300
	$A$ / (kg m <sup>-2</sup> a <sup>-1</sup> )	28	[20 to 600]
	Accu <del>repartition</del> <del>distribution</del>	<del>Constant-Uniform</del>	throughout the year
HNO <sub>3</sub> deposition	$10^3 \times \epsilon_{\text{dep}}^{15}$		<del>+10</del>
Nitrate diffusion in snow	$D$ / (m <sup>2</sup> s <sup>-1</sup> )	<del>1.3-0</del>	<del>10<sup>-11</sup> at T = 237 K</del>
TUV-snow parameters and variables	<b>Optical &amp; physical prop. snowpack</b>	DC snowpack, from France et al., 2011	
	O <sub>3</sub> column	DC observations 2000-2009	
	$k$	1	
Nitrate photolysis	$\Phi$	0.026	
	$\sigma$ and $\sigma'$	From Berhanu et al. (2014a)	
	$q$	1	
Cage effect	$f_{\text{cage}}$	0.15	
	$10^3 \times \Delta^{17}\text{O}(\text{H}_2\text{O})$	0	
Cycling/ <del>oxidation</del> of NO <sub>2</sub>	$[\text{BrO}]$ / pptv	2.5 (Frey et al., 2014)	
	$[\text{RO}_2]$ / (molecule cm <sup>-3</sup> )	= $7.25 \times 10^{159} \times (J(\text{NO}_2) / \text{s}^{-1})$ (Kukui et al., 2014)	
	$[\text{HO}_2]/[\text{RO}_2]$	0.7 (Kukui et al., 2014)	
	$[\text{O}_3]$ / ppbv	From Legrand et al. (2009)	
	$10^3 \times \Delta^{17}\text{O}(\text{O}_3)_{\text{bulk}}$	25.2 ( <del>Vicars and Savarino et al., submitted Savarino, 2014</del> ) 3 (Savarino et al., submitted)	
Atmospheric properties	$T$ / K	Concordia AWS (8989) in 2009-2010	
	$P$ / mbar	Concordia AWS (8989) in 2009-2010	
Nitrate export	$f_{\text{exp}}$	20 %	
	$FPI$ / (kgN m <sup>-2</sup> a <sup>-1</sup> )	8.2 10 <sup>-6</sup> (Muscari and de Zafra, 2003)	
Mass balance in the atmosphere	$FS/FPI$	50 %	
	$FS$	Plateau from May 16 to October 18	
	<del>repartition</del> <del>distribution</del>	<del>Constant-Uniform</del> throughout the year	
	$FT$	<del>Constant-Uniform</del> throughout the year	
	$h_{\text{AT}}$ / m	50	
	$\nu(\text{NO}_3^-)$	Idealized DC	
	$10^3 \times \Delta^{17}\text{O}(FS)$	42	
$10^3 \times \delta^{15}\text{N}(FS)$	19		
$10^3 \times \Delta^{17}\text{O}(FT)$	30		
$10^3 \times \delta^{15}\text{N}(FT)$	0		

Mis en forme : Exposant

4

1 Table 4. Simulated nitrate concentration and isotopic composition at the air-snow interface in  
 2 the case of the DC realistic simulation.

	Atmosphere			Skin layer		
	$\nu(\text{NO}_3^-)$ / (ng m <sup>-3</sup> )	$10^3 \times \delta^{15}\text{N}$	$10^3 \times \Delta^{17}\text{O}$	$\omega(\text{NO}_3^-)$ / (ng g <sup>-1</sup> )	$10^3 \times \delta^{15}\text{N}$	$10^3 \times \Delta^{17}\text{O}$
average	31.9			3074		
weighted		0.2	23.7		34.9	25.5
average						
min	5.0	-17.0	20.8	707	10.1	20.5
max	110.0	19.4	39.3	5706	58.1	38.9

3

4 [Table 5. Simulated nitrate mass fluxes and their isotopic composition in the case of the DC](#)  
 5 [realistic simulation.](#)

Flux	Annual flux	Seasonal flux			Seasonal $10^3 \times \delta^{15}\text{N}$			Seasonal $10^3 \times \Delta^{17}\text{O}$		
	/( $10^{-6}$ kgN m <sup>-2</sup> a <sup>-1</sup> )	Mean	Min	Max	Mean	Min	Max	Mean	Min	Max
<i>FP</i>	32.07	1.02	0.00	3.27	12.6	-23.8	29.3	21.7	20.4	25.0
<i>FD</i>	32.22	1.02	0.10	2.72	13.9	-7.0	29.4	24.8	20.8	39.3
<i>FE</i>	8.05	0.26	0.03	0.68	3.9	-17.0	19.4	24.8	20.8	39.3
<i>FA</i>	0.15	0.00	0.00	0.00	317.7	317.6	317.8	17.8	17.8	17.8
<i>FS</i>	4.10	0.13	0.00	0.45	19.0	19.0	19.0	42.0	42.0	42.0
<i>FT</i>	4.10	0.13	0.13	0.13	0.0	0.0	0.0	30.0	30.0	30.0

6

7 Table 6. Simulated nitrate mass, concentration and isotopic composition in the top 50 cm of  
 8 snow and in the archived flux as well as the apparent fractionation constants.

	Nitrate in top 50 cm			Nitrate in archived flux			Fractionation constants		
	$m_{50\text{cm}}(\text{NO}_3^-)$ / (mgN m <sup>-2</sup> )	$10^3 \times \delta^{15}\text{N}$	$10^3 \times \Delta^{17}\text{O}$	$\omega(\text{NO}_3^-)$ / (ng g <sup>-1</sup> )	$10^3 \times \delta^{15}\text{N}$	$10^3 \times \Delta^{17}\text{O}$	$10^3 \times {}^{15}\epsilon_{\text{app}}$	$10^3 \times {}^{17}\epsilon_{\text{app}}$	$10^3 \times {}^{15}\epsilon_{\text{pho}}$
average	8.1±1.6			23.0±0.0			-49.5±3.7	1.4±0.6	
weighte		100.5	23.3		317.7	17.8			-55.1
d									
average									
min	6.2	77.4	20.0	22.9	317.6	17.8	-53.6	0.7	-78.8
max	11.0	127.5	27.4	23.0	317.8	17.8	-43.0	2.4	-52.9

9

10 [Table 6. Simulated nitrate mass fluxes and their isotopic composition in the case of the DC](#)  
 11 [realistic simulation.](#)

Flux	Annual flux	Seasonal flux			Seasonal $10^3 \times \delta^{15}\text{N}$			Seasonal $10^3 \times \Delta^{17}\text{O}$		
	/( $10^{-6}$ kgN m <sup>-2</sup> a <sup>-1</sup> )	Mean	Min	Max	Mean	Min	Max	Mean	Min	Max
<i>FP</i>	32.07	1.02	0.00	3.27	12.6	-23.8	29.3	21.7	20.4	25.0
<i>FD</i>	32.22	1.02	0.10	2.72	13.9	-7.0	29.4	24.8	20.8	39.3
<i>FE</i>	8.05	0.26	0.03	0.68	3.9	-17.0	19.4	24.8	20.8	39.3

<u>FA</u>	<u>0.15</u>	<u>0.00</u>	<u>0.00</u>	<u>0.00</u>	<u>317.7</u>	<u>317.6</u>	<u>317.8</u>	<u>17.8</u>	<u>17.8</u>	<u>17.8</u>
<u>FS</u>	<u>4.10</u>	<u>0.13</u>	<u>0.00</u>	<u>0.45</u>	<u>19.0</u>	<u>19.0</u>	<u>19.0</u>	<u>42.0</u>	<u>42.0</u>	<u>42.0</u>
<u>FT</u>	<u>4.10</u>	<u>0.13</u>	<u>0.13</u>	<u>0.13</u>	<u>0.0</u>	<u>0.0</u>	<u>0.0</u>	<u>30.0</u>	<u>30.0</u>	<u>30.0</u>

1  
2





1 Table 57. Overview of the TRANSITS results for the sensitivity tests.

2  
3  
4

Tested variable	Tested values (reference value)	FA / ( $10^{-6}$ kgN m <sup>2</sup> a <sup>-1</sup> ) (abs. diff.)	FA/FPI in % (abs. diff.)	$10^3 \times \delta^{15}\text{N}(FA)$ (abs. diff.)	$10^3 \times \Delta^{17}\text{O}(FA)$ (abs. diff.)
<b>Realistic simulation for DC (reference)</b>		<b>0.15</b>	<b>1.77</b>	<b>317.7</b>	<b>17.8</b>
$h_{AT}$ / m	500 ( <b>50</b> )	0.15 (=)	1.77 (=)	317.7 (=)	17.8 (=)
$\gamma(\text{NO}_3^-)$ / (ng m <sup>-3</sup> )	Real. ideal. DC $\times 10$ (Real. ideal. DC)	0.15 (=)	1.77 (=)	317.7 (=)	17.8 (=)
FPI / ( $10^{-6}$ kgN m <sup>-2</sup> a <sup>-1</sup> )	82 ( <b>8.2</b> )	1.45 (+1.31)	1.77 (=)	317.7 (=)	17.8 (=)
$10^3 \times \delta^{15}\text{N}(FS)$	+119 ( <b>+19</b> )	0.15 (=)	1.77 (=)	376.0 (+58.4)	17.8 (=)
$10^3 \times \delta^{15}\text{N}(FT)$	+100 ( <b>0</b> )	0.15 (=)	1.77 (=)	388.5 (+70.9)	17.8 (=)
$10^3 \times \delta^{15}\text{N}_{dep}$	0 ( <b>+10</b> )	0.15 (=)	1.77 (=)	303.5 (-14.2)	17.8 (=)
$10^3 \times \Delta^{17}\text{O}(FS)$	0 ( <b>42</b> )	0.15 (=)	1.77 (=)	317.7 (=)	16.0 (-1.8)
$10^3 \times \Delta^{17}\text{O}(FT)$	0 ( <b>30</b> )	0.15 (=)	1.77 (=)	317.7 (=)	15.1 (-2.7)
$10^3 \times \Delta^{17}\text{O}(\text{O}_3)_{bulk}$	0 ( <b>25.2</b> )	0.15 (=)	1.77 (=)	317.7 (=)	7.4 (-10.4)
$10^3 \times \Delta^{17}\text{O}(\text{OH})$	0 ( <b>3</b> )	0.15 (=)	1.77 (=)	317.7 (=)	17.2 (-0.6)
[BrO] / pptv	5.0 ( <b>2.5</b> )	0.15 (=)	1.77 (=)	317.7 (=)	18.2 (+0.4)
[HO <sub>2</sub> ]	Est. DC $\times 10$ ( <b>Est. DC</b> )	0.15 (=)	1.77 (=)	317.7 (=)	16.6 (-1.2)
[CH <sub>3</sub> O <sub>2</sub> ]	Est. DC $\times 10$ ( <b>Est. DC</b> )	0.15 (=)	1.77 (=)	317.7 (=)	17.3 (-0.5)
[O <sub>3</sub> ] / ppbv	Obs. DC $\times 10$ ( <b>Obs. DC</b> )	0.15 (=)	1.77 (=)	317.7 (=)	18.6 (+0.8)
T / K	Obs. DC -10 ( <b>Obs. DC</b> )	0.15 (=)	1.77 (=)	317.7 (=)	17.5 (-0.3)
FS/FPI	0.6 ( <b>0.5</b> )	0.14 (-0.0)	1.73 (-0.04)	322.4 (+4.7)	17.8 (=)
$f_{cage}$	0.18 ( <b>0.15</b> )	0.17 (+0.03)	2.11 (+0.34)	305.5 (-12.2)	16.8 (-1.0)
$f_{exp}$	0.24 ( <b>0.2</b> )	0.11 (-0.03)	1.36 (-0.41)	322.1 (+4.5)	18.1 (+0.4)
A / (kg m <sup>-2</sup> a <sup>-1</sup> )	33.6 ( <b>28</b> )	0.32 (+0.17)	3.90 (+2.13)	263.9 (-53.8)	18.6 (+0.8)
$\rho$ / (kg m <sup>-3</sup> )	360 ( <b>300</b> )	0.06 (-0.09)	0.72 (-1.05)	373.8 (+56.1)	17.0 (-0.8)
k	1.2 ( <b>1.0</b> )	0.35 (+0.21)	4.28 (+2.51)	252.0 (-65.6)	18.8 (+1.1)
q	1.2 ( <b>1.0</b> )	0.06 (-0.09)	0.70 (-1.07)	375.2 (+57.5)	16.9 (-0.9)
$\Phi$	0.0336 ( <b>0.026</b> )	0.06 (-0.09)	0.70 (-1.07)	375.2 (+57.5)	16.9 (-0.9)
D / ( $10^{-11}$ m <sup>2</sup> s <sup>-1</sup> )	1.2 ( <b>1.0</b> )	0.16 (+0.01)	1.89 (+0.12)	309.4 (-8.2)	17.9 (+0.1)
Accumulation	Winter = 2 $\times$ summer	0.16 (+0.02)	1.98 (+0.21)	306.1 (-11.6)	18.0 (+0.3)
repartition distribution	Summer = 2 $\times$ winter (flat)	0.13 (-0.01)	1.64 (-0.13)	325.9 (+8.2)	17.6 (-0.2)
O <sub>3</sub> column	100 DU flat	0.01 (-0.14)	0.08 (-1.69)	344.1 (+26.4)	15.3 (-2.5)
	300 DU flat	0.19 (+0.05)	2.33 (+0.56)	309.1 (-8.6)	18.1 (+0.3)
	500 DU flat	0.70 (+0.56)	8.58 (+6.81)	252.1 (-65.5)	19.6 (+1.8)
	300 DU / 100 DU hole (real. DC)	0.06 (-0.08)	0.76 (-1.01)	328.3 (+10.6)	16.9 (-0.9)

5  
6

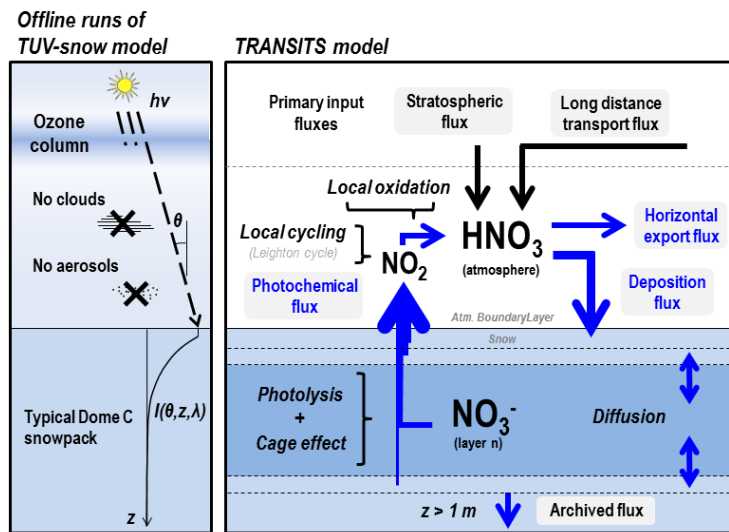
1 **Figures**

2

3

4 ~~Figure 1. Two cycles overlapping at the air snow interface of Dome C in summer. The~~  
5 ~~calculation of the photochemical, chemical and archiving lifetimes of  $\text{NO}_2$  and  $\text{NO}_3^-$  for summer~~  
6 ~~solstice conditions are explained in the text. Numbers in the black boxes represent the number~~  
7 ~~of cycles undergone by  $\text{NO}_2$  and  $\text{NO}_3^-$  before their oxidation and archiving, respectively.~~

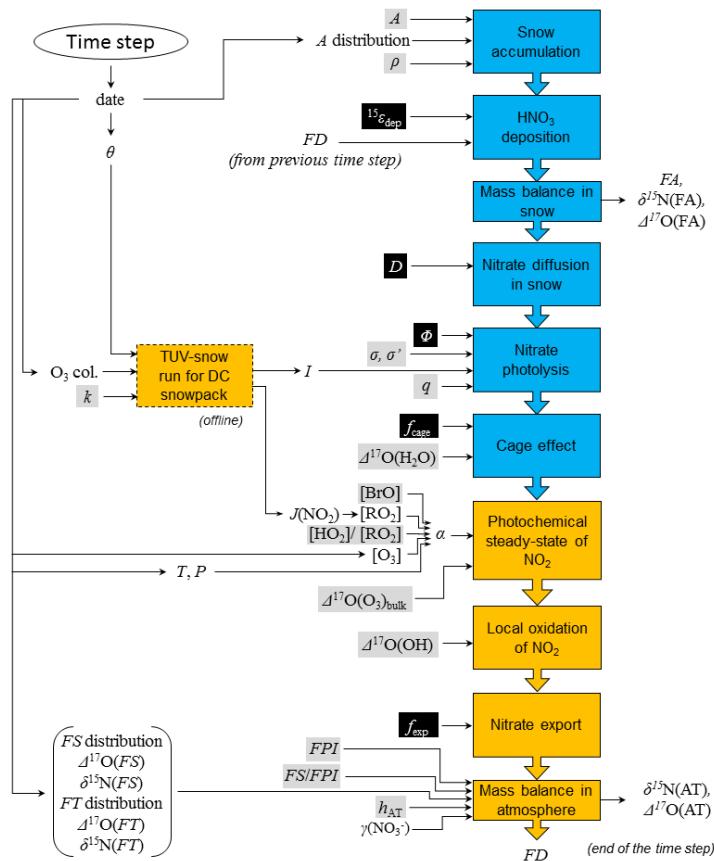
8



9

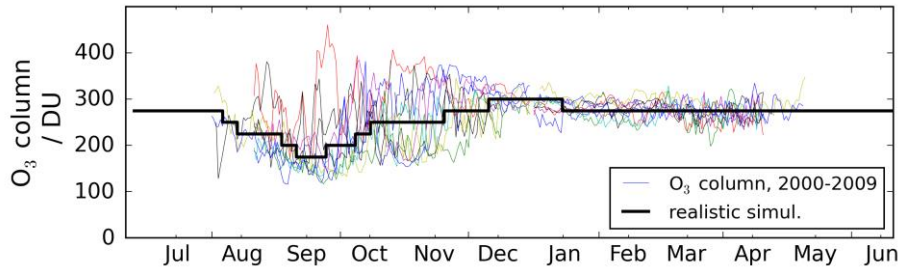
10 Figure 12. Overview of the TRANSITS model.

11



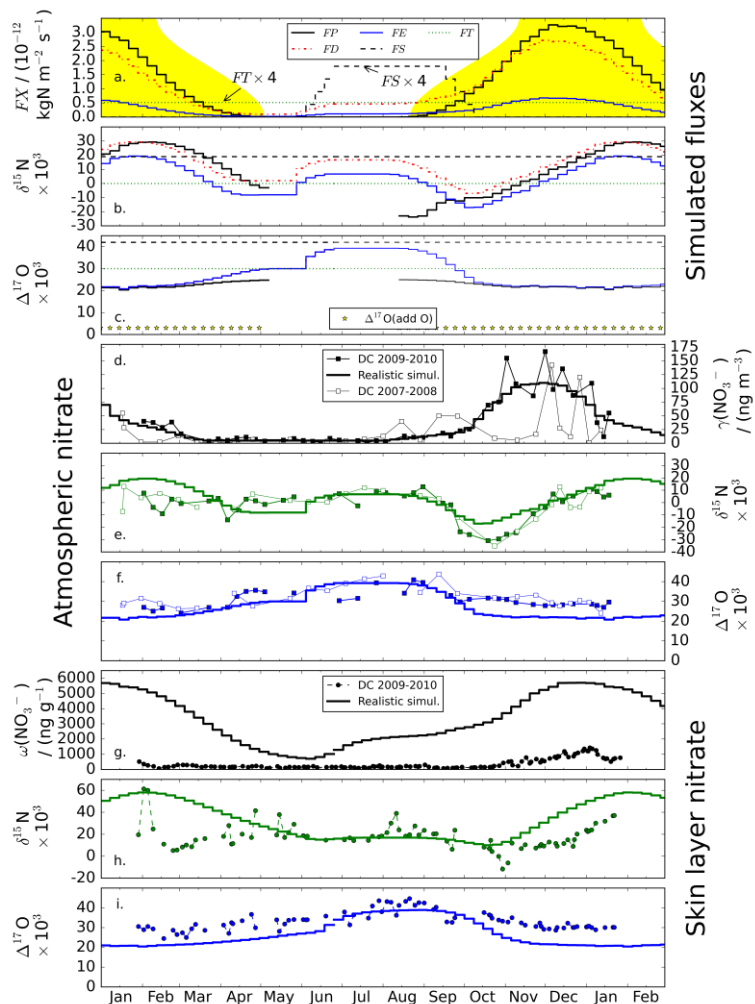
1  
 2 Figure 23. Schematic view of the processes included in TRANSITS (one time step is shown).  
 3 The orange and blue boxes represent processes occurring in the atmosphere and the snowpack,  
 4 respectively. Arrows entering from left and right sides of each box represent required inputs to  
 5 the calculation of each process. For the sake of clarity, we only display the input time-variables  
 6 (black font on white background), the fixed parameters (black on grey) and the  
 7 adjustment parameters (white on black).

8

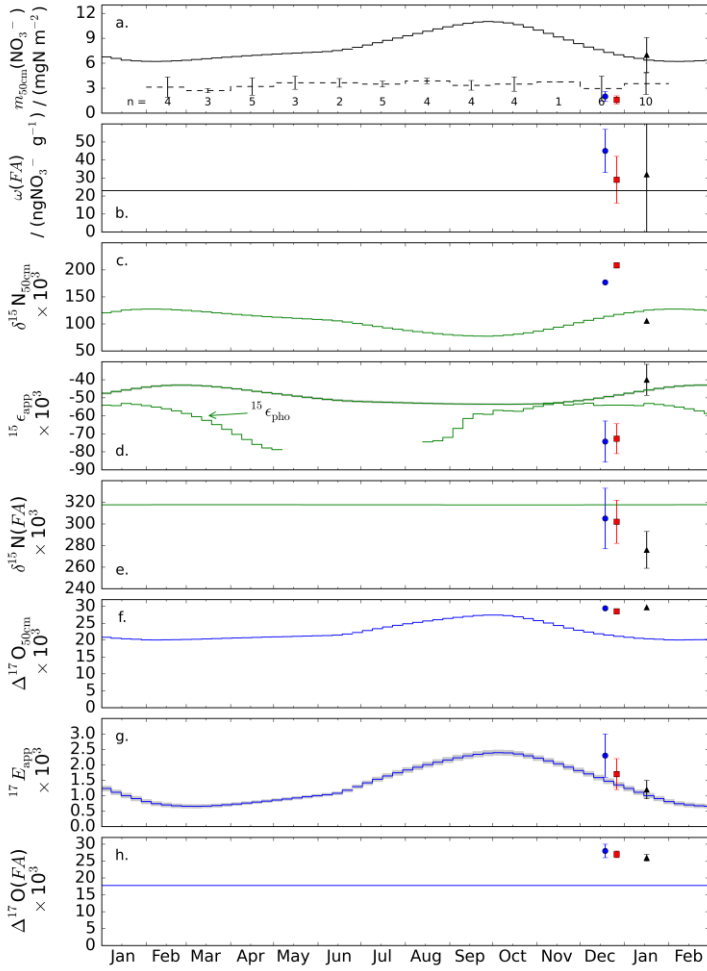


1  
 2 Figure 34. Driving data-~~ozone column data~~ for the DC realistic simulation versus observed  
 3 time series for years over the 2000-2009 (a) snow accumulation rates shared over the 52 time  
 4 steps (A is set to  $28 \text{ kg m}^{-2} \text{ a}^{-1}$ ). (b) ozone column. The ozone column scenarios are given with  
 5 the annual cycles measured at a daily time resolution over the period 2000-2009.

6

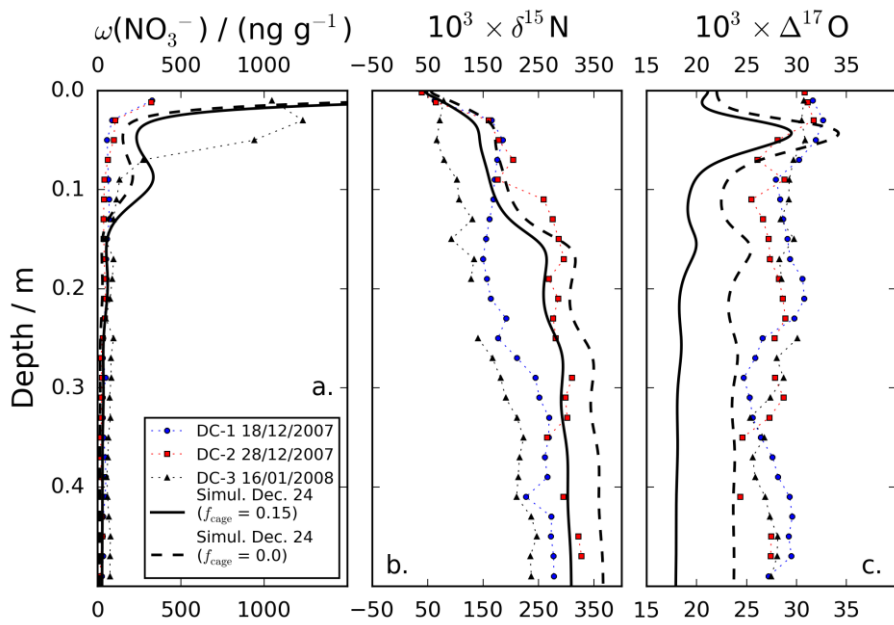


1  
 2 Figure 45. Realistic simulation results and comparison to the observations at Dome C. (a–c)  
 3 simulated fluxes (mass and isotopic composition) and  $\Delta^{17}\text{O}$  in the additional O atom (panel c).  
 4 The legend in panel a also applies to panels b and c. The yellow filled curve in panel a.  
 5 represents the day length at Dome C. Note that  $\delta^{15}\text{N}$  and  $\Delta^{17}\text{O}$  in FE and FD are equal. (d–f)  
 6 simulated and observed concentrations of  $\delta^{15}\text{N}$  and  $\Delta^{17}\text{O}$  in atmospheric nitrate. (g–i) simulated  
 7 and observed mass fractions of  $\delta^{15}\text{N}$  and  $\Delta^{17}\text{O}$  in skin layer nitrate. The 2007–2008 and 2009–  
 8 2010 observed data originate from Frey et al. (2009) and Erbland et al. (2013) respectively.



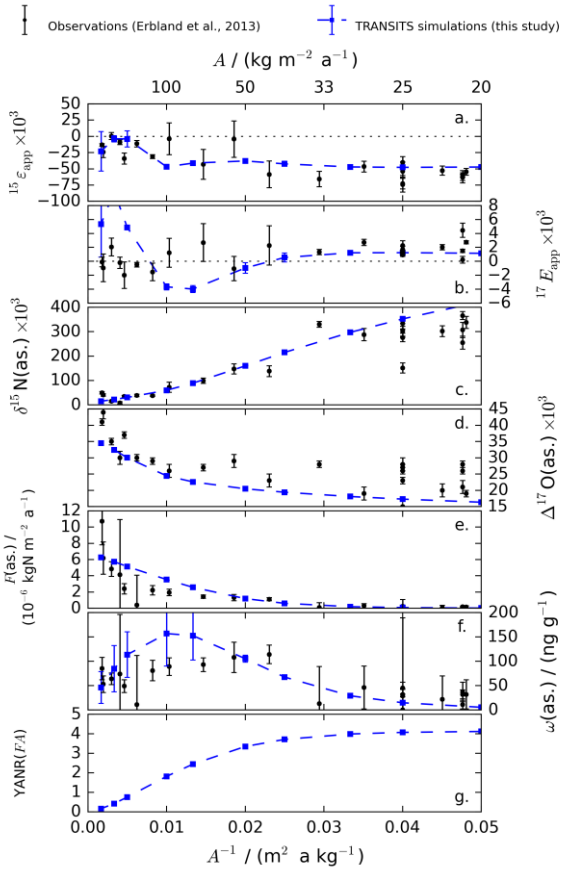
1  
2 Figure 56. Realistic simulation results for the snowpack and comparison to the observations at  
3 Dome C. (a) nitrate mass in the top 50 cm (the dashed curve represents the observed monthly  
4 values), (b) archived nitrate mass fractions, (c)  $\delta^{15}\text{N}$  of nitrate in the top 50 cm, (d) apparent  
5 and photolytic  $^{15}\epsilon$  fractionation constants (in grey, the range  $\pm 1\sigma$ ), (e)  $\delta^{15}\text{N}$  in the archived  
6 nitrate, (f)  $\Delta^{17}\text{O}$  of nitrate in the top 50 cm, (g) apparent  $^{17}E$  fractionation constant (in grey, the  
7 range  $\pm 1\sigma$ ) and (h)  $\Delta^{17}\text{O}$  in the archived nitrate. In each panels, the observed data from the  
8 three DC snowpits (Frey et al., 2009; Erbland et al., 2013) are represented by the same symbols  
9 as in Fig. 6-7).

1



2

3 Figure 67. Realistic simulation results: nitrate in the 50 top cm of the snowpack on 24 December  
 4 and comparison to the three observed profiles at Dome C in summer 2007-2008 (Frey et al.  
 5 (2009) and Erbland et al. (2013)). (a) nitrate mass fractions, (b)  $\delta^{15}\text{N}$  in nitrate and (c)  $\Delta^{17}\text{O}$  in  
 6 nitrate.

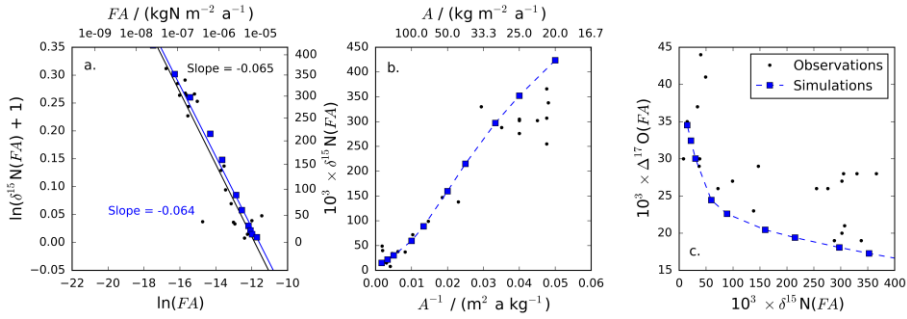


1  
 2 Figure 78. Reduced data in the TRANSITS simulations across East Antarctica and in the  
 3 observations (Erbland et al., 2013) as a function of the snow accumulation rates (top x-axis)  
 4 and their inverse (bottom x-axis). (a–b)  $^{15}\text{N}/^{14}\text{N}$  and  $^{17}\text{O}$ -excess apparent fractionation constants  
 5 (simulated dots and errors bars represent the mean and standard deviation values over the  
 6 December/January period), (c–d) Asymptotic (observed) and archived (modeled/simulated)  
 7  $\delta^{15}\text{N}$  and  $\Delta^{17}\text{O}$  values (simulated dots represent annual average values), (e) Asymptotic and  
 8 archived nitrate mass, (f) Asymptotic and archived nitrate mass fractions (simulated dots and  
 9 errors bars represent the mean and standard deviation values over the whole year), (g) Yearly  
 10 Average Number of Recyclings in the archived nitrate (YARN(FA)):-

Mis en forme : Police :Italique

Mis en forme : Police :Italique

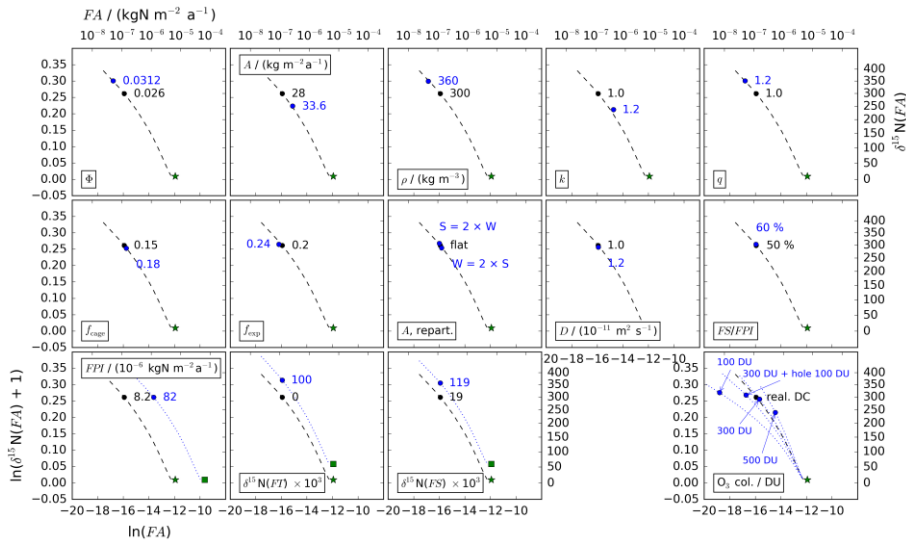




1  
 2 Figure 89. Realistic simulation with varying snow accumulation rates (blue squares) versus  
 3 observations along the D10–Dome C–Vostok route (black dots). (a) modified Rayleigh plot.  
 4 The two lines are linear fit to the data and the slopes are given in the respective colors. (b)  
 5  $\delta^{15}\text{N}(FA)$  versus the inverse of the snow accumulation rates, (c)  $\Delta^{17}\text{O}(FA)$  versus  $\delta^{15}\text{N}(FA)$ .

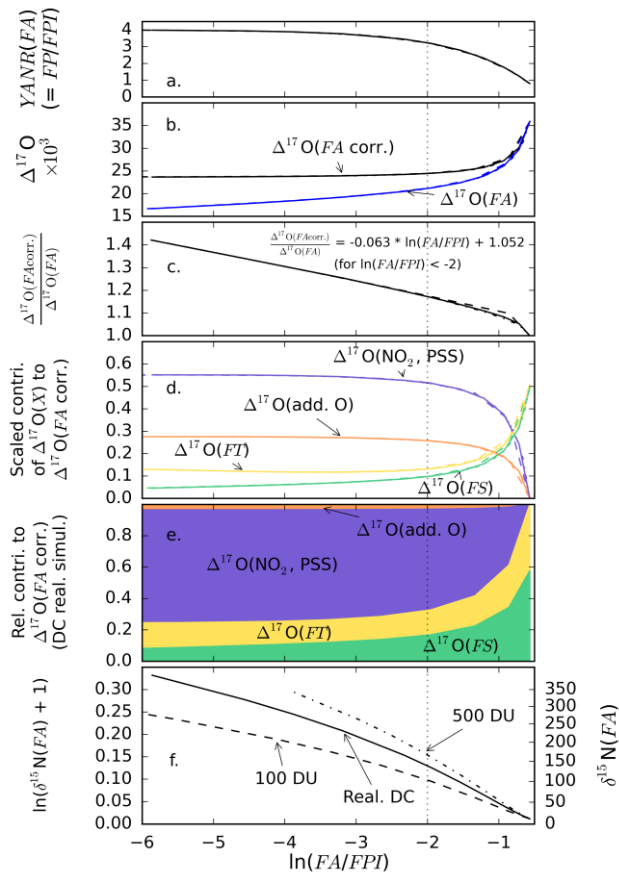
6

1



2

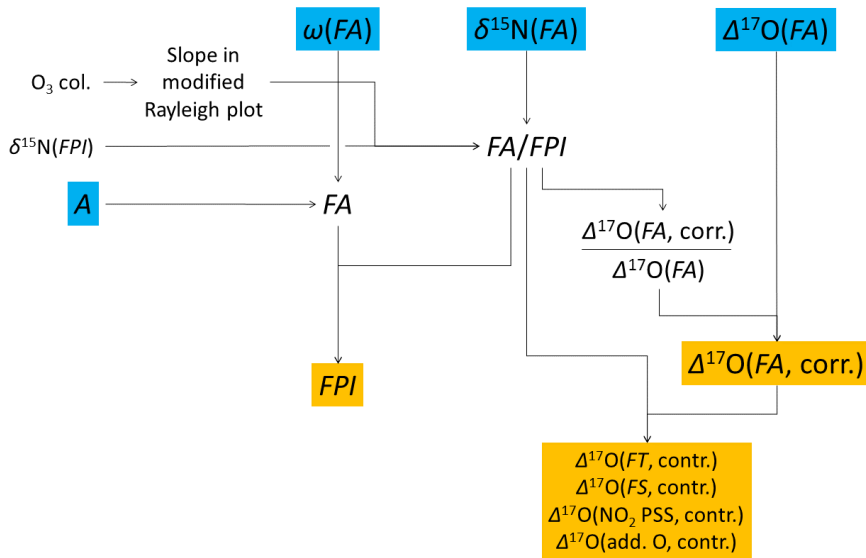
3 Figure 940. Modified Rayleigh plots of the sensitivity tests to the TRANSITS model. Only the  
 4 tests which imply significant changes in  $FA$  and  $\delta^{15}N(FA)$  are shown. The green star represents  
 5 the starting point whose coordinates are  $(\ln(FPI), \ln(\delta^{15}N(FA) + 1))$  and thick dashed lines  
 6 represent the curve which is obtained for the realistic DC simulation ( $\Phi$  varied). The other blue  
 7 dashed curves represent the consequences of a change in the starting point (squares) or in the  
 8 ozone column.



1  
2 Figure 10-4. TRANSITS simulations of the reduction in  $\Delta^{17}\text{O}(\text{FA})$  under the cage  
3 effects and scaled contributions to  $\Delta^{17}\text{O}(\text{FA, corr.})$  as a function of nitrate trapping efficiency  
4 ( $\ln(\text{FA}/\text{FPI})$ ). (a) average number of recycling cycles undergone by the archived nitrate at the  
5 air-snow interface ( $\text{YANR}(\text{FA})$ ), (b) deposition ratio ( $\text{FD}/\text{FPI}$ ), (c)  $\Delta^{17}\text{O}(\text{FA})$  with and without  
6 cage effect and (d) the associated  $\Delta^{17}\text{O}(\text{FA, corr.})/\Delta^{17}\text{O}(\text{FA})$  ratio, (e) the scaled contributions  
7 of  $\Delta^{17}\text{O}(\text{NO}_2, \text{PSS})$ ,  $\Delta^{17}\text{O}(\text{add. O})$ ,  $\Delta^{17}\text{O}(\text{FT})$  and  $\Delta^{17}\text{O}(\text{FS})$ , (f) the relative contributions to  
8  $\Delta^{17}\text{O}(\text{FA, corr.})$  in the DC case ( $\Delta^{17}\text{O}(\text{NO}_2, \text{PSS}) = 31.3\%$ ,  $\Delta^{17}\text{O}(\text{add. O}) = 3\%$ ,  $\Delta^{17}\text{O}(\text{FT}) =$   
9  $30\%$  and  $\Delta^{17}\text{O}(\text{FS}) = 42\%$ ), and (g) the  $\delta^{15}\text{N}(\text{FA})$  as a function of the ozone column. Note  
10 that for the (a-e) panels, the curves for the three  $\text{O}_3$  column case almost superimpose. The  
11 vertical dashed line at  $\ln(\text{FA}/\text{FPI}) = -1.22$  represents a threshold value below which  $\Delta^{17}\text{O}(\text{FA, corr.})/\Delta^{17}\text{O}(\text{FA})$   
12 ratio is linear with  $\ln(\text{FA}/\text{FPI})$ .

Mis en forme : Police :Italique

Mis en forme : Police :Italique



1  
 2 Figure 1142. Schematic of the suggested methods to retrieve information about the variables in  
 3 orange boxes using the measurement of from  $\omega(FA)$ ,  $\delta^{15}N(FA)$ , and  $\Delta^{17}O(FA)$  and the annual  
 4 snow accumulation rates accessible in ice cores. Orange boxes at the bottom of the figure  
 5 represent the variable, which can be retrieved from variables measured in ice cores.